Behaviour of nourishments in quasi 3-dimensional graded sediment models

Weir at Iffezheim, Rhine river, southern Germany

Report graduation project of Erik Ravenstijn

Delft, August 2009

Graduation commitee:
Prof.dr.ir. H.J. de Vriend
dr.ir. C.J. Sloff
dr.ir. M. Snellen
dr.ir. E. Mosselman

In cooperation with:

Preface

For support during this graduation project I would like to thank all members of my graduation committee. Also Mohammed Yossef, Andries Paarlberg, my friends and family are deeply thanked for all their support.

Delft, August 2009.

Index

Executive summary

Bed degradation in a number of Dutch river branches, like the Bovenrijn, can cause various problems in the near future. At low waters the navigation depth at the non-erodible layer near Emmerich can become too small. Other problems could be lower ground water levels and stability of structures in and near the river, like groynes. To diminish negative effects of bed degradation, nourishing material can be an effective solution. For a better understanding of nourishment behaviour and a better prediction of nourishment propagation, a tracer nourishment released in Germany in 1996 has been modeled and compared with field data. This tracer nourishment was released in the river Rhine at Iffezheim, Southern Germany, chainage kilometre 336.
Propagation of this tracer has been recorded to approximately 60 kilometres downstream of the dumpsite. The model used in this research, is a quasi-3D model with a graded sediment module. Simulating with a graded sediment module is important, since the mixture of the tracer nourishment modeled is different from the original bed material and there is an interest in the difference in behaviour between the finer and coarser tracer fractions. A quasi-3D format is used, because spatial scales less than the river width and transverse sorting effects might be important, as well as the parameterization of important 3D effects, like spiral flow. For the description of sediment transport a modified Meyer-Peter-Müller formula is used, the sediment balance of the river bed is described by the model of Hirano. Hiding and exposure effects are implemented by the formulation of Egiazaroff, modified by Ashida & Michiue. The bed load transport vector is adjusted by formulations for the effects of spiral flow and transverse bed slope. The roughness is calibrated against the water level for several relevant discharges. The sediment transport formula is calibrated against the yearly sediment transport. The discharge is schematized in two ways: either a constant representative discharge that yields the same yearly transport, or a hydrograph with five different discharge levels is used. Results of case studies show that the thickness of the active layer, hiding and exposure effects and the discharge schematization are important parameters for propagation of the tracer nourishment. Hiding and exposure effects appear to be quite different for a number of existing formulations. Simulation with a hydrograph instead of a constant representative discharge shows important differences: the propagation speed of specific sediment fractions is different. The coarsest fractions move just a little bit, but are still hardly mobile, though not completely immobile as in the computations with the constant representative discharge.
Compared to the field data, the finer fractions propagate too slowly, but the coarser fractions hardly move at all. To change this, relevant parameters that can be changed within the model concept used are the active layer thickness, critical Shields value and hiding and exposure relation. It is uncertain however, if the model concept used can represent a satisfactory approximation of the behaviour of all nourishment fractions simultaneously.
A number of physical processes that occur in the river reach just downstream Iffezheim, are not included in the model concept. Significant dunes appear to be present in this river reach, introducing vertical and horizontal sorting processes and different hydrodynamic conditions. Furthermore, it is questionable if the critical Shields value should not be variable with the sediment diameter. Finally, navigation appears to be possibly important.
Development of a model which takes into account these physical considerations, could be beneficial for prediction of sediment nourishments. On locations where a nourishment could be an effective solution, field data of the propagation of specific tracer fractions could give important information for rough estimations of nourishment behaviour.

With the currently available knowledge about the Dutch river branches, a number of practical recommendation can be done, for nourishing material as a measure against bed degradation. Dumping large amounts of nourishment in a short period of time is not recommended, since it is difficult to forecast the behaviour precisely, starting with smaller amounts is safer. It is advised to measure the bottom regularly, to see where the nourishment has had effect so far. A nourishment that is relatively coarse compared to the original bed material, will armour the bed more and results in less nourishments needed to keep the river bed on a certain level. Another advantage of a coarsening of the bed could be the river slope, which could be steeper for coarser material.

1 Introduction, problem definition and outline

1.1 Introduction

Bed degradation in a number of Dutch river branches, like the Bovenrijn, can cause various problems in the near future.

Just across the border in Germany, there is a nearly non-erodible layer at Emmerich (chainage km 853). Continuing degradation in the Bovenrijn, just downstream of Emmerich, creates a 'jump' in the bed, since the non-erodible layer does not degrade. The water levels at Emmerich are affected by the degradation more downstream, which results in a lower navigation depth. At low water this can cause serious problems for navigation.

Bed degradation will also result in lower water levels. This causes lower ground water levels. This can for example lead to drier winter beds. The lower bed also causes more water to flow in the summerbed, what results in even more degradation. At last the stability of structures can also be an issue, due to erosion there can be problems with groynes, for instance.

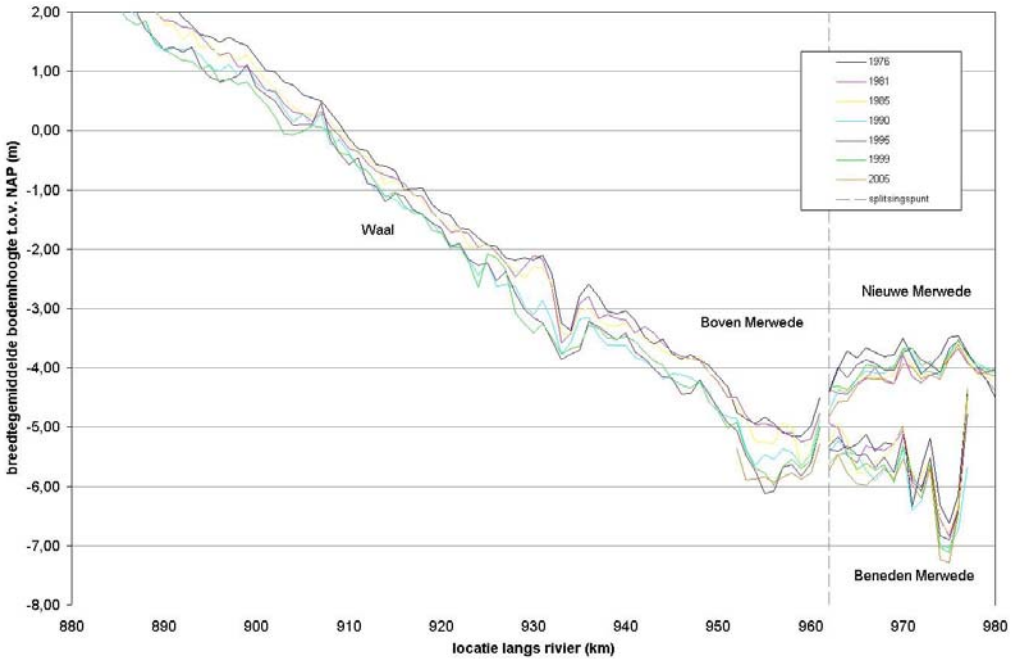

Figure 8.2: bed degradation in the Waal and Merwede according to *Mosselman and Wijbenga (2007)*

Bed degradation occurs for instance in the Bovenrijn, the Waal and the Merwede river. These river sections together have a length of approximately 150 km. The average degradation from 1970 to 2000 in the Bovenrijn is a few centimers per year, between chainage km 859 and km 867 *(RIZA, 2005)*. Predictions *(RIZA, 2005)* conclude that this degradation will continue during the following decades.

To stop bed degradation problems, nourishing material onto the riverbed is an effective solution. In Germany nourishments already have been applied successfully as a measure against bed degradation.

When the scale of the bed degradation is considered, large volumes of nourishment might be needed. When for instance nourishments are done which are in volume equal to an average thickness of 0.2 m along the Bovenrijn, Waal and Merwede, with an average width of 150 m, around 4.5 million m^3 of nourishment is needed. Nourishing this volume has serious consequences for river morphology on a large scale, obstruction of navigation and for logistics needed to supply the nourishment. Thus, the complexity of the nourishment strategy and the period of time needed for nourishing the riverbed of the Dutch river branches, is significant.

For nourishing material more efficiently, making better predictions of the nourishment behaviour is beneficial.

1.2 Problem of this research

With the currently available knowledge about river morphology it is hard to make rough predictions of nourishment behaviour, for instance of the propagation speed of the sediment within the nourishment. There are no useful field data from the Dutch river branches, which could lead to more insight into the nourishment behaviour. The predictive capability of the existing modeling tools is uncertain.

1.3 Outline of report

In chapter 2 the goal and comprehending methodology of this research will be stated. Chapter 3 describes the computational model, along with the physical relationships and parameters used in this model. Chapter 4 gives the results of the hydraulic calibration. Chapter 5 handles the schematization of the discharge at the upstream boundary of the model. The morphological set-up is done in chapter 6. Results of several case-studies are shown and discussed in chapter 7, after which final conclusions and recommendations are drawn in chapter 8.

2 Project objective and methodology

2.1 Goal

- Building a computational model to simulate a nourishment and judge it's predictive capability by comparing the results with field data.
- Identification of possible physical shortcomings of this computational model.
- Gaining a better insight into physical processes in the river that are important for nourishment behaviour, by performing this study.
- Giving practical recommendations for nourishing as a measure against bed degradation, with the currently available knowledge.

2.2 Methodology

In the Netherlands there are no useful field data of nourishment material for a comparison with a model simulation, but in Germany there are. Downstream the weir of Iffezheim in the Rhine river, in southern Germany, many nourishments have been done since 1978, also to prevent bed degradation. In December 1996 a graded tracer was released just downstream the weir at Iffezheim, along chainage kilometre 336-337. This tracer has been monitored intensively over a period of 5 years (until 2001), and over 60 kilometres along the river. Field data from this monitoring were provided by the BfG (Bundesanstalt für Gewässerkunde), for this study. With the help of a quasi-3D computational model containing a graded sediment module, the tracer nourishment released just downstream the weir at Iffezheim in 1996, has been modeled. In this model testing with morphological parameters and other conditions that influence the prediction of nourishment behaviour, has been done.

The use of a fully 3D modeling approach would create an unnecessary computational burden, since a large resolution in the vertical direction of the hydrodynamic grid does not contribute to a better representation of the physical processes that are important to model. Computing with a 1D model would not be satisfactory, since spatial scales of less than the river width and transverse sorting effects might be important. Computing with a 2D model would also not be satisfactory, since 3D effects like spiral flow are important to take into account. This is done by a parameterization of the important 3D effects for the 2D hydrodynamic grid. Representation of typical features as point bars and side channels should be satisfactory. This has consequences for the size of the grid cells.

The model used in this study contains a graded sediment module. Both the tracer nourishment and the river bed are significantly graded. Moreover, the tracer nourishment is coarser than the original bed material. These aspects are very important for morphological developments of the tracer nourishment. Not taking these aspects into account would result in the ignorance of many relevant phenomena, such as the difference in propagation speed of the available sediment sizes present in the nourishment.

The computational model used in this project, is a model constructed with the program Delft3D. The Delft3D instruments have a good functionality for modeling nourishments. Furthermore, it is one of the few models available in Holland with relatively good experience according to the quasi-3D approach with a graded sediment module.

3 Computational model

3.1 Physical relations

3.1.1 Hydrodynamic equations

To prescribe the flow, a transport equation for momentum and a continuity equation are needed. All the symbols are explained in appendix III.

Transport equations for momentum:

$$\frac{\partial u}{\partial t}+u\frac{\partial u}{\partial x}+v\frac{\partial u}{\partial y}+g\frac{\partial (h+z_b)}{\partial x}+g\frac{u\sqrt{u^2+v^2}}{C^2h}=\frac{\varepsilon_H}{\rho h}\left(2\frac{\partial^2 u}{\partial x^2}+\frac{\partial^2 u}{\partial y^2}+\frac{\partial^2 v}{\partial x\partial y}\right)$$

$$\frac{\partial v}{\partial t}+u\frac{\partial v}{\partial x}+v\frac{\partial v}{\partial y}+g\frac{\partial (h+z_b)}{\partial y}+g\frac{v\sqrt{u^2+v^2}}{C^2h}=\frac{\varepsilon_H}{\rho h}\left(2\frac{\partial^2 v}{\partial y^2}+\frac{\partial^2 v}{\partial x^2}+\frac{\partial^2 u}{\partial x\partial y}\right)$$

Continuity equation:

$$\frac{\partial h}{\partial t}+h\frac{\partial u}{\partial x}+u\frac{\partial h}{\partial x}+h\frac{\partial v}{\partial y}+v\frac{\partial h}{\partial y}=0$$

In the transport equation for momentum, the Chézy coefficient is used to express the roughness. In the model Nikuradse values are chosen for the roughness, but these are interrelated with Chézy coefficients by the White-Colebrook formula:

$$C=18\log_{10}\left(\frac{12h}{k}\right)$$

3.1.2 Morphological relations

To prescribe morphological change, a formula for sediment transport is needed and a formula for sediment balance is needed.

3.1.2.1 Sediment transport equations

For each sediment fraction i the bedload transport is calculated with a modified Meyer-Peter-Müller transport model:

$$q_{s,i} = \alpha D_i \sqrt{\Delta g D_i} \left(\mu\theta_i - \xi\theta_{cr} \right)^c \; p_{i,a}$$

In which:

$\theta_i = \left(\frac{\sqrt{u^2 + v^2}}{C} \right)^2 \frac{1}{\Delta D_i}$, this is the Shields parameter.

$\mu = \min\left(\left(\frac{C}{C_{g,90}} \right)^{1.5}, 1.0 \right)$, this is the ripple factor.

$$\xi_i = \left\{ \begin{array}{l} 0.8429 \frac{D_m}{D_i}, if \; \frac{D_i}{D_m} \le \frac{7}{18} \\ \left[\frac{\log_{10} 19}{\log_{10} 19 + \log_{10}\left(D_i / D_m \right)} \right]^2, otherwise \end{array} \right\}$$

The above equation for ξ_i *(Egiazaroff, modified by Ashida & Michiue, 1973)* produces the hiding and exposure value for each fraction. The critical Shields value in the sediment transport formula is expressed as θ_{cr}. This formula is chosen, because it is suited and valid the constraints (mainly bottom transport, $w_s / u_* \ge 1$) are fulfilled and there is good experience with this formula in the Rhine river.

The total amount of sediment transport is easily obtained by summation over all fractions:

$$q_{s,total} = \sum_{i=1}^{n} q_{s,i}$$

In this equation n is the number of fractions.

3.1.2.2 Sediment balance equations

To prescribe which sediment fraction, and how much of it, is present at each location, a concept of different layers in the bottom is used. The top layer is the active layer. Sediment from this layer is directly available for transport. This layer has a constant thickness. The active layer is the representation of the mixing layer of a river bed.

Below the active layer there is an underlayer system. A number of underlayers with a certain thickness define this system. Sediment material in the underlayer system cannot erode directly, first it has to move to the active layer. Something similar holds for deposition of material. Sediment from the highest underlayer can move to the active layer if this active layer is eroded. Because the active layer thickness is constant, erosion from this layer means that material from the highest underlayer moves into the active layer. When deposition occurs, a part of the active layer, equal to the amount of deposition, moves into the highest underlayer. All layers are assumed to be fully mixed at all times.

For each fraction the sediment balance equation for the active layer can be written as *(Hirano, 1971)*:

$$(1-\varepsilon)\left[\frac{\partial(\delta p_{i,a})}{\partial t} + p_i(z_0)\frac{\partial z_0}{\partial t}\right] + \frac{\partial q_{sx,i}}{\partial x} + \frac{\partial q_{sy,i}}{\partial y} = 0$$

For sedimentation, $(\partial z_0 / \partial t \geq 0)$, holds:

$$p_i(z_0) = p_{i,a}$$

For erosion, $(\partial z_0 / \partial t \leq 0)$, holds:

$$p_i(z_0) = p_i(z_0)$$

The transport for each fraction is:

$$q_{s,i} = p_{iT} q_{s,total}$$

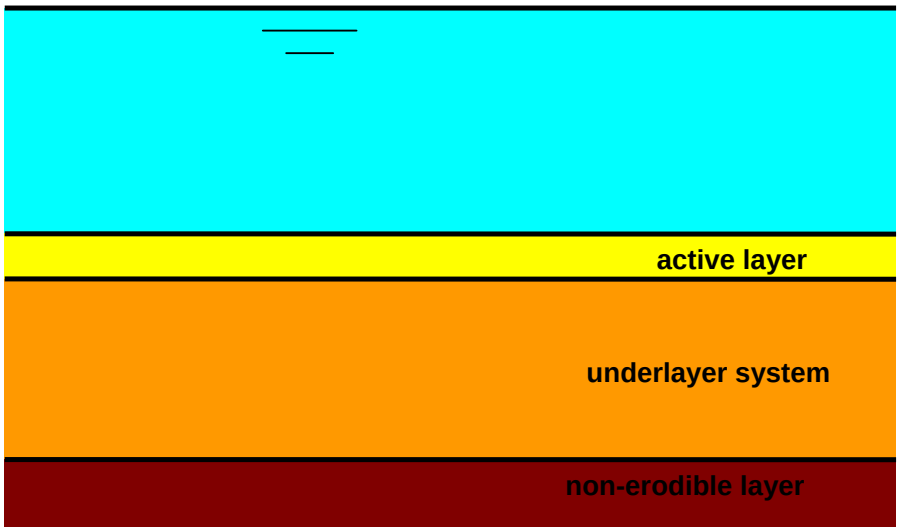

Figure 3.1: sketch of schematization of river bottom into layers

3.1.2.3 3D effects

The direction of the bedload transport is different from the depth averaged velocity in quasi-3D calculations. This direction is adjusted by helical flow and by transverse bed slope effects.

By implementing helical flow in the model, the near-bed flow direction is different from the depth-averaged flow direction. This has consequences for the bedload transport vector and hence for morphology. Helical flow is 3-dimensional by nature, but can be included in a quasi-3D model by means of a parameterization.

The equilibrium intensity of the helical flow is formulated as:

$$I_e = \frac{hu}{R}$$

Variable R is the radius of the streamline curvature, defined as:

$$\frac{1}{R} = \frac{1}{u_s}\frac{\partial u_r}{\partial s}$$

The actual helical flow intensity, I, adapts to the equilibrium flow intensity, I_e, as described by an advection-diffusion equation.

The angle between the near-bed flow direction and the depth averaged flow, caused by helical flow, can be calculated with the help of the following equation:

$$\tan\alpha_\tau = -\frac{2}{\kappa^2}\left(1-\frac{\sqrt{g}}{2\kappa C}\right)\frac{I}{u}$$

The effect of the transverse bed slope is implemented with the help of the following equation *(Koch&Flokstra 1980, extended by Talmon et. al 1995)*:

$$\tan(\varphi_s) = \frac{\sin(\varphi_\tau) + \frac{1}{f(\theta)}\frac{\partial z_b}{\partial y}}{\cos(\varphi_\tau) + \frac{1}{f(\theta)}\frac{\partial z_b}{\partial x}},$$

in which φ_τ is the direction of the bedload transport already adjusted for helical flow, and φ_s is the direction of the bedload transport adjusted for both helical flow and the transverse bed slope. The formulation for $f(\theta)$ is:

$$f(\theta) = A_{sh}\theta_i^{Bsh}\left(\frac{D_i}{H}\right)^{Csh}\left(\frac{D_i}{D_m}\right)^{Dsh}$$

3.2 Model set-up and input

3.2.1 Construction of the computational grid

The first step in making a computational model with Delft3D is the grid. The grid is curvi-linear and defined such that it follows the normal lines, i.e. the extent of the summerbed. This prevents the occurrence of a stepwise or staircase grid representation along the river banks or normal lines. Such stepwise banks are known to generate numerical disturbances on the bed.

Values for a number of parameters have to be chosen.
One is the number of grid cells in the cross direction of the summer bed, in between the normal lines of the river. The choice is dependent on the representation of large scale river morphology and is 12 cells in this case, 6 is believed to be the minimum for representing large scale summerbed morphology of the river Rhine. A second value is the ratio of the length of the grid cells to the width, in the summer bed. The length is chosen three times the width of the grid cells. Longer cells save computational effort, but when the ratio exceeds a value of 4, significant errors in the computation can occur. This results in summerbed grid cells of approximately 40 meters long, and 13 meters wide. The above choices affect the number of grid cells in the horizontal plane. In the vertical plane there is only one grid cell, because the approach is to calculate with a quasi-3D model.

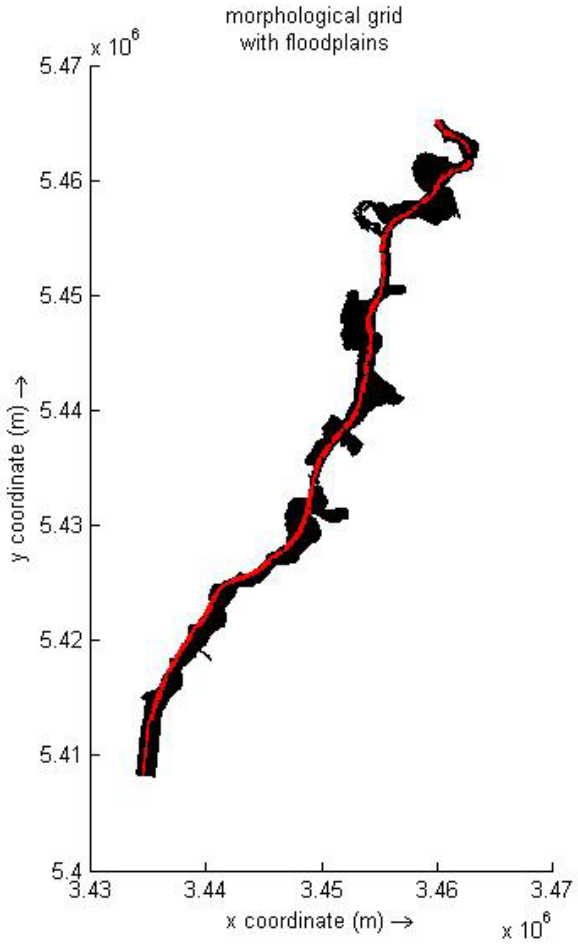

Figure 3.2: morphological grid with floodplains

There are a number of other restrictions considering this grid. To prevent an unrealistic flow pattern, the orthogonality and the smoothness of the grid should be within certain limits. For the orthogonality it holds that **Error! Objects cannot be created from editing field codes.**, where **Error! Objects cannot be created from editing field codes.** is the angle between two intersecting grid lines.

For the smoothness it holds that the ratio of the lengths and the ratio of the widths, of adjacent grid cells, should be smaller than the value of 1.2. In the floodplains the grid cells are constructed as large as possible, to save computational time.

3.2.2 Topographic data

The topography is obtained by averaging data points per grid cell. The resolution of the original topographic data is one data point per 10 m^2 of the grid. This results is about 4 to 5 data points per grid cell in the summerbed and more in the winter bed, since the grid cells are larger there. This resolution is high enough to average the data per grid cell, obtaining values for each grid cell. The available topographic data are from 2004, while the interesting modeling period is around 1996-2001, because the tracer nourishment was dumped in 1996 and has been recorded until 2001. Using a spin-up period before the period of 1996-2001 is modeled, the bottom of 2004 is adjusted by the hydraulic forcing based on data of the period 1993-2004 (see chapter 5) and the sediment composition of autumn 1991 (see section 3.2.6 and 6.1.2).

3.2.3 Groynes

The groynes are schematized as weirs in this model. The height of the crest of the groynes can only be specified as one horizontal level in this model, whereas in practice the crests of the groynes have a slope. The crest levels are determined from the topographic data, which give a rough approximation. In a later stage data were provided with accurate heights of the groynes, unfortunately no time was left to implement these data in the model. Figure 3.3 shows the roughly chosen groyne height, used in the model, and the more accurate data, gained from the BfG. Regarding the more accurate data, the average value of the crest height of each groyne is chosen as groyne height.

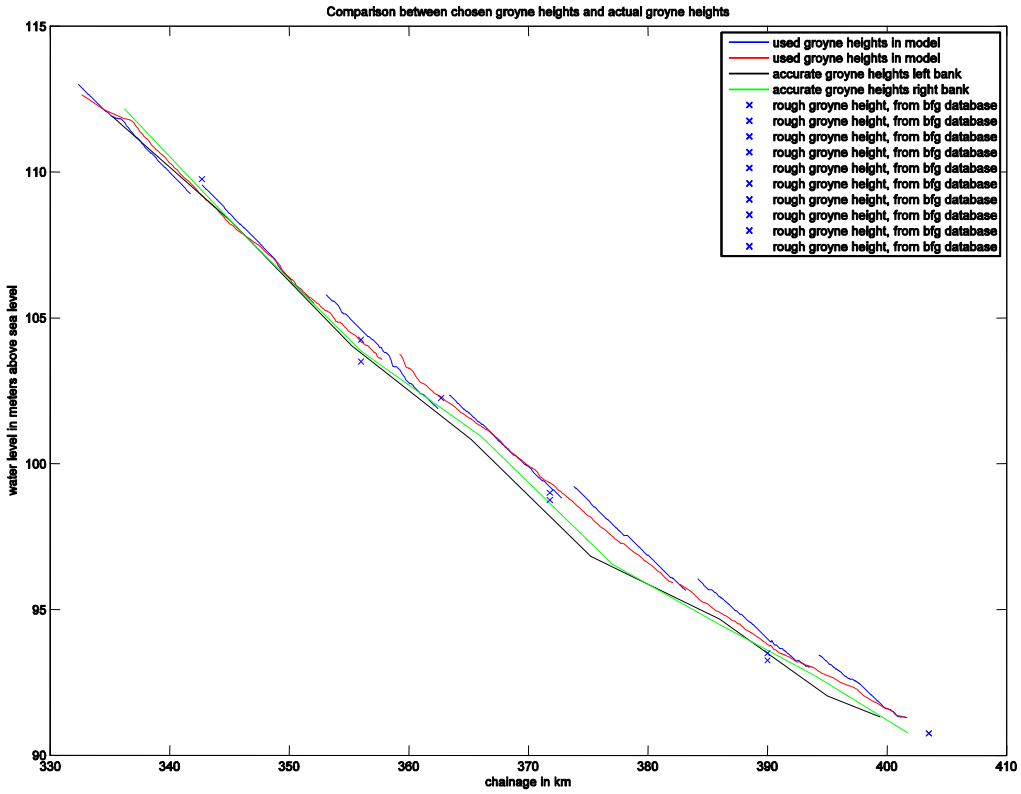

Figure 3.3: Comparison of groyne crest elevations used in the model and more accurate data gained later

The difference is less than 0.5 m in most cases. Around chainage km 375 the difference is larger, around 1 m. The accuracy of measurements is limited by the order of the stone sizes found in the groynes. Since these stones typically have a size in the order of decimeters, the error in the heights will not be far less than 0.5 m anyway. Besides this, the height of each groyne varies along its crest, making it more difficult to find one representative crest height for the whole groyne. Since the errors in the crest height do not influence the amount of time the groynes are submerged in the model computation, the influence on the tracer nourishment is negligible.

3.2.4 Hydraulic boundary conditions

One boundary condition at the upstream boundary and one at the downstream boundary is needed. A discharge is prescribed at the upstream boundary and a discharge related water level is chosen at the downstream boundary. The discharge at the upstream boundary is only released in the summerbed, to prevent unrealistic flows through the winterbed. At the downstream boundary the water level is prescribed along the whole downstream end of the grid. For every constant discharge a fixed water level is set according to the Q-H relationship for this part of the river.

3.2.5 Morphological boundary condition

One morphological boundary condition at the upstream boundary is needed for this model. This boundary is represented as a fixed bed level. Artificial disturbances will travel downstream from the upstream boundary. That is why a rectangular virtual extension to the grid of 5km has been build, upstream of the upstream boundary. Figure 3.4 shows this virtual extension, the extension is the green part of the grid in this picture.

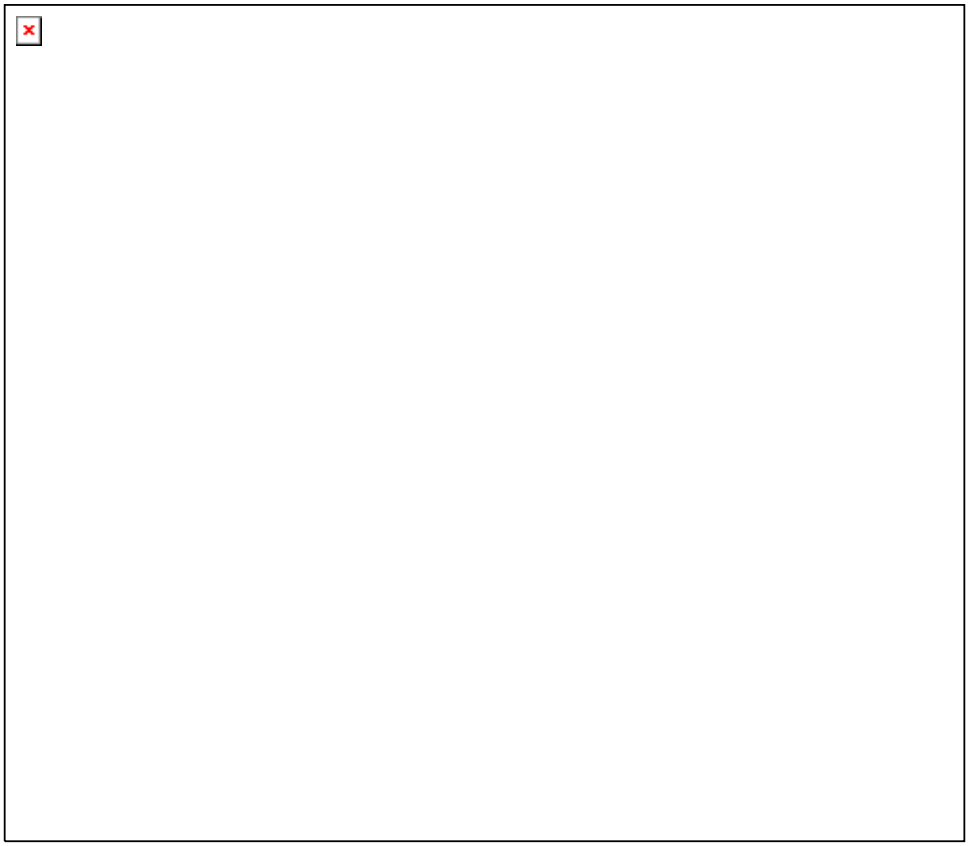

Figure 3.4: rectangular virtual extension to grid

The celerity of bed perturbations, for a quasi-steady approximation, states:

$$c_b = \frac{bs}{Fr^2(1-\varepsilon)h}.$$

For the modeled river reach, this celerity is around 1.5 km/year. This means that bed perturbations travel into the 'real' model, when considering the simulation period of 5 year (see also 3.2.15). This should be taken into consideration for this research. A larger virtual grid could resolve this, but demands more computational effort. Another way to represent the morphological boundary is to prescribe the sediment transport time series or to prescribe the bed level time series. This is more work, and since the focus of this study is exploratory and qualitative, this will not provide more information.

3.2.6 Initial sediment conditions

When modeling with graded sediment, a discrete number of sediment fractions, with a characteristic sediment diameter, must be chosen. The initial sediment conditions are prescribed as the mass of each sediment fraction present in the bottom for each grid cell, together with the initial bed level. This initial bed level is constructed from the topographic data, as described in 3.2.2. A number of sediment transport algorithms of the model are calculated for each sediment fraction separately.

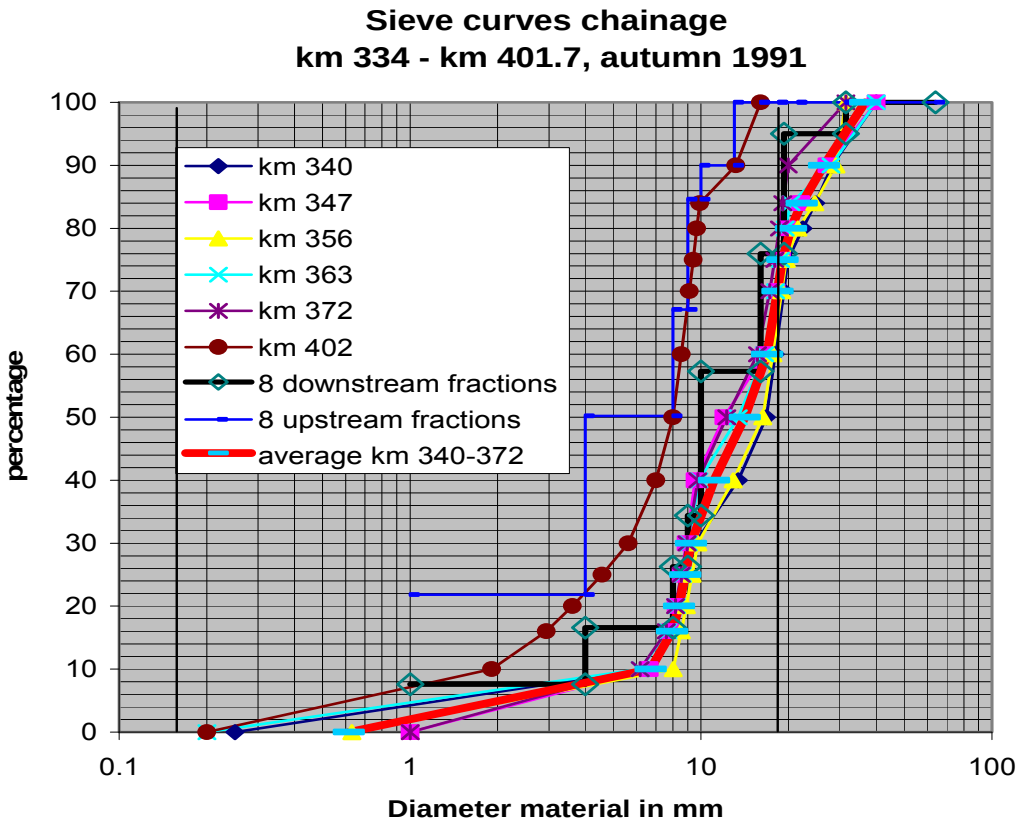

Figure 3.5: division of sieve curves in discrete classes

Figure 3.5 shows the constructed classes for a discrete number of sediment fractions, for both the upstream part and the downstream part of the river. The number of fractions and their borders are uniform for the whole model, only the percentages of the material present in these fractions varies. Having a distribution of percentages of the sediment fractions at two locations, the percentages along the whole river can be interpolated linearly from this data.

The borders (maximum and minimum grain size) of each fraction are chosen according to the sieve curve data, and the percentages present in each fraction are dependent on this choice.

For each sediment fraction, the characteristic diameter is calculated according to the following relationship:

$$D_i = \sqrt{D_{\min} \bullet D_{\max}}$$

This characteristic diameter is used for all morphological algorithms in which it is present.

Initially, the sediment fractions per grid cell are assumed fully mixed in the bottom.

3.2.7 Initial hydraulic conditions

The initial water level and the initial velocity field has to be prescribed. These are chosen values from rough estimations, or these are obtained from data from previous simulations. In the first case a spin-up period is needed before morphological calculations are implemented in the computation.

3.2.8 Type of transport

Both bedload and suspended load do occur within the reach of the model, chainage km 336 – 401. According to the BfG (Bundesanstalt für Gewässerkunde), distinction can be made between coarser material (bedload), sand (most bedload, but also some suspended load) and finer materials (suspended load, the type of material is not specified). The finer materials (<0.063 mm) are all washload and hence not important for this project. The BfG itself does not know the division between the types of transport for the sand material exactly, but estimates that material with a diameter of more than 0.1-0.2 mm can be defined as bedload. As can be seen from figure 3.5, there is almost no material smaller than 0.1-0.2 mm present in the data range available. Of course smaller sand can be present occasionally, but the data proofs that for the modeled river reach almost all the sand is bedload. This justifies to model the sand as bedload.

3.2.9 Exclusion of floodplains

From model results it appeared that most of the time there is almost no flow through the winterbed. For a discharge of 2330 m^3/s and a stationary situation, there is hardly any flow through the winterbed. Only at the downstream end of the model a side channel is present, which is visible in the figure below. This side channel is approximately half a kilometre long.

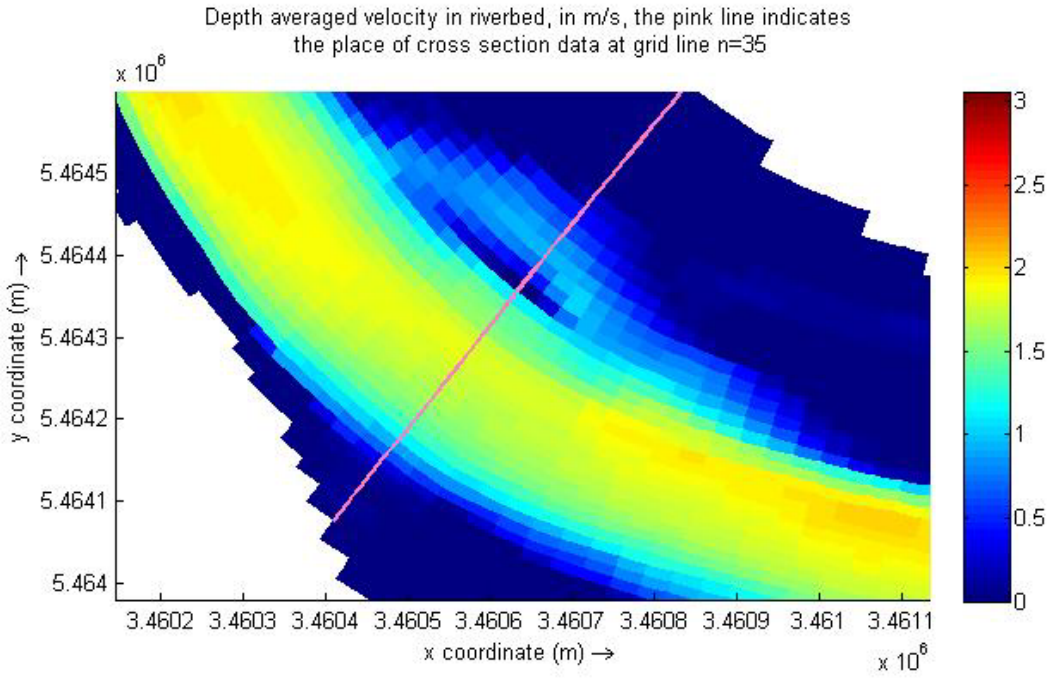

Figure 3.6: side channel at downstream end of model

A cross section at the pink line of figure 3.6 is given below:

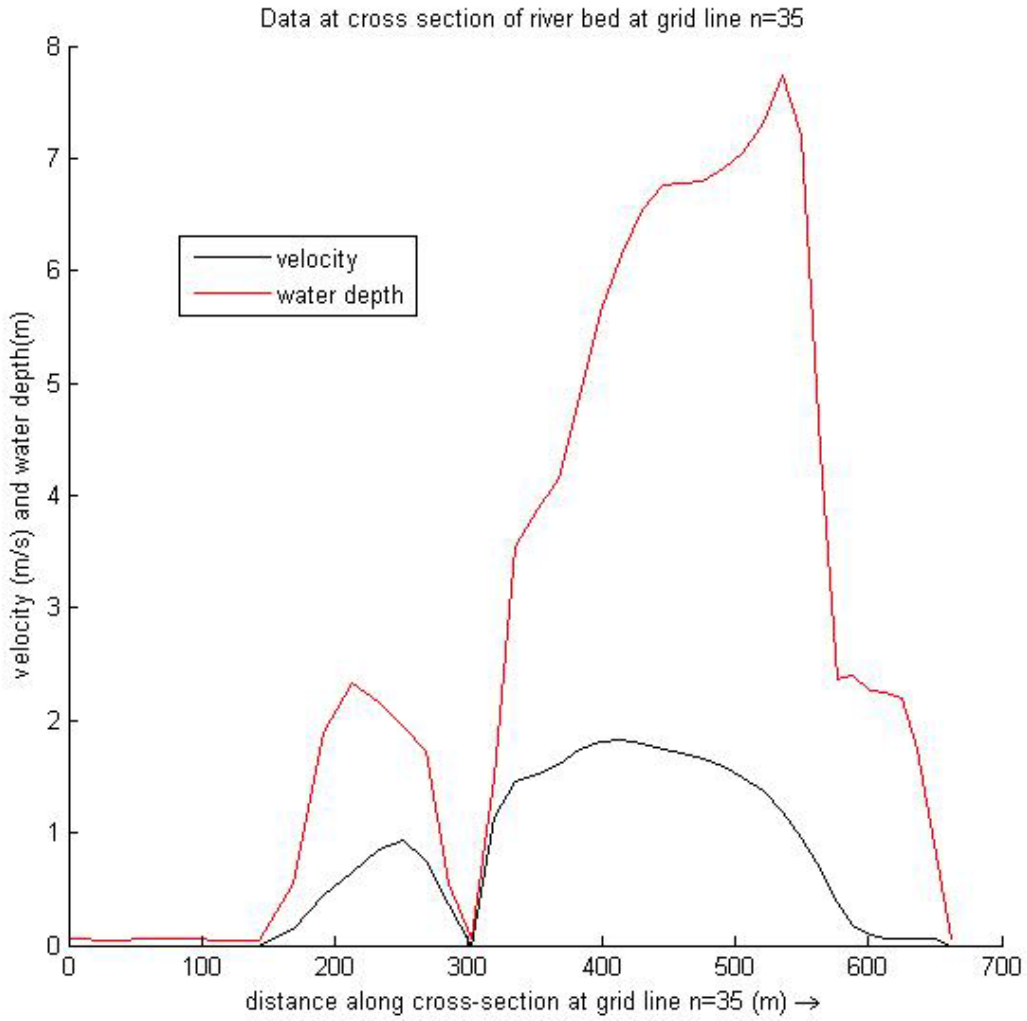

Figure 3.7: velocities and water depth in side channel and summerbed

The side channel is present around 150 to 200 meters along the river. A comparison of the depth averaged velocity and waterdepth in the side channel to those of the complete cross section, shows that the discharge per unit width in the side channel is in the order of 2% of the total discharge per unit width through the cross section. Nonetheless, this side channel can have a significant influence on morphology. However, it is located at the downstream end of the model. Since this exploratory study is about a tracer which is supplied at the upstream end of the model, excluding this side channel at the downstream end would not interfere much with results in the largest part of the model.

At a discharge of 3400 m^3/s, more flow through the winterbed occurs, although most of the discharge still goes through the summerbed. An indication of the difference in velocity with a discharge of 2330 m^3/s is in figure 3.8.

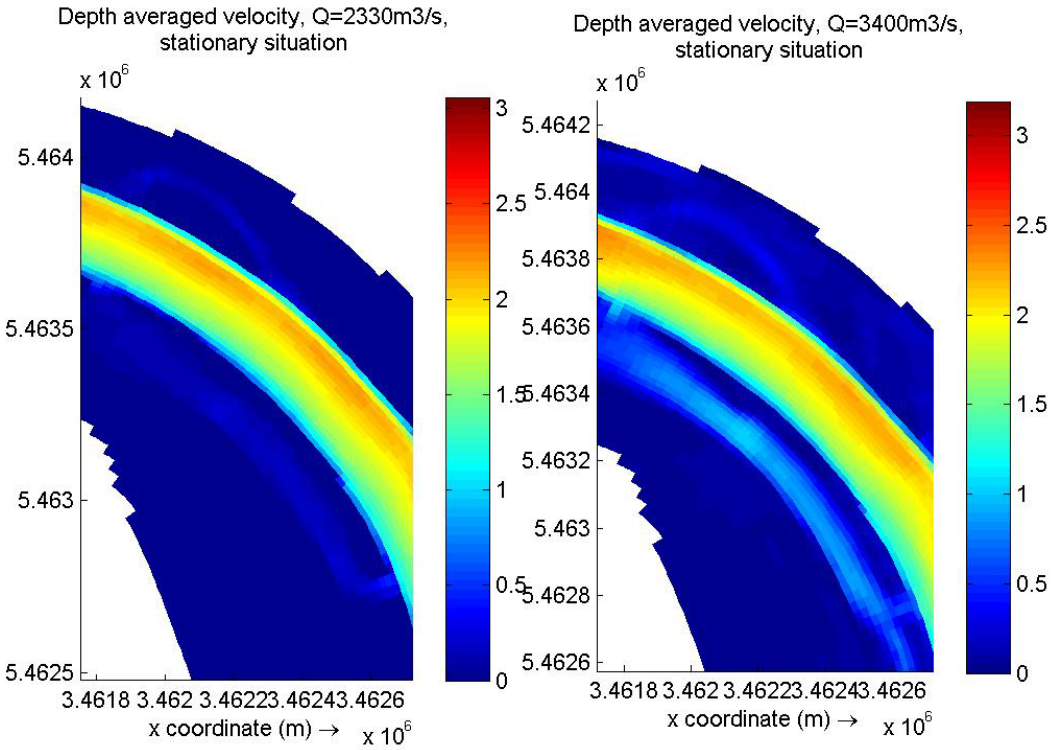

Figure 3.8: velocities is m/s for different discharges

This leads to the decision to exclude the floodplains from the model. Only with the high discharge of Q=3400 m^3/s there is a bit more flow through the floodplains. Because this high discharge occurs for only a few days per year on average, approximately the same behaviour of the tracer nourishment will occur when the floodplains are excluded. The result of the exclusion of the floodplains is a 4 times smaller grid, which leads to a significantly smaller computational effort.

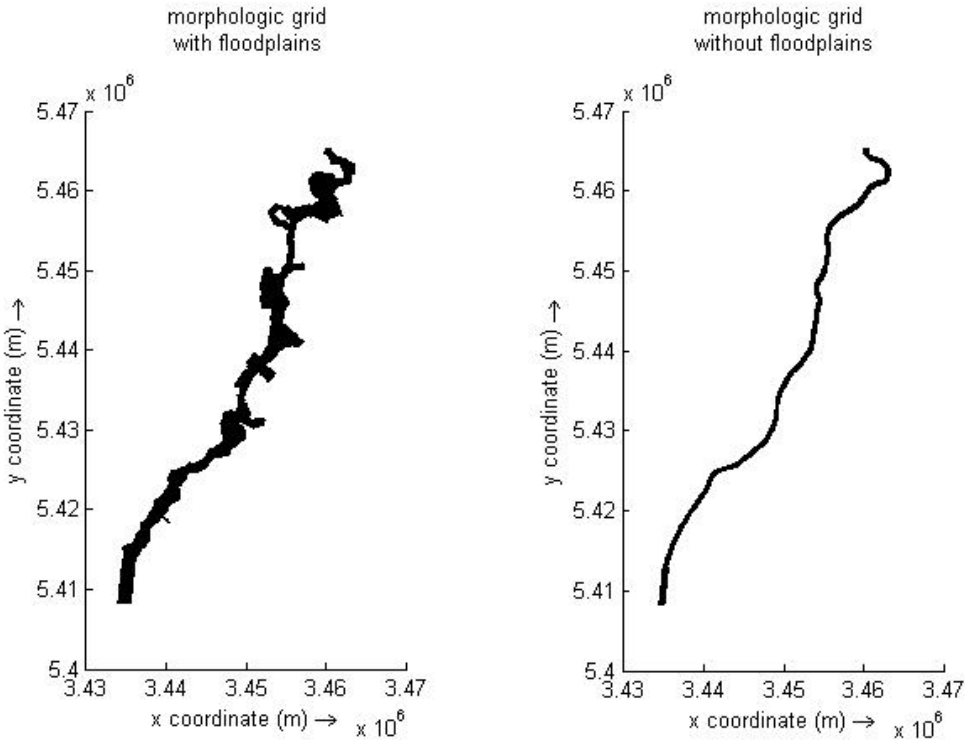

Figure 3.9: morphological grid with and without floodplains

3.2.10 Discharge schematization

Both runs with a constant discharge and with a hydrograph have been done during this project. A run with a hydrograph is a run with a fixed number of different discharges per year, in a specified sequence. This issue is further discussed in chapter 5.

3.2.11 Roughness

The roughness is chosen as a constant in this model, and hence is not affected by morphological change. Information about the determination of the roughness coefficient can be found in section 3.3.1 and chapter 4.

3.2.12 Tracer nourishment

On top of the initial conditions for the original bed, the nourishment of the tracer should be prescribed. This includes the description of the volume, type of nourishment, and the material. This description is given in section 6.4.

3.2.13 Morphological updating

After every computational time step, the topography and sediment composition are updated according to the morphological changes. To reduce computational time, the morphology is speeded up. This is simply done by multiplying erosion and deposition rates by a constant value, resulting in less computational time needed for a certain morphological period. Example: when a period of 5 'morphological' years needs to be modeled and the morphology is speeded up by a factor 5, only 1 year of flow needs to be computed.

3.2.14 Discharge variation along river

During most discharges, the variation along the river due to contributions of tributary streams is quite small, in the order of 30 m^3/s. The discharge data from the middle of the model (station Maxau, around chainage km 362) is used for set-up of this model. Only during flood peaks the variation is significantly larger, in the order of 250 m^3/s.

3.2.15 Modeling period

The interesting modeling period is of course the period in which movement of the tracer is recorded, from December 1996 to 2001. A spin-up period is needed before the modeling of the tracer starts, for adjustment towards a proper bed level and bed composition, corresponding to the forcing of the model. More information about this spin-up period is given in chapter 6 and 7.

3.2.16 Runtime

In appendix IV a table is given with runtime indications of several simulations done in this project.

3.3 Physical and numerical parameters

3.3.1 Roughness

For the roughness spatially varied Nikuradse values are chosen, resulting in the following values:

- Trees: Nikuradse = 10 m
- Grass: Nikuradse = 0.4 m
- Ponds and channels: Nikuradse = around the same as summerbed = 0.035 m

The same roughness coefficients are used for both the u and v flow velocity component. The roughness data are gained by hydraulic calibration, which is described in chapter 4.

3.3.2 Other constant physical parameters

The values of other constant physical parameters can be found in the list of symbols in appendix III.

3.3.3 Constraints for the flow

The Courant number for the flow must be low enough, to prevent instabilities and loss of information. The Courant number for the flow is written as:

$Courant = c_w \Delta t / \Delta x$,

in which: $c_w = \sqrt{gh}$

The numerical scheme used in this model is unconditionally stable for open surface waves. Above a value of approximately 10, the model is still stable, but errors in the water level and velocity become less workable.

3.3.4 Constraints for the bed

The Courant number for bed perturbations must be low enough, to prevent instabilities and loss of information. The Courant number for bed perturbations is written as:

$Courant = c_b \Delta t / \Delta x$,

in which: $c_b =$ celerity of bed perturbations in m/s

The numerical scheme used is implicit, nonetheless this Courant number should be smaller than 1.

4 Hydraulic calibration

4.1 Calibration setup

Nikuradse roughness values are calibrated with the help of four different discharges. For every discharge a stationary situation is computed, after which the results are compared to water level measurements from a number of stations along the river. The values for the spatially varying Nikuradse roughness are defined in section 3.3.1.

The downstream boundary is a fixed water level. This boundary is located at chainage kilometre 400,8 of the Rhine river. In table 4.1, the water levels at the downstream boundary are given for the occurring discharge at Maxau (chainage km 362).

discharge at Maxau	water level at downstream boundary
838 m^3/s	91.121 m
1200 m^3/s	92.21 m
1700 m^3/s	93.23 m
2330 m^3/s	94.530 m

Table 4.1: Q-H relation for discharge at Maxau and water level at downstream boundary

4.2 Results

The blue points in the figures are measurements, the red lines are model results.

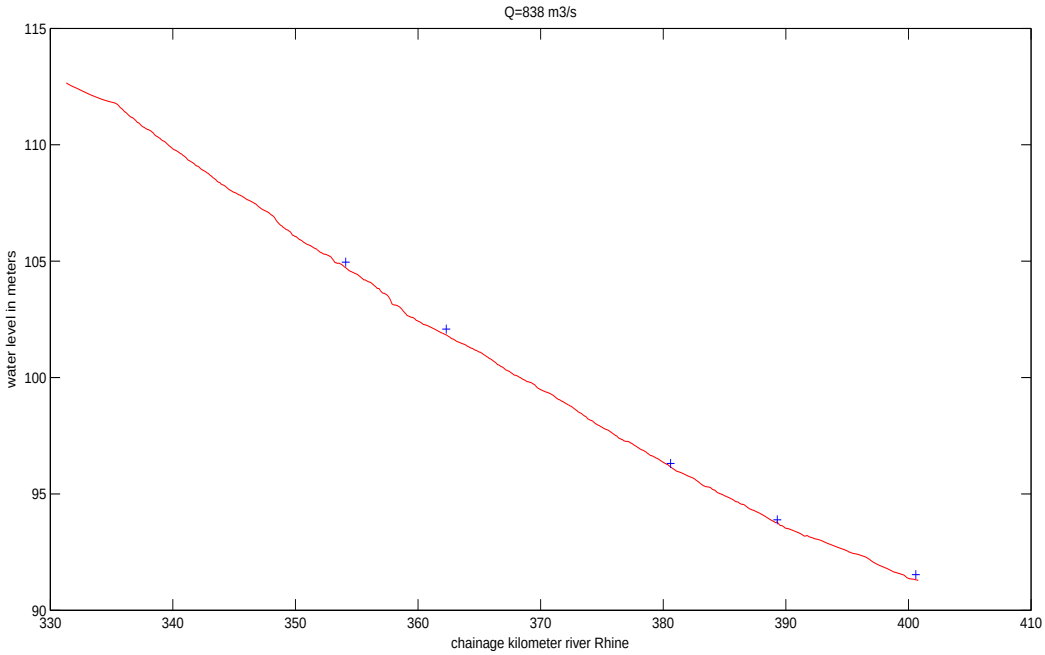

Figure 4.1: results at a discharge of 838 cubic meters per second

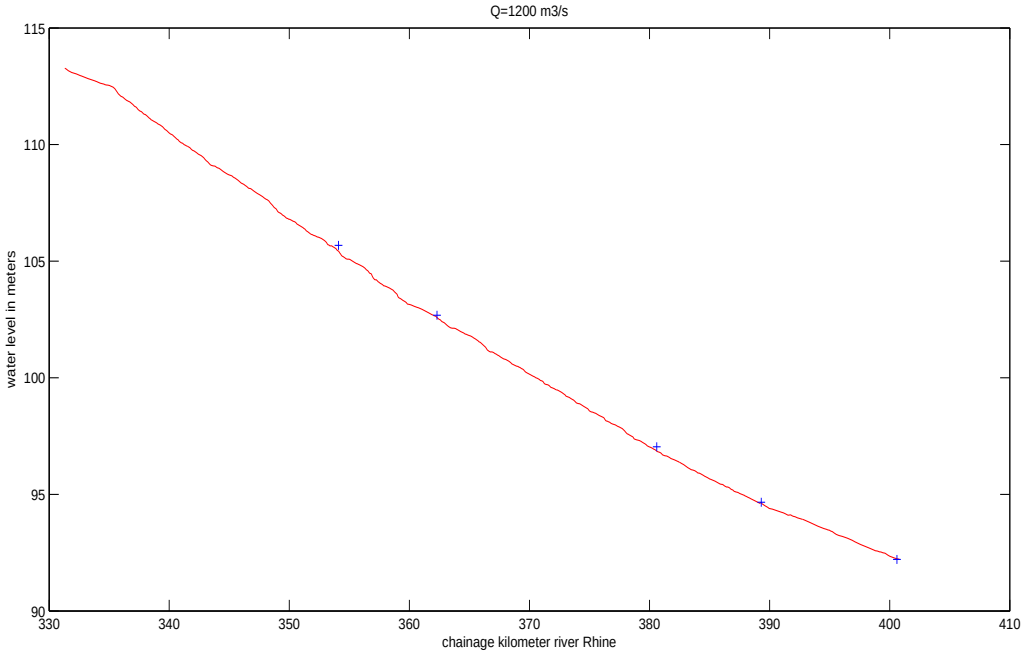

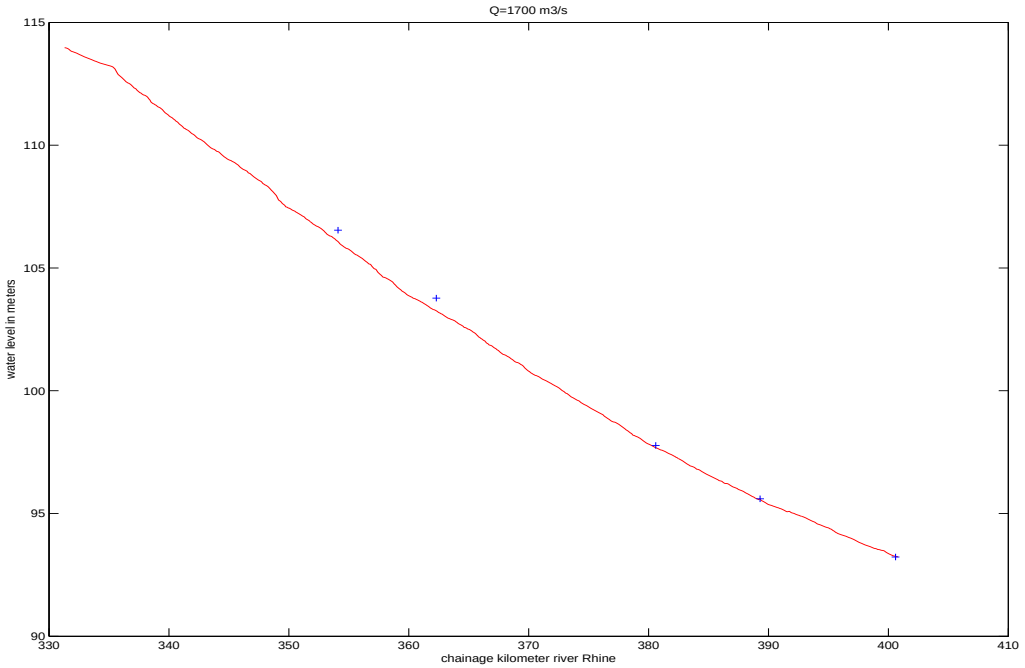

Figure 4.2 and 4.3: results at a discharge of 1200 and 1700 cubic meters per second

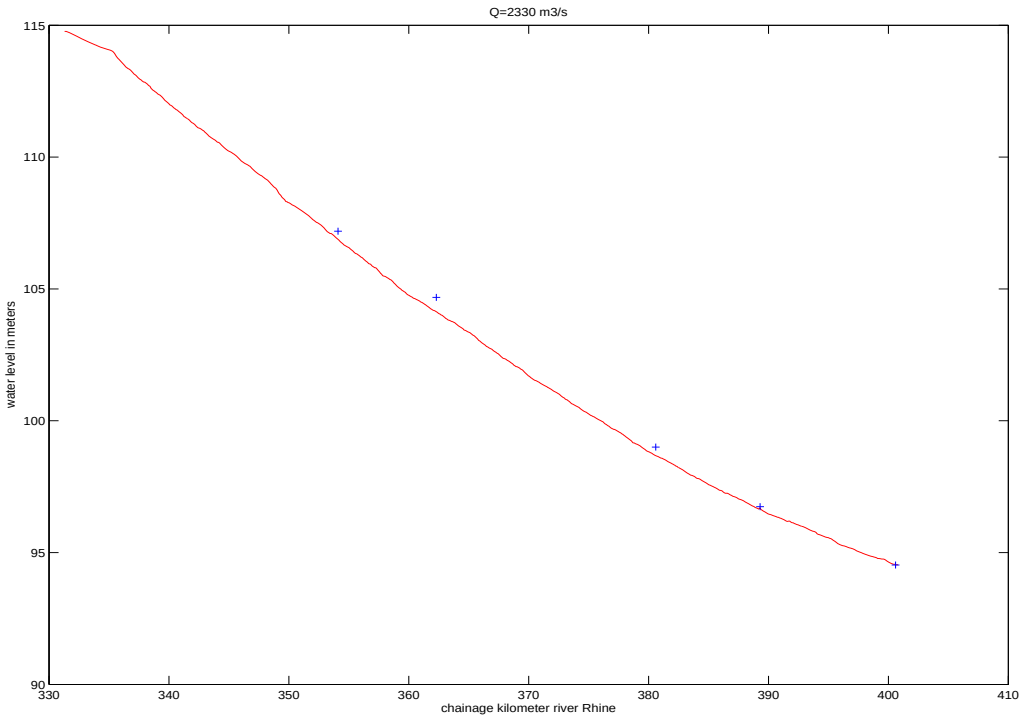

Figure 4.4: results at a discharge of 2330 cubic meters per second

The error found in the water levels is never more than 0.4m, this is around 7% of the water depth. This does not have an significant impact on morphology. Since the primary purpose of this model is investigation in morphological parameters, the error of 0.4m is acceptable for this study. The conclusion is that the roughness values defined in 3.3.1 will be used for further computations.

5 Discharge schematization

5.1 Constant discharge and hydrograph

Morphological runs are made with a constant discharges or with a hydrograph. In this case a hydrograph is a sequence of a limited number of constant discharges, with the total duration of one year. When calculating with a hydrograph, a number of different discharge levels are chosen from appropriate time series. The hydrograph is constructed from these different levels. For every computational year, this constructed hydrograph is used for computation. To calculate with detailed time series in the model, could raise problems in combination with speeding up morphology as described in 3.2.13, during a flood peak.

5.2 Choice of discharge levels for hydrograph

The period of the time series used to choose the discharge levels is from 01-01-1993 to 31-12-2004. This is the time series of the discharge at Maxau, around chainage km 362, which is approximately in the centre of the model. This data covers the period of time over which movement of the tracer was recorded (1996-2001).

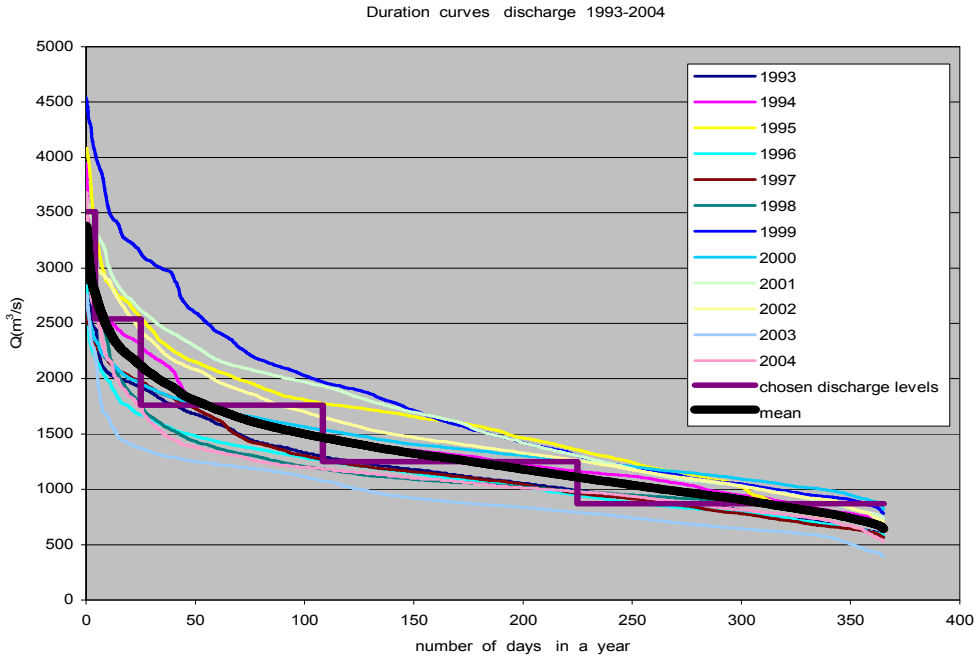

Figure 5.1: discharge duration curves for period 1993-2004

In the above figure the discharge curves for each year of the time series are shown, as well as the mean of all these years. The discharge levels are chosen from these data, together with the duration of these discharge levels. The discharge levels are situated around the mean discharge curve of this period, but also the curves of each separate year should be taken into account in this analysis. The total water volume of

the chosen discharge levels equals the total water volume of the mean discharge curve. In this case 5 different discharge levels are chosen. More levels would result in a computational time which is less workable, and less levels would result in too much loss of detail.

5.3 Construction of hydrograph

With information about the discharge levels and their duration, the hydrograph for the computational model, based on the chosen data, can be constructed.

When constructing the hydrograph, attention must be given to the flood peaks that occur. Flood peaks have a relatively short duration, but their high discharge can be important for the model. During a flood peak coarse material might become mobile, for instance.

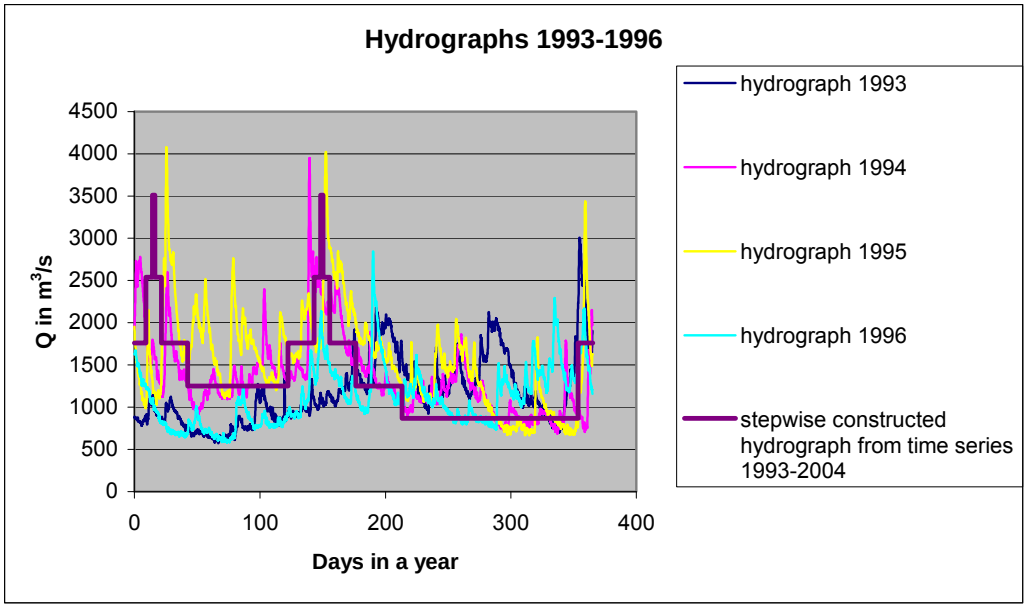

Figure 5.2: comparison between chosen hydrograph for computation and data

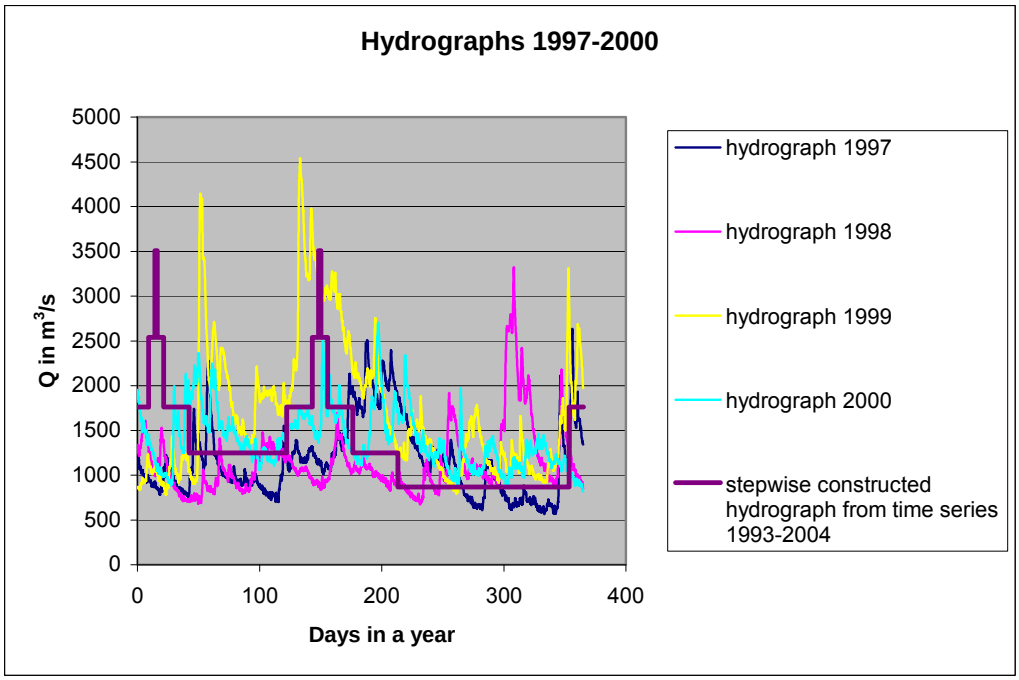

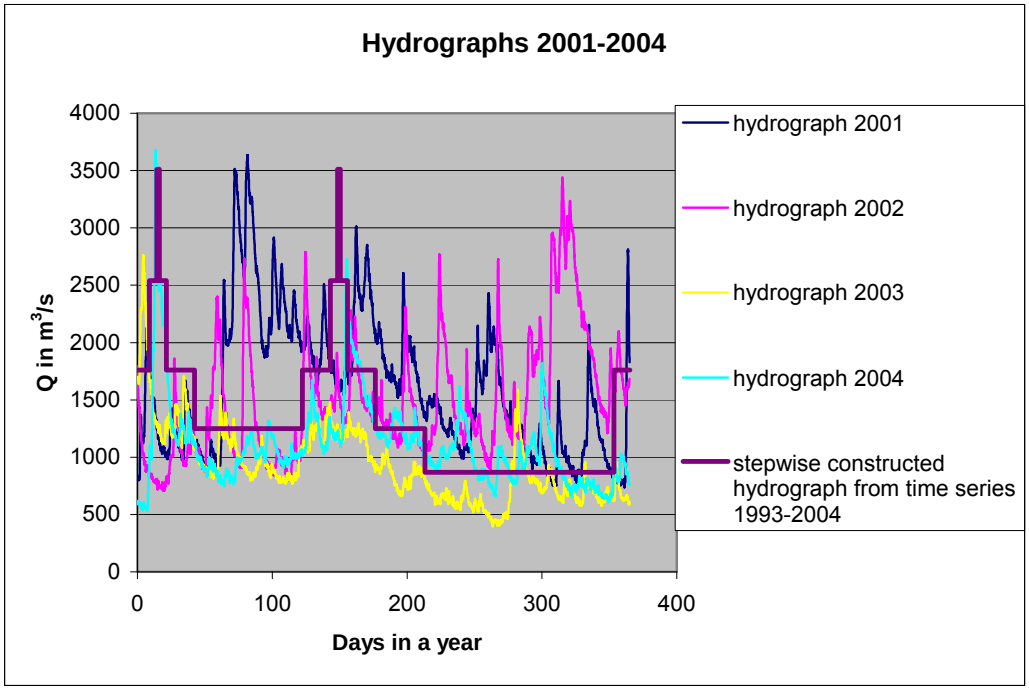

Figure 5.3 and 5.4: comparison between chosen hydrograph for computation and data

From the above figures it appears that most years have multiple flood peaks, mostly occurring in winter or in spring. That is why two flood peaks, one in January and one in May, are chosen in this constructed hydrograph.

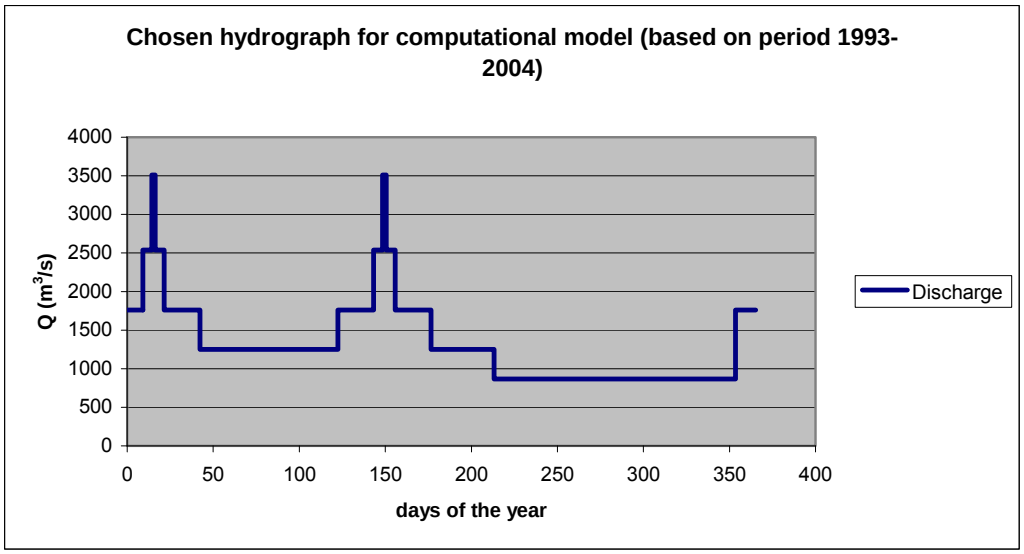

Figure 5.5: chosen hydrograph for computation

The chosen hydrograph is of course just one of the many possible options. It is dependent on the chosen time series used in construction, the choice of the discharge levels, their duration, the number of discharges present in the hydrograph, and the sequence of the discharge levels in the hydrograph.

6 Morphological set-up

6.1 Morphological set-up of 1D behaviour

6.1.1 Sediment transport formula

The coefficients of the sediment transport formula are roughly set with the help of data from the BfG in Germany (Bundesanstalt für Gewässerkunde). Morphological runs with a representative constant discharge are made with different combinations of coefficients, to see which combination represents the sediment transport best. The representative constant discharge should produce the measured yearly transport.

6.1.1.1 Representative discharge

With the knowledge of the total yearly transport along the section of the river where the model is located, the representative discharge can be calculated. In Appendix I data are given about the total yearly transport present between chainage km 325 - 625. With the help of other data from the BfG, discharge-transport relations for several points along the river can be constructed, which are shown in the graphs of figures 6.1 to 6.3:

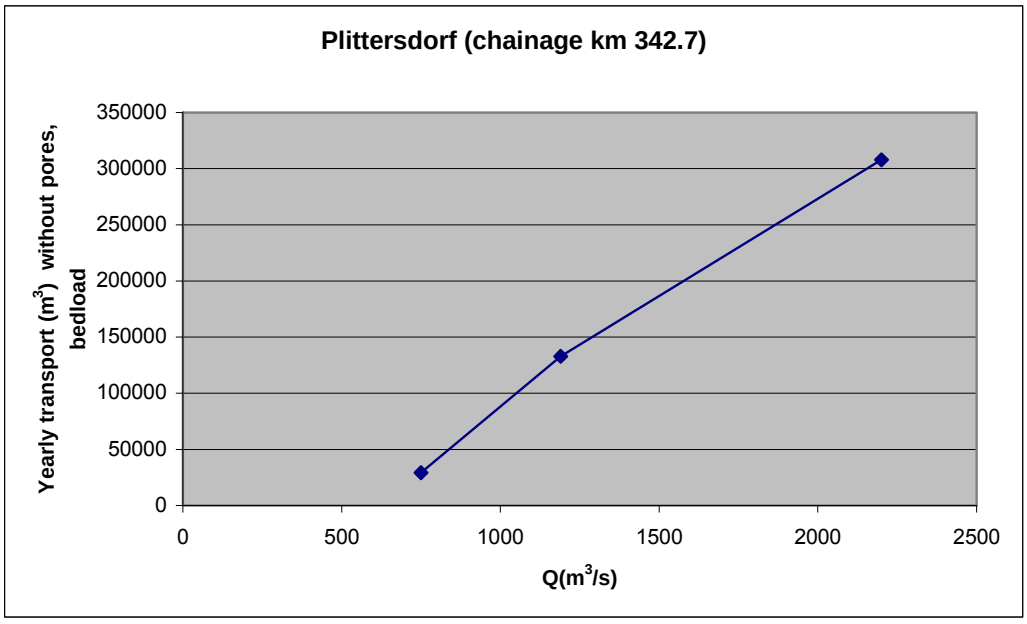

Figure 6.1: yearly transport at Plittersdorf

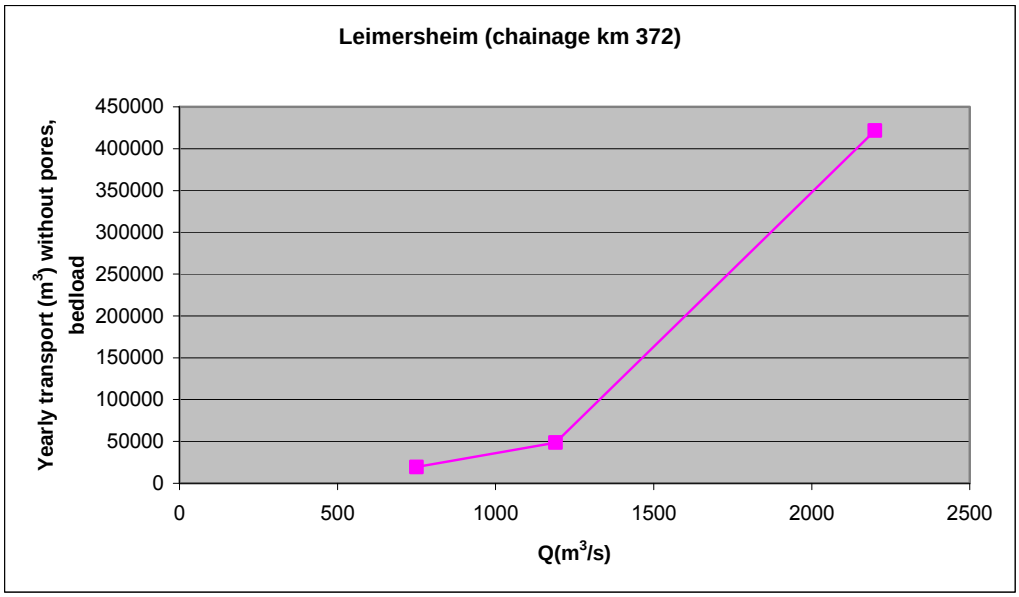

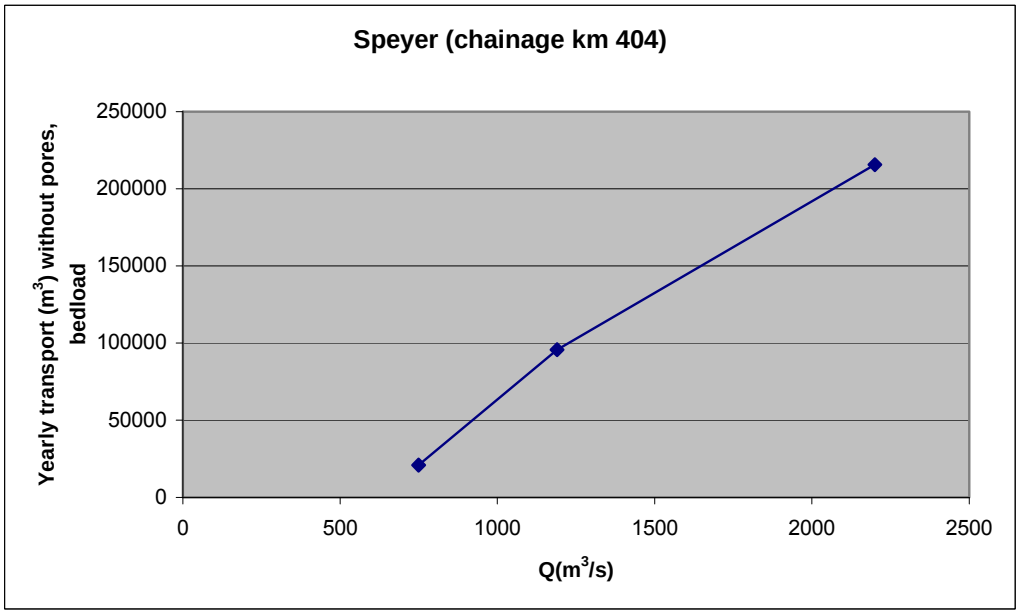

Figure 6.2 and 6.3: yearly transport at Leimersheim and Speyer

In the above graphs the data points represent an averaging over 3 samples, hence the averaging is done over a rather limited data range. When the data of the above graphs are averaged over the 3 locations, and compared with the data from Appendix I, it appears that the representative discharge is around 2000 m^3/s.

6.1.1.2 Total amount of sediment transport summed across summerbed.

The transport is bedload, and without pores.

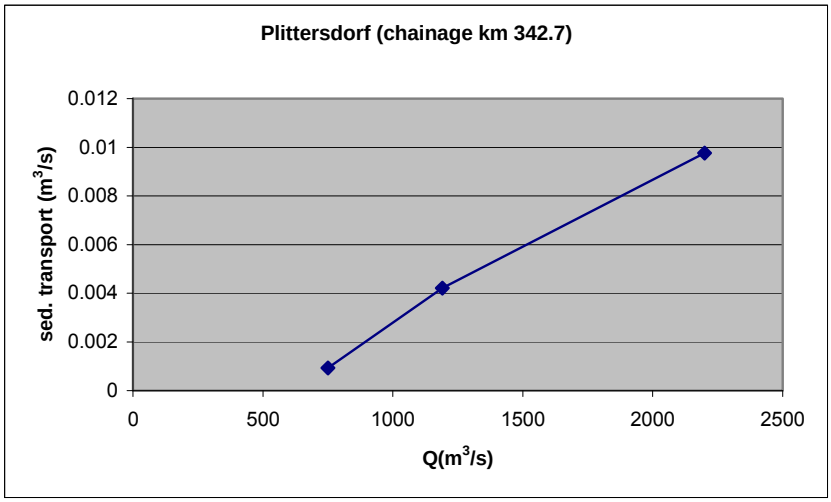

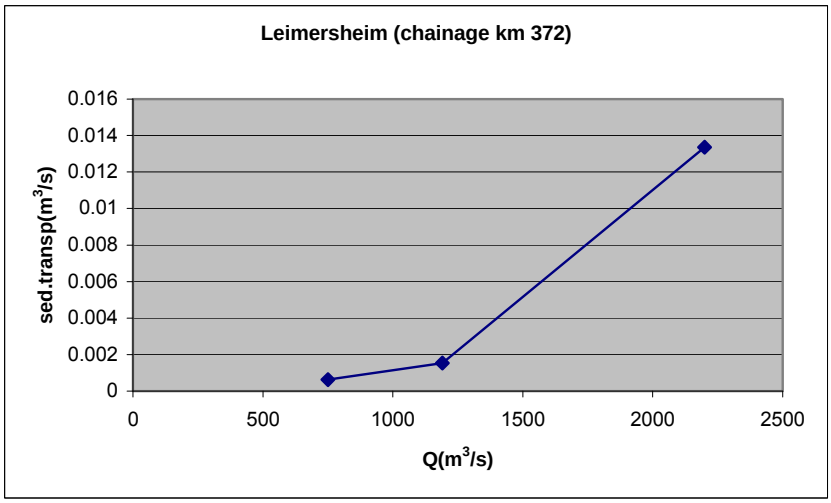

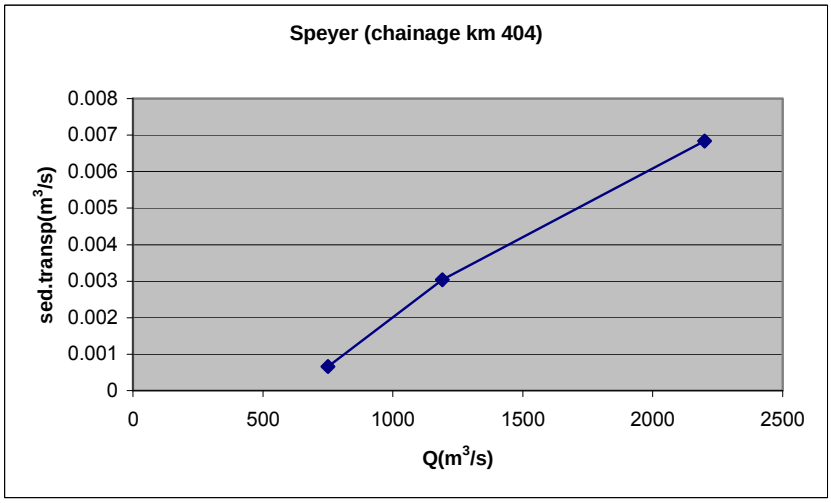

Figure 6.4, 6.5 and 6.6: sediment transport at Plittersdorf, Leimersheim and Speyer

When averaging over the above 3 locations, the sediment transport occurring at the representative discharge is around 0.0075 m^3/s.

6.1.1.3 Runs with representative discharge to determine coefficients

Several coefficients of the sediment transport formula are varied in model runs with the representative discharge, to see the effect on the summerbed averaged sediment transport along the river, estimated in 6.1.1.2. The combination of coefficients which represent this sediment transport approximately correctly is:

coefficient	value
α	2.5
μ (ripple factor)	1
θ_{cr} (critical Shields value)	0.05
c	1.5

Table 6.1: calibrated coefficients of sediment transport formula

Below is the sediment transport formula (see also section 3.1.2.1) in which the above coefficients are implemented.

$$q_{s,i} = \alpha D_i \sqrt{\Delta g D_i} \left(\mu \theta_i - \xi \theta_{cr} \right)^c \; p_{i,a}$$

6.1.2 Initial bed composition

The interesting modeling period, is the period in which the tracer is supplied and recorded. The nourishment of the tracer was done in December 1996 from chainage km 336.2 - 337, unfortunately data about bed composition are only available at limited moments in time. Before the tracer nourishment is modeled, a morphological spin-up period is needed, as is stated in 3.2.15. This spin-up period will shift the start time of the simulation from December 1996 to an earlier date. This is why the bed composition data of the autumn of 1991 is used for the initial bed composition of the model. The schematization of the 1991 bed composition data into 8 discrete fractions is shown below. The details of this schematization and further implementation in the model were already discussed in section 3.2.6.

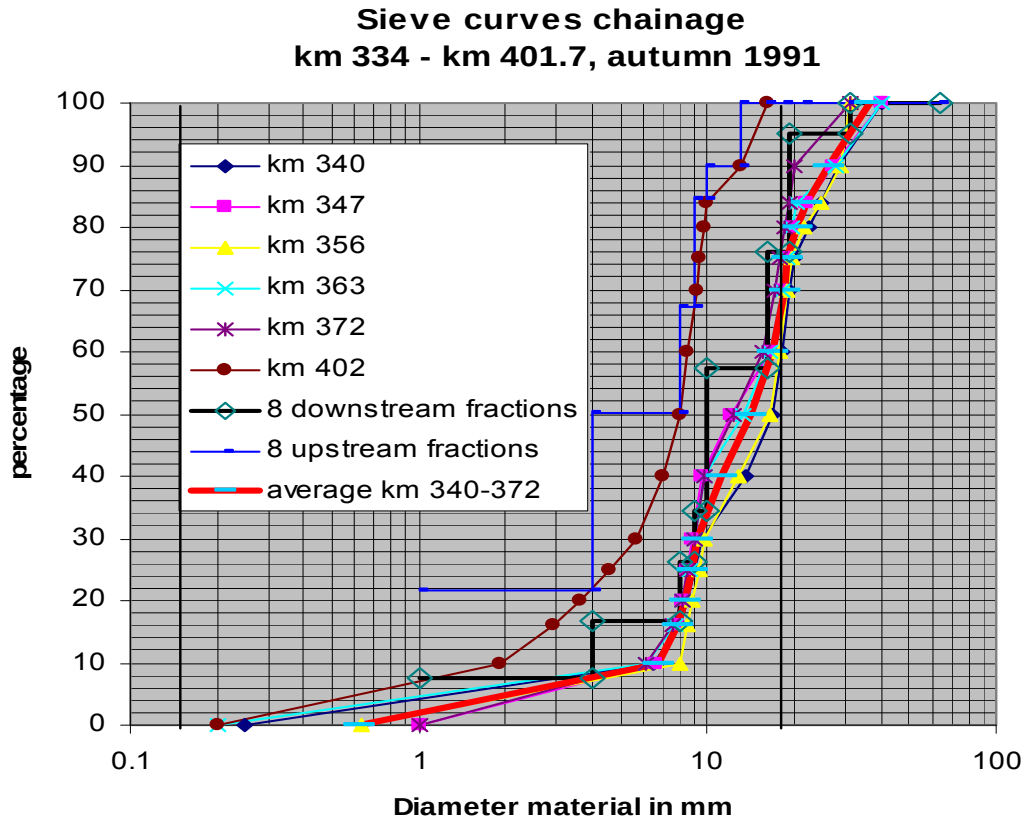

Figure 6.7: sieve curve data used for initial morphological conditions

The change of bed composition in time can be significant, as can be seen in the graphs below:

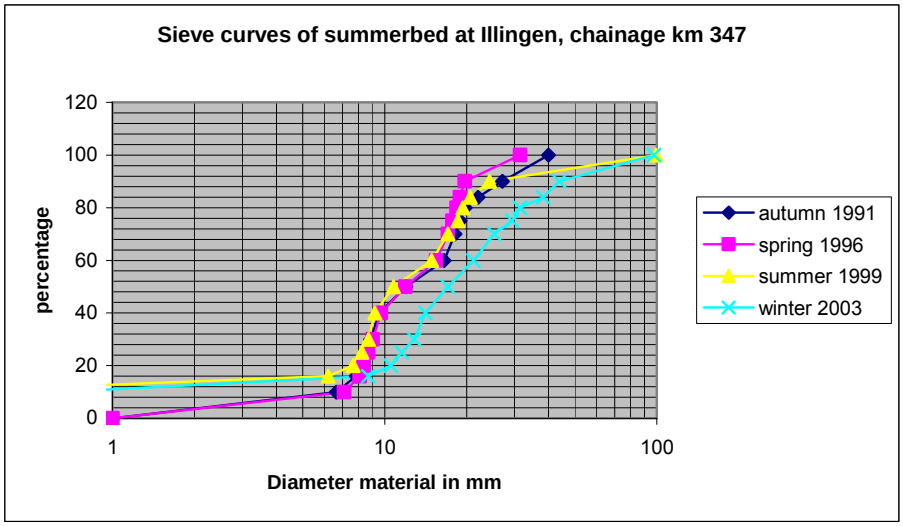

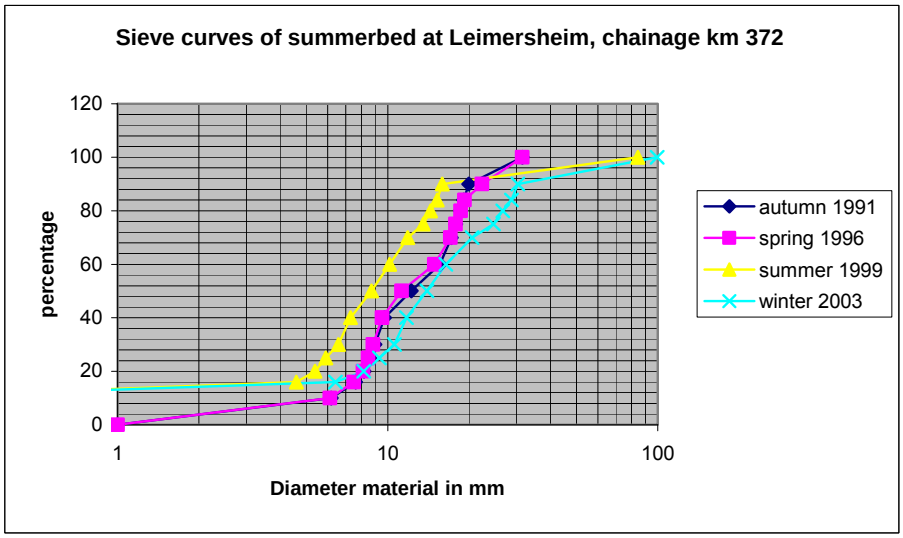

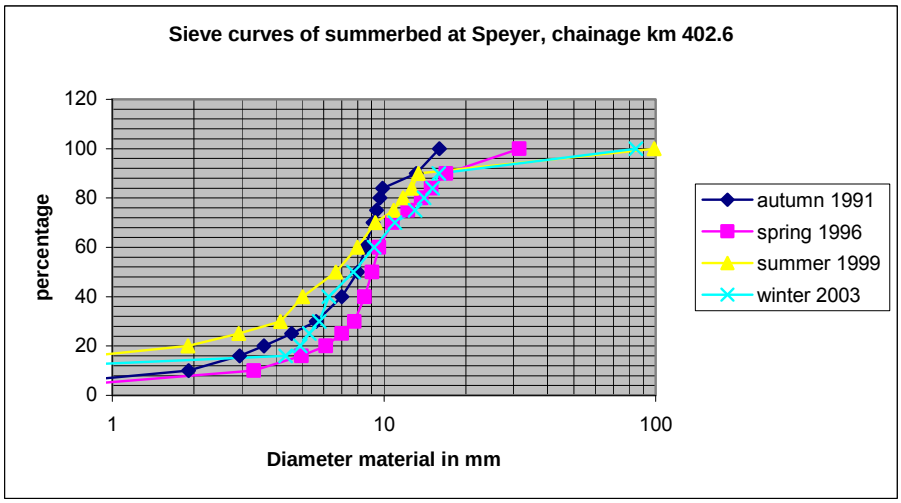

Figure 6.8, 6.9 and 6.10: variation in bed composition

The difference between the bed composition of spring 1996 and autumn 1991 appears to be insignificant for the stations at Illingen and Leimersheim, but for the station of Speyer this is not the case.

The bed composition of spring 1996 might have been a better choice for the initial bottom of the model compared to autumn 1991. This date is closer to the date on which the tracer is nourished. However, with a large spin-up period the start time of the simulation can be closer to autumn 1991 than spring 1996. In a later stage of this project, this did not appear to be the case.

The data shows that there is quite some difference in the bed composition in time, changing the initial bed composition is an interesting case study.

6.2 Morphological set-up of 2D behaviour

As stated in section 3.1.2.3, an algorithm for the adjustment of the bedload transport vector is needed. This adjustment affects the transverse slope of the river bed. To know how large this slope approximately should be, use is made of data of the BfG.

The sections below present a comparison between data of the BfG and model results from a morphological run (without tracer material) is made. A constant, representative discharge, and the following coefficients regarding the algorithm for the adjustment of the bedload transport vector, are used:

coefficient	value
A_{shld}	**1.5**
B_{shld}	**0.5**
C_{shld}	**0**
D_{shld}	**0**

Table 6.2: coefficients used for equation of Koch and Flokstra (1980) for adjustment of bedload transport vector

In the sections below (6.2.1, 6.2.2 and 6.2.3) each first figure is data from the BfG of 16-06-1993. Each second figure of the sections contains model results, with the above parameters as input. The bed level after 1.25 morphological years is stationary.

From 6.2.1, 6.2.2 and 6.2.3 it appears that the bed levels are approximately correct, but the transverse slopes are not, these slopes seem to be too steep at some places. Since this study is mainly exploratory, no further adjustments are made to the above parameters.

6.2.1 Phillipsburg, chainage km 390

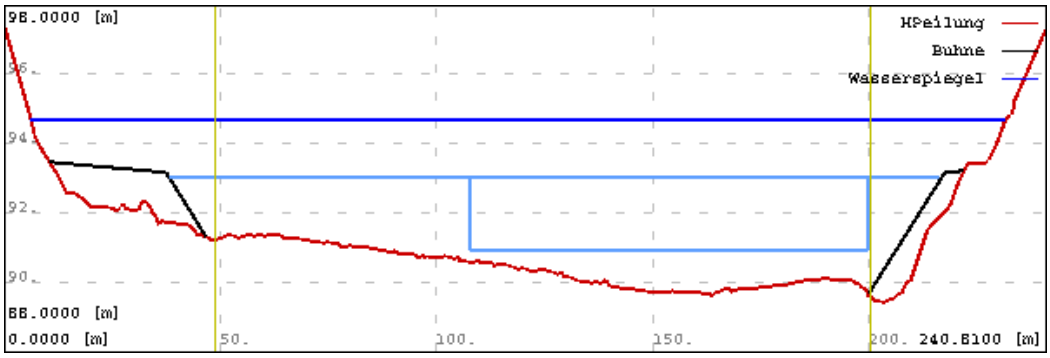

Figure 6.11: cross section at Phillipsburg at 16-06-1993, according to BfG data

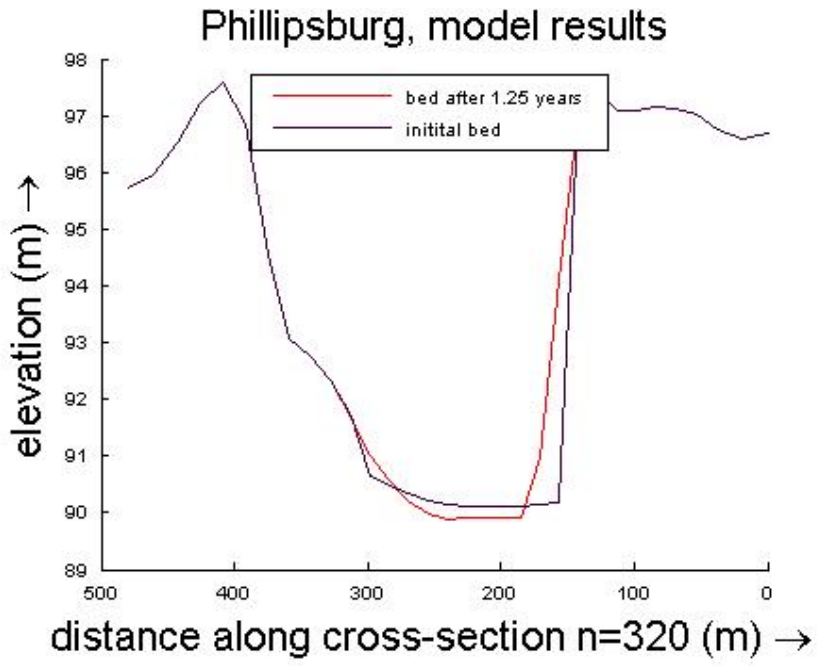

Figure 6.12: model results

6.2.2 Leimersheim, chainage km 371.8

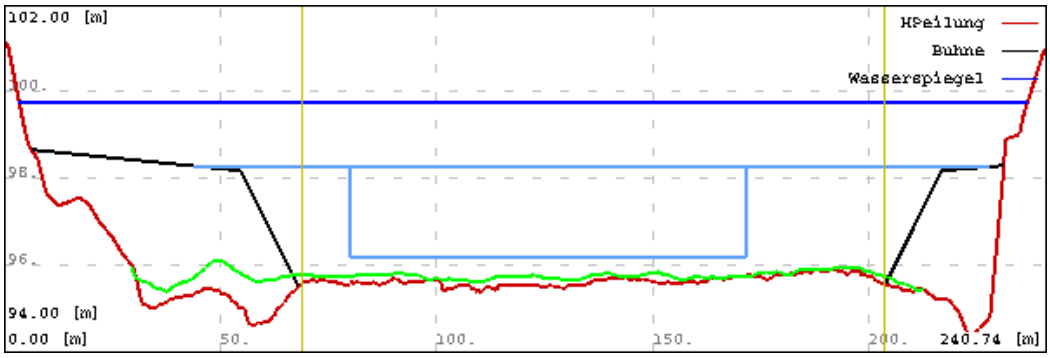

Figure 6.13: cross section at Leimersheim at 16-06-1993, according to BfG data

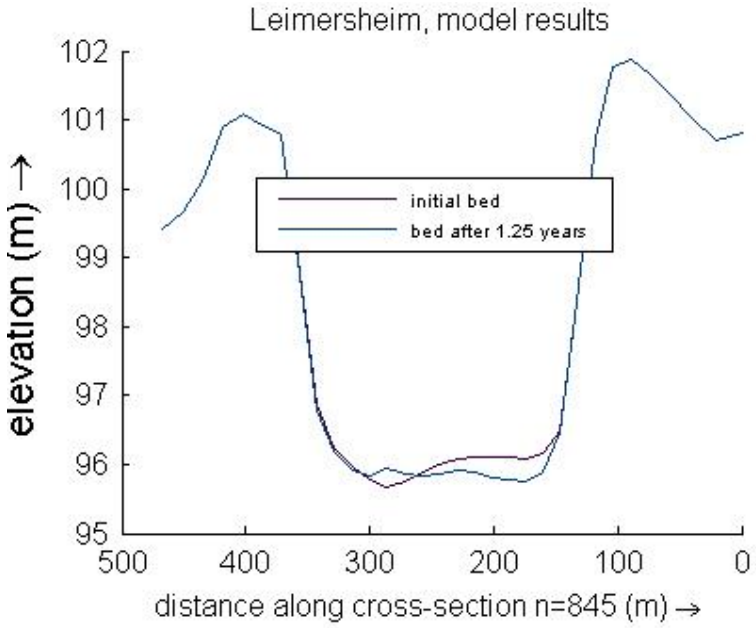

Figure 6.14: model results

6.2.3 Plittersdorf, chainage km 342.7

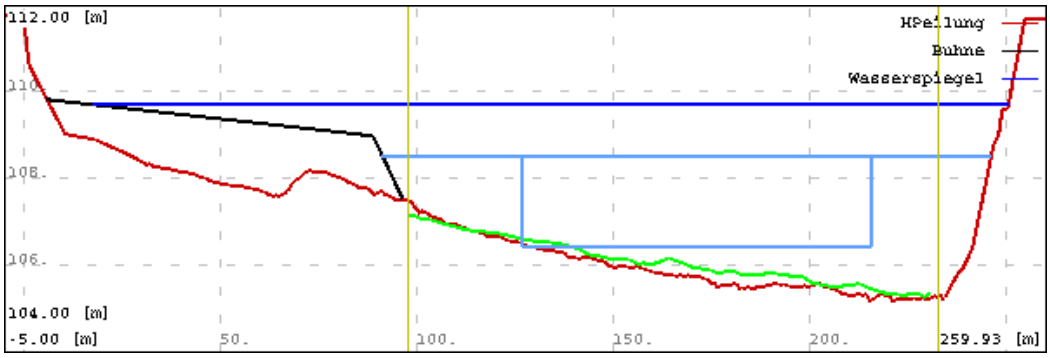

Figure 6.15: cross section at Plittersdorf at 16-06-1993, according to BfG data

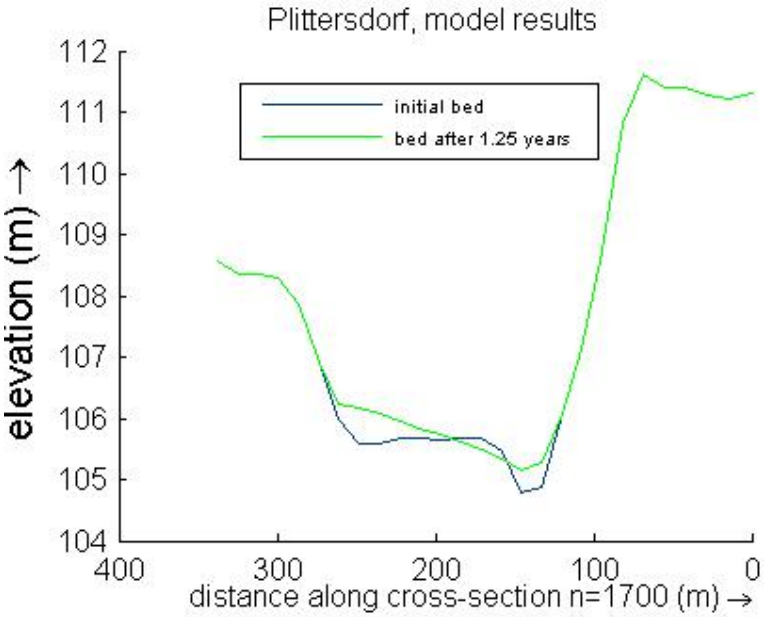

Figure 6.16: model results

6.3 Dredging and nourishment

Apart from the tracer nourishment, there is quite some regular dredging and nourishment done in the region that is modeled. Most of it is done just downstream of the weir at Iffezheim (chainage km 336-337), to compensate bed degradation. A run with the representative discharge and without any dredging and nourishment is done, too see the effects.

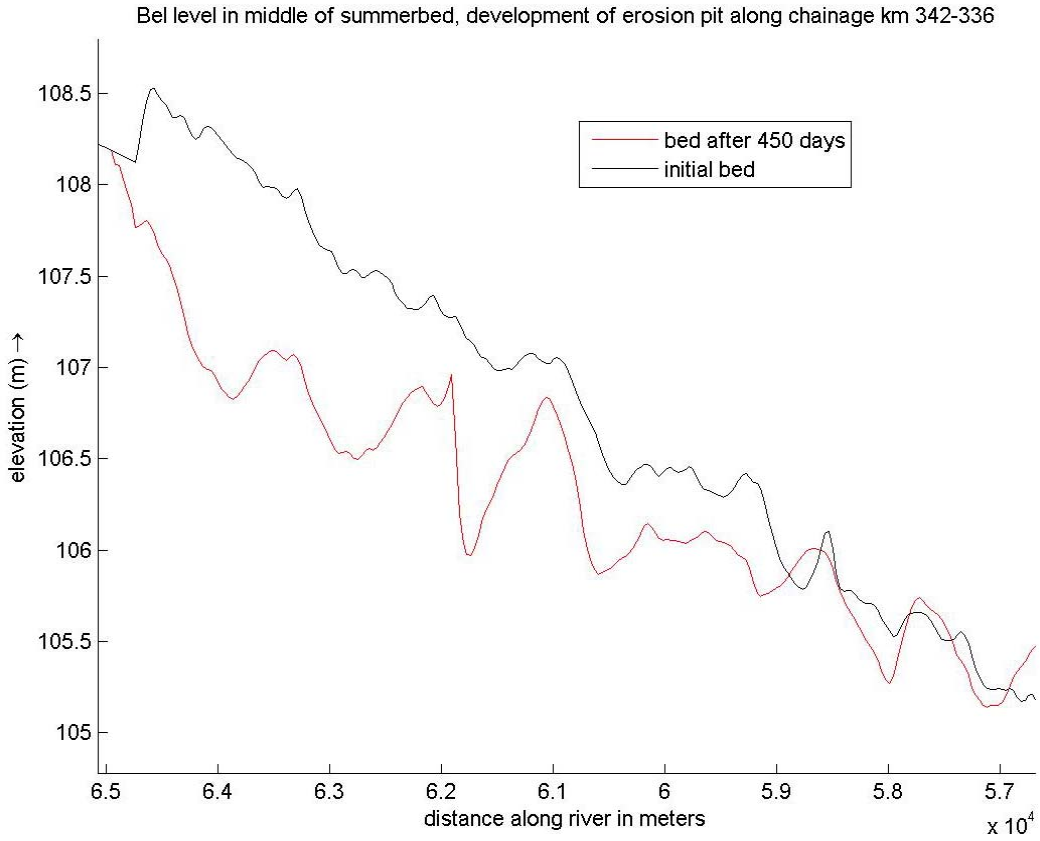

Figure 6.17: growth of erosion area around chainage km 336-342.

The visible erosion area is situated approximately from chainage kilometre 336 to 342, this is the region just downstream of the weir at Iffezheim (located around chainage km 334).

After 450 morphological days there is no excessive sedimentation or erosion in the model, except for the region just downstream of the weir at Iffezheim. This could be expected, since regular nourishments are done in this region. Most of these nourishments are done from chainage km 336.2 to km 336.6. From nourishment data of the period 1991-2005, it appears that yearly a nourishment around 150000 – 200000 m^3 (probably pores included, although the available data are not totally clear about this) is done. The growth of the erosion area is around the same.

In simulations for case studies, different nourishment volumes have been added. In the morphological set-up of the model, no extra nourishment was done.

6.4 Tracer nourishment

The whole tracer is nourished from chainage km 336.2 – 337, across the total width of the summerbed. The tracer has a volume of 17500 m^3 (including pores), unfortunately this is not the same as was supplied in reality (which is around 29000 m^3), due to a calculation error. The tracer has the following composition:

Fraction	*Percentage*
0-4 mm	11.98%
4-16 mm	24.98%
16-31.5 mm	34.98%
31.5-45 mm	18.02%
45-56 mm	10.04%

Table 6.3: gradation of tracer nourishment

The tracer is dumped in 5 discrete classes as described above. For all simulations a spin-up period is used in the computation, before the tracer is dumped. At runs with constant discharges this spin-up period is around 150 days. At runs with a hydrograph this period is longer, around 2 years.

The nourishment has an equal thickness for the whole area where this nourishment is dumped. The dumping is done at once. Dumping at once is an approximation of reality, where the dumping is done in a period of a month. The equal thickness is of the nourishment is also an approximation. In reality the tracer is spread quite equally over the nourishment area, but significant differences between dump thicknesses do exist. In reality the nourishment thickness is around 0.1m-0.3m.

7 Results of case studies

In this chapter case studies of several parameters will be discussed. Runs are made with the representative discharge, 2000 m^3/s, with a higher discharge, 3000 m^3/s and with a hydrograph.

7.1 Reference case

7.1.1 Set-up

The following parameters have been used in the reference case:

Parameter	*value*
Thickness active layer	0.5 m
Number of fractions	10
Thickness underlayer	0.5m
Number of underlayers	2
Discharge	2000 m^3/s
Dredging and nourishment	not implemented
Other parameters	As described in morphological set-up or in list of symbols

Table 7.1: important parameters reference case

This reference case has another number of fractions than used in the morphological set-up. In this set-up only 8 fractions were used. In section 7.2 the difference between calculating with 10 or 8 fractions is discussed.

Other model settings are discussed in chapter 3 and 6.

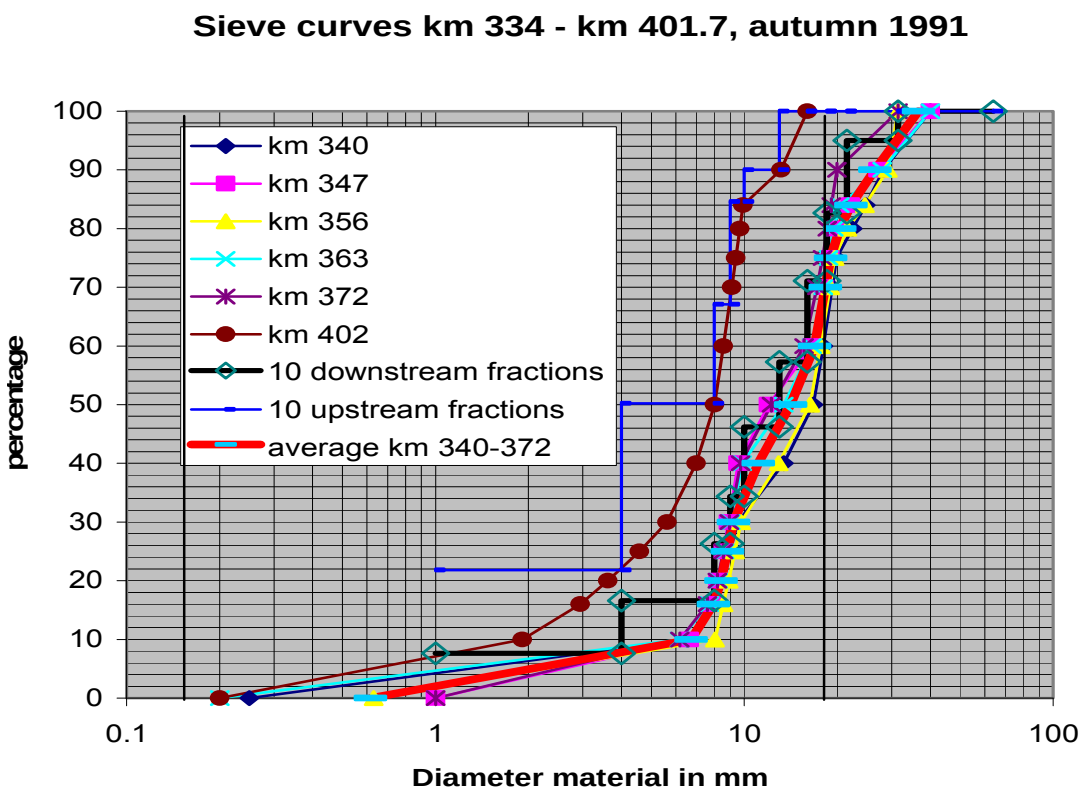

Figure 7.1: division of sieve curve data in 10 discrete fractions

Fraction schematization	sed1	sed2	sed3	sed4	sed5	sed6	sed7	sed8	sed9	sed10
lower (mm) border	2E-04	4	8	9	10	13	16	18.5	22	31.5
upper (mm) border	4	8	9	10	13	16	19	21.5	32	64
occurrence at upstream boundary	0.08	0.09	0.10	0.08	0.12	0.11	0.14	0.12	0.12	0.05
occurrence at downstream boundary	0.22	0.28	0.17	0.18	0.05	0.10	0.00	0.00	0.00	0.00

Table 7.2: fraction schematization

In the model with 10 fractions, the number of fractions in the coarse area of the sieve curve has been increased. This change might have an effect on the sediment transport, since the relation between the diameter of the transported material and the transport is non-linear. The effect on the sediment transport could have consequences for the sediment balance, and hence for the sediment composition.

Considering the number of the lower border of the finest fraction, there is a mistake. Unfortunately this border was set at 0.0002mm, which is far too small. Since the representative diameter of the finest fraction is calculated by $D_i = \sqrt{D_{\min} \bullet D_{\max}}$, this diameter will also be far too small compared with reality, leading to a different behaviour.

Considering the data from figure 7.1, 0.4 mm could for instance be a better choice for the lower border of the finest fraction. The representative diameter D_i turns out to be 1.26 mm for this choice.

In this reference case, the tracer is already supplied. A spin-up period is used of approximately half a morphological year, before the tracer is supplied.

In the following figure a comparison is made between the bed level at 125, 150 and 175 morphological days.

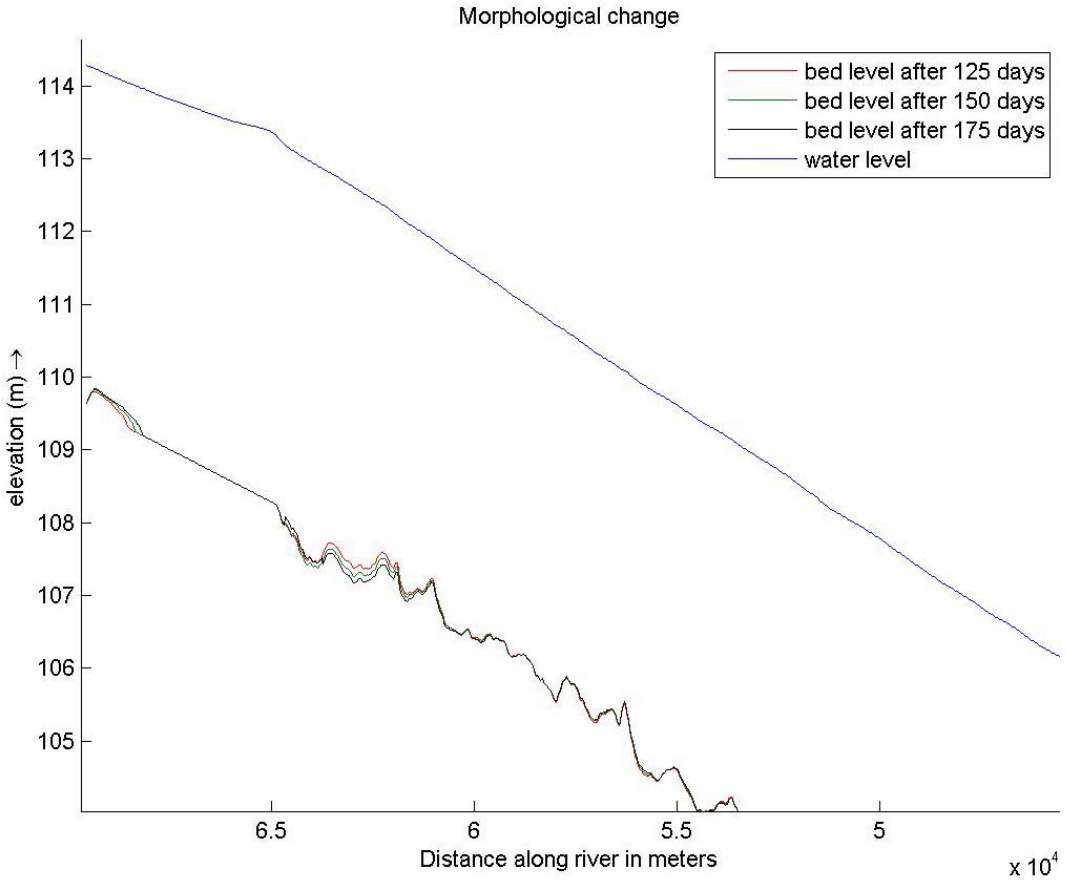

Figure 7.2: bed level change in computation

These are bed levels averaged over the cross direction of the summerbed. The 2D topography is also stationary after 150 morphological days. Stationary does, of course, not mean that the bed does not change, but that large adjustments due to a different initial bottom are not present anymore.

The sediment composition also appeared to be ‘stationary’ after 150 days, at first glance. A more detailed view shows that the composition takes a longer time to adjust. After 150 days the global pattern is already quite stationary, but slight changes still occur after 1 morphological year of computation. After 2 morphological years, the composition has become more or less stationary. Unfortunately this only became clear after all runs with a constant discharge were made.

Initial hydraulic data are gained from a previous run without the implementation of morphology. This means the hydraulic data are already approximately stationary at the start.

7.1.2 Bed level

Because of the not-implemented regular nourishment in the bed degradation zone just downstream the weir at Iffezheim (chainage km 336-342, around 65000 – 60000m in the figure below), a large erosion area starts growing here.

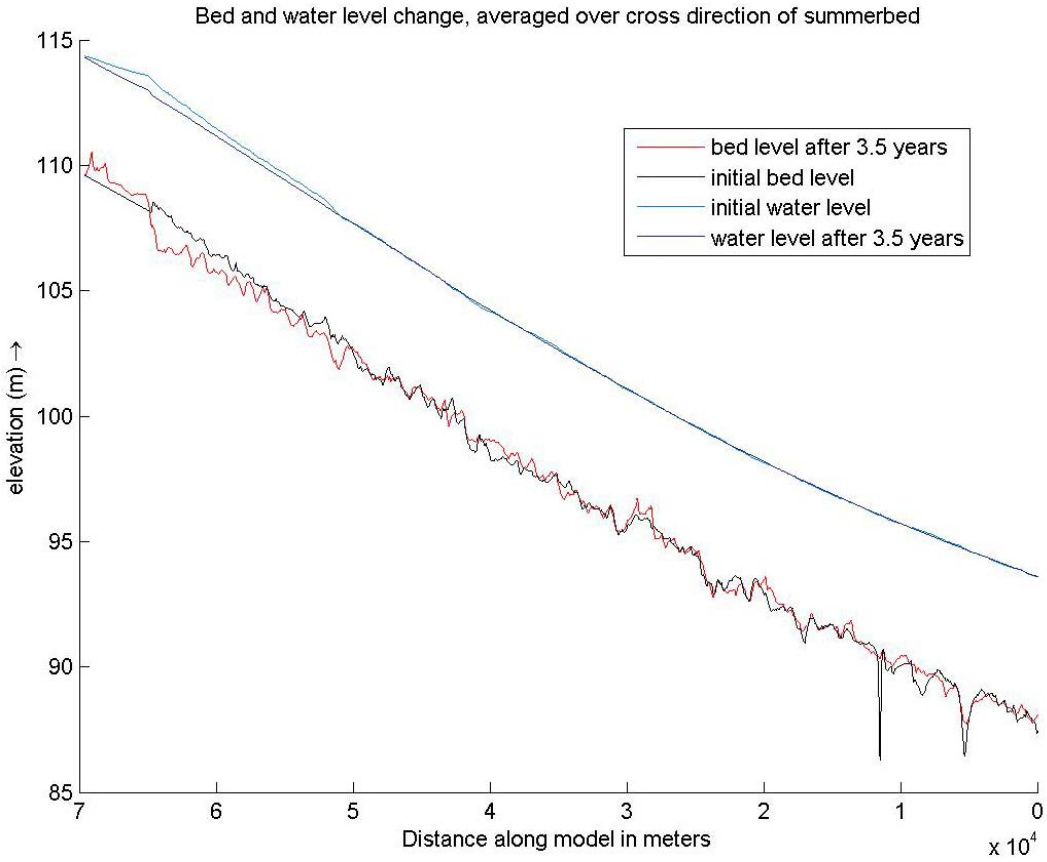

Figure 7.3: Difference between bed and water level after 3.5 morphological years, chainage km ~ 334 to 401

For a 'translation' of the numbers along the x-axis, which are given in meters in the figures, to a corresponding chainage kilometer, a table is given below.

Distance along model on the x-axis, in meters	*Corresponding chainage kilometer*
69500	331.3
0	400.8

Table 7.3: comparison between units on figure's horizontal axis and chainage kilometres

The erosion area has consequences for the mobility of fractions, which has to be taken into account during analysis.

Just downstream the upstream boundary (around 70000-65000m in the figure), in the virtual extension of the model, sediment deposition is found. This is the consequence of the fixed bed level at the upstream boundary. To keep the bed at the same level at this boundary, Delft 3D gives a sediment transport at the upstream boundary. This material sedimentates due to the relatively lower velocity, caused by relatively lower water level slope at the start of the simulation.

Sometimes quite a lot of cumulative sedimentation or erosion can be found in the model, like in the river bend below.

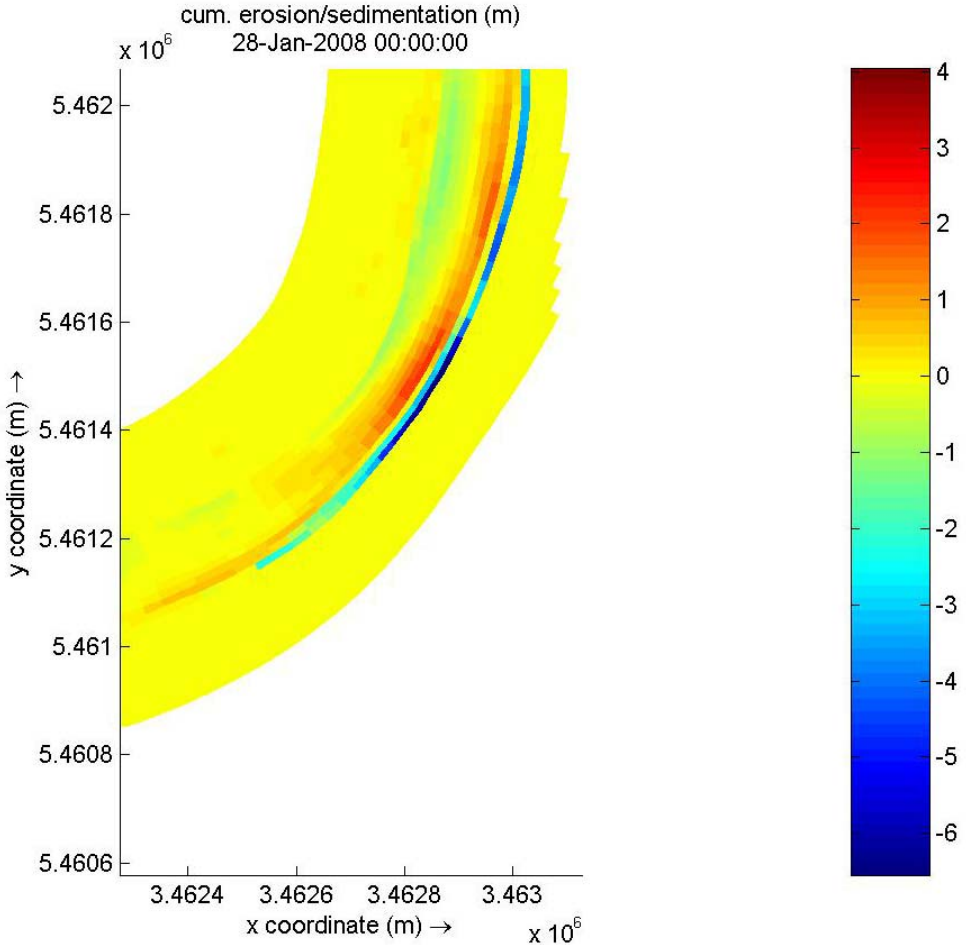

Figure 7.4: cumulative erosion and sedimentation in bend

Large amounts of cumulative erosion or sedimentation are mainly caused by some shifts of cross sections, as shown below:

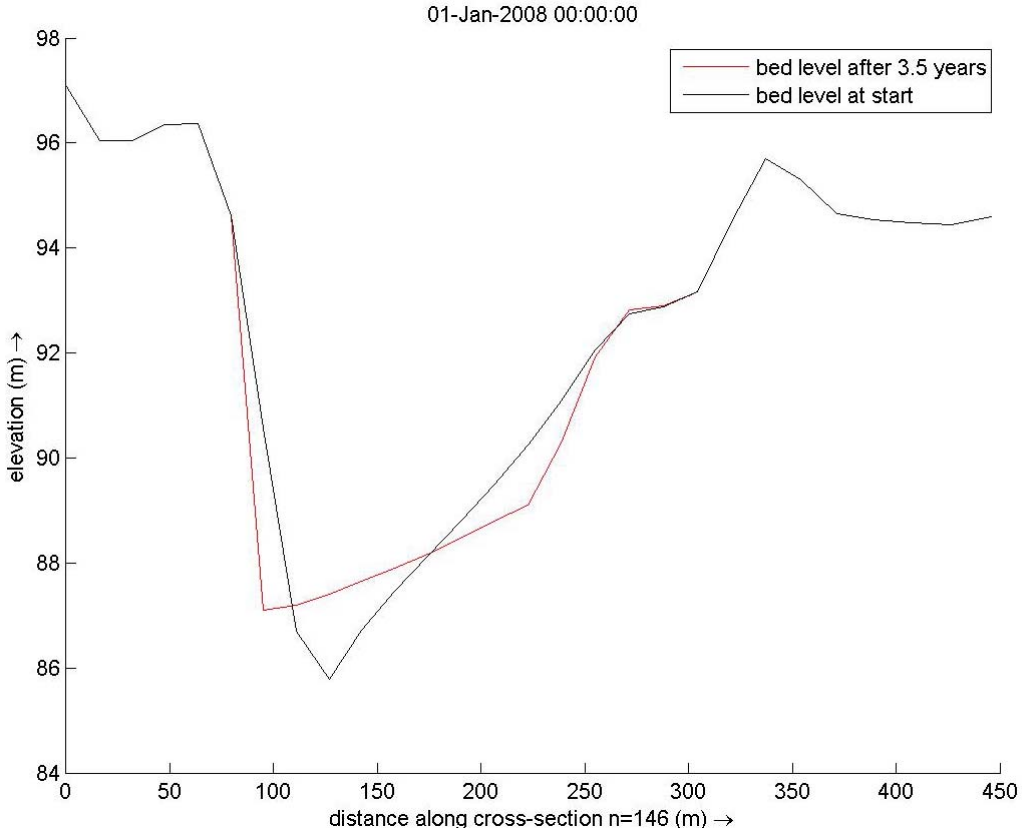

Figure 7.5: cross profile in bend with cumulative erosion and sedimentation shown.

Around 100m on the horizontal axis, there is relatively slight shift of the cross section in the horizontal direction, which causes a relatively large shift in the vertical direction.

The large majority of bed level changes is less than 1-2 m, compared with the level at the start.

7.1.3 Sediment data

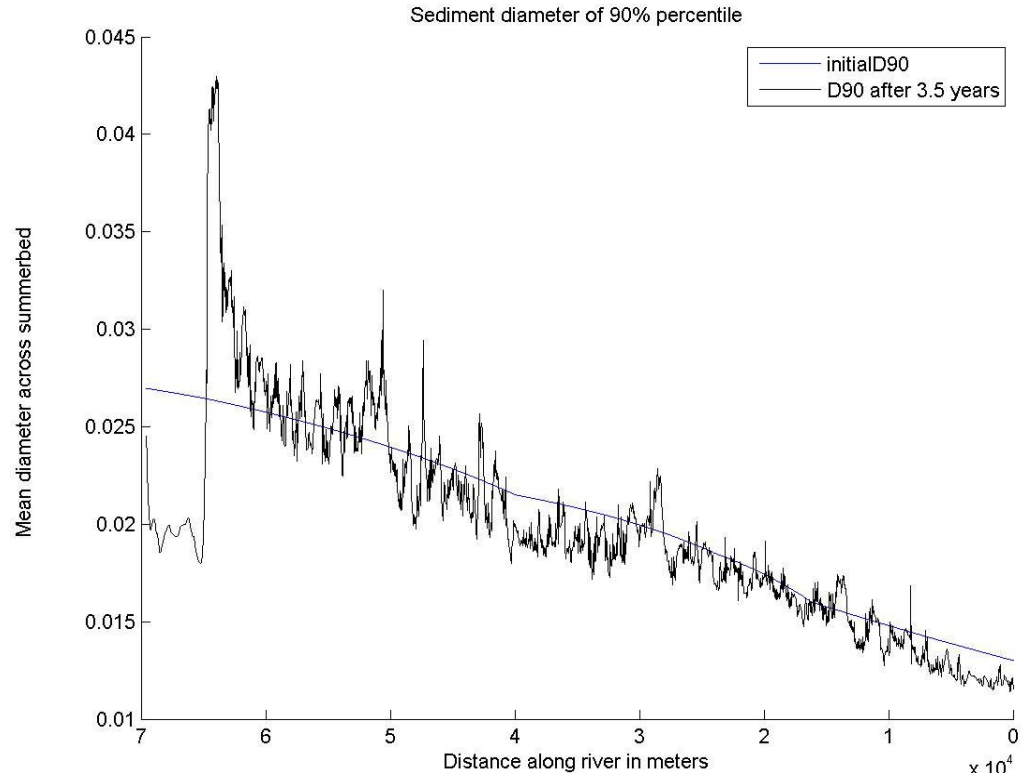

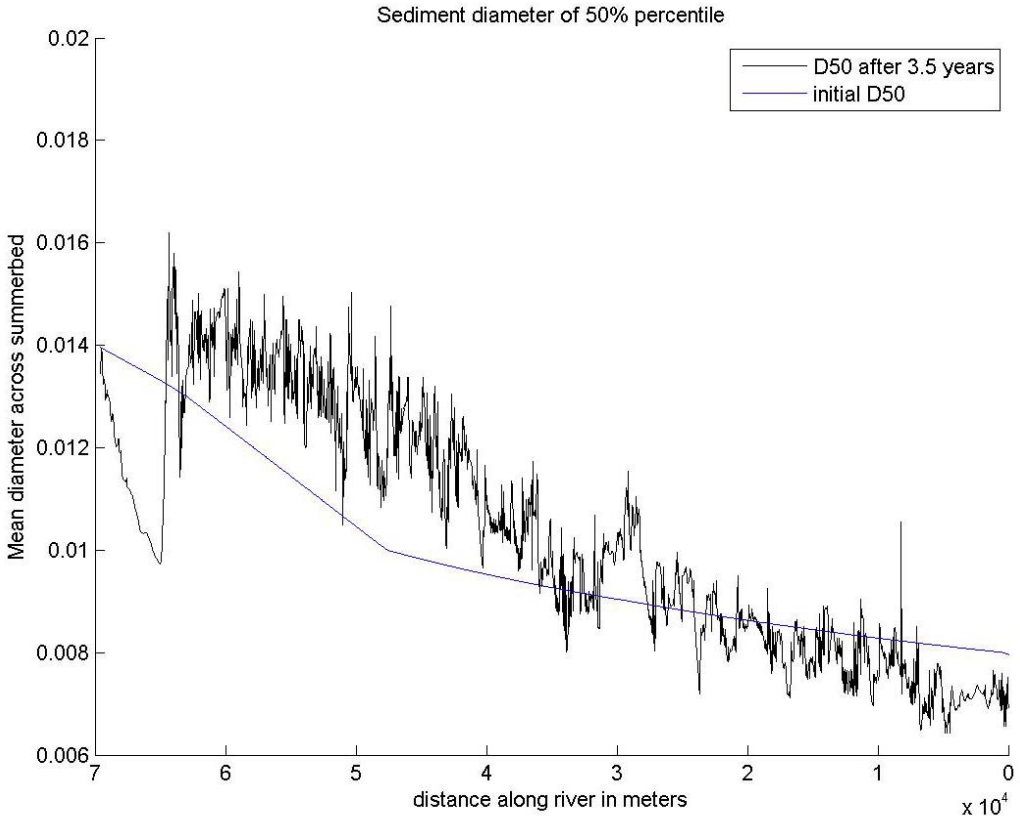

Figure 7.6 and 7.7: sediment diameters of percentiles, averaged across summerbed, in meters.

As can be seen in the figure 7.6 and 7.7, from 70000 m to 65000 meters there is a fining of material. For the 90% percentile of the material, there is a significant coarsening around 65000 meters – 60000 meters (around chainage km 336 -342), this is the part of the model where also the large erosion area develops. Also for the 50% percentile of the material, there is a coarsening visible, but far less extreme than for the 90% percentile at chainage km 336-342. These percentiles also include the tracer material.

The coarsening means a significant change in the environment where the tracer is supplied (around chainage km 336.2-337). The tracer itself is a bit coarser than the original material, but the significant coarsening around chainage km 336-342 will mainly be caused by the erosion area.

The coarsening has, for example, an effect on hiding and exposure related to the tracer. This has consequences for the mobility of the tracer.

7.1.4 Tracer

As can be seen below, transport of the tracer material is only occurring in the summerbed, the tracer material outside the summerbed hardly moves.

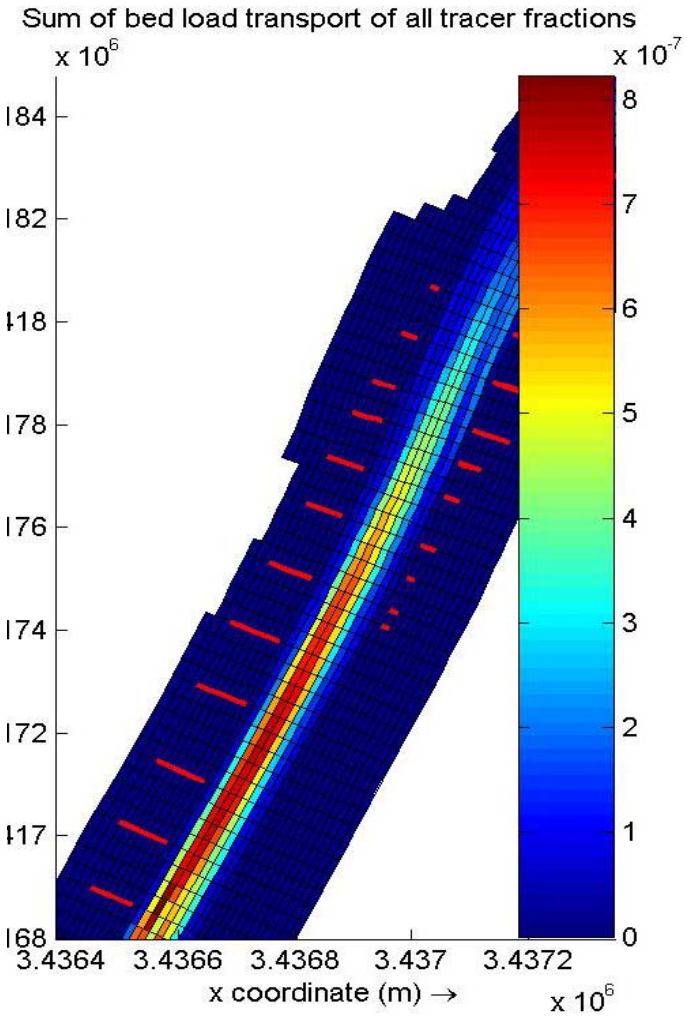

Figure 7.8: transport of tracer material, the red stripes are the weirs, the summerbed is in between them.

Below the relative occurrence of the tracer fractions per grid cell is shown, as a function of the coordinate along the river axis. This occurrence is not only relative to the other tracer fractions in the grid cell, but also to the original bed material.

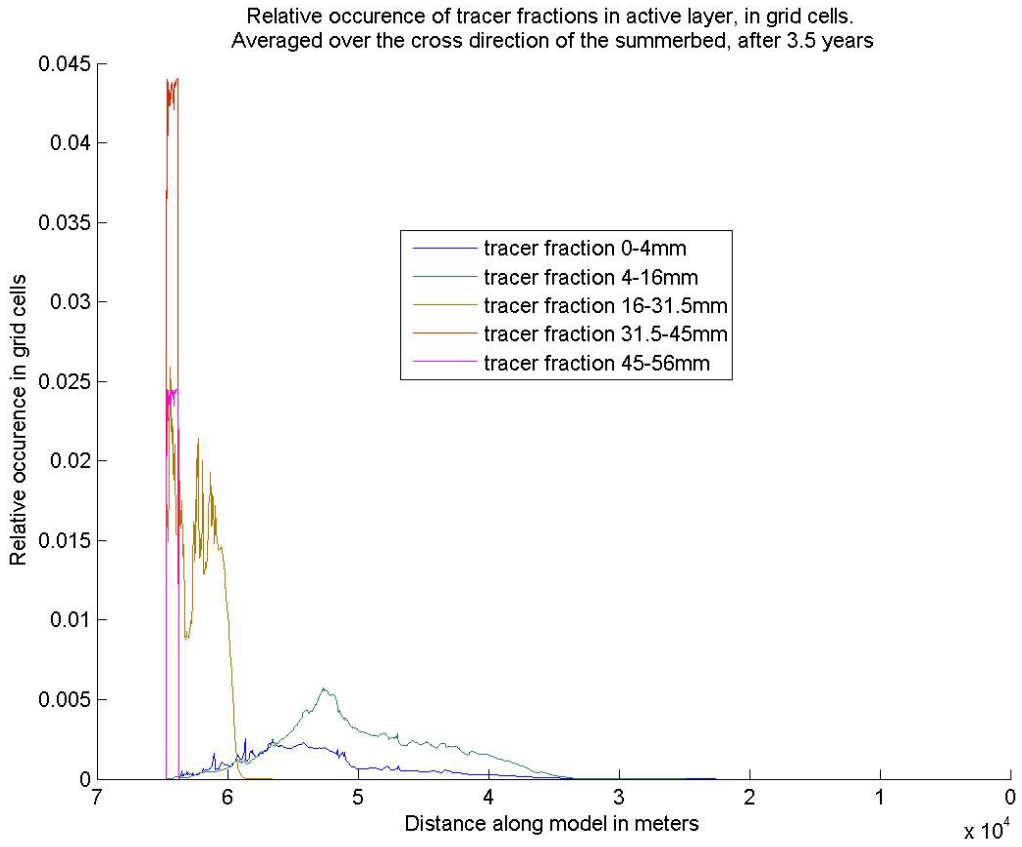

Figure 7.9: propagation of tracer fractions in model

As can be seen in figure 7.9, the coarsest two tracer fractions hardly move. Recorded data *(Gölz, E., Theis, H., Trompeter, U., 2006)* of the tracer shows different results. Recorded data shows significant movement of the two coarsest fractions. Immobility of the coarsest fractions can be caused by the erosion area described in section 7.1.2. On top of this, the model calculates with a constant discharge. In reality there is a lot of discharge variation, as could be seen in chapter 5. Flood peaks could move the coarser fractions.

The smallest fraction seems to move at the same rate, or even a bit slower, as the tracer fraction of 4-16 mm. One of the possible reasons could be the hiding and exposure relationship.

The celerity of the 4-16mm tracer fraction is around 15 kilometers in 3.5 years. The celerity of the data is a factor 2.5 larger. Unfortunately there are no data about the smallest tracer fraction, 0-4mm. The tracer fraction 16-31.5mm moves significantly slower in the model compared to the data. This can have the same reasons as discussed for the two coarser fractions.

From German data it is clear that the tracer material is frequently located down to 1 meter below the bed.

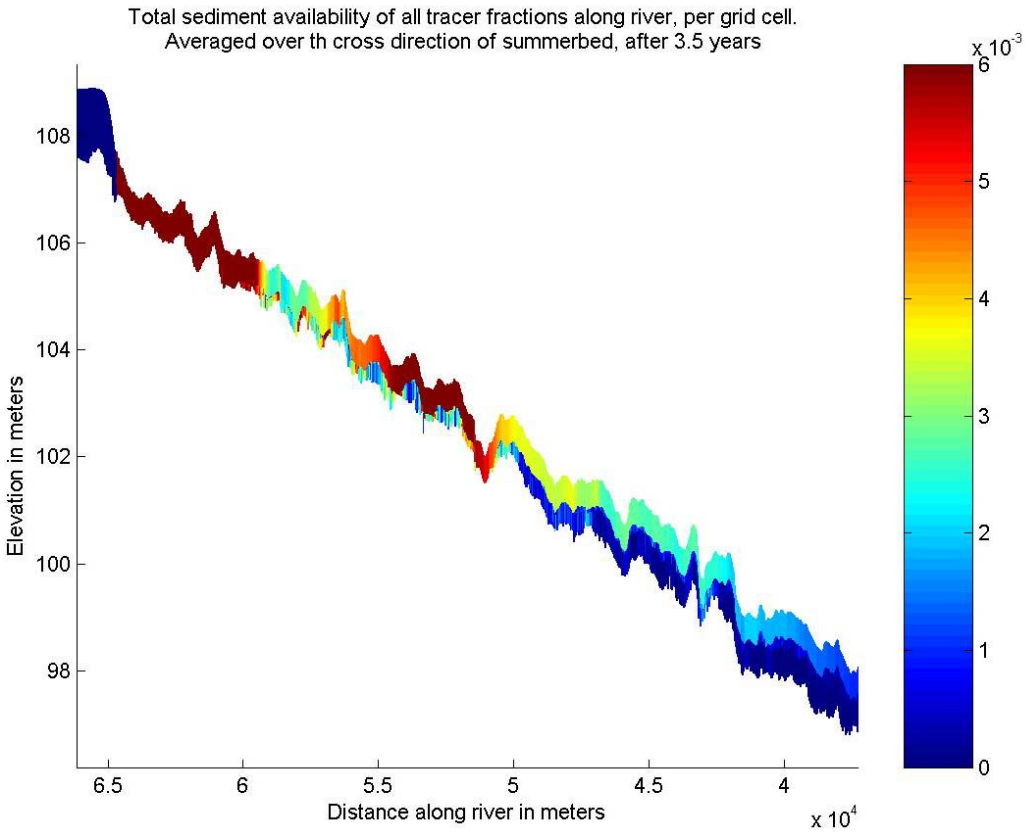

Figure 7.10: occurrence of tracer fractions in active layer and underlayer system

In figure 7.10 two layers are visible. The layer on top is the active layer, the layer below represents the sediment that is available below the active layer.

From the simulation it appears that most of the tracer material stays within the top 0.5 m below the bed, this is exactly the thickness of the active layer. This can also be seen in figure 7.10: the availability of all tracer fractions is the highest in the top layer.

The figure below gives a plane view of the bed load transport per unit width in the river. The unit of the transport is m^2/s.

The figure shows that the transport of the tracer material is very small compared with the transport of the original bed material. The figure also shows that there are significant gradients in the tracer transport. In the figure two areas can be distinguished were significant transport occurs. The area further downstream will represent transport of finer fractions, the area more upstream will represent transport of more coarser fractions.

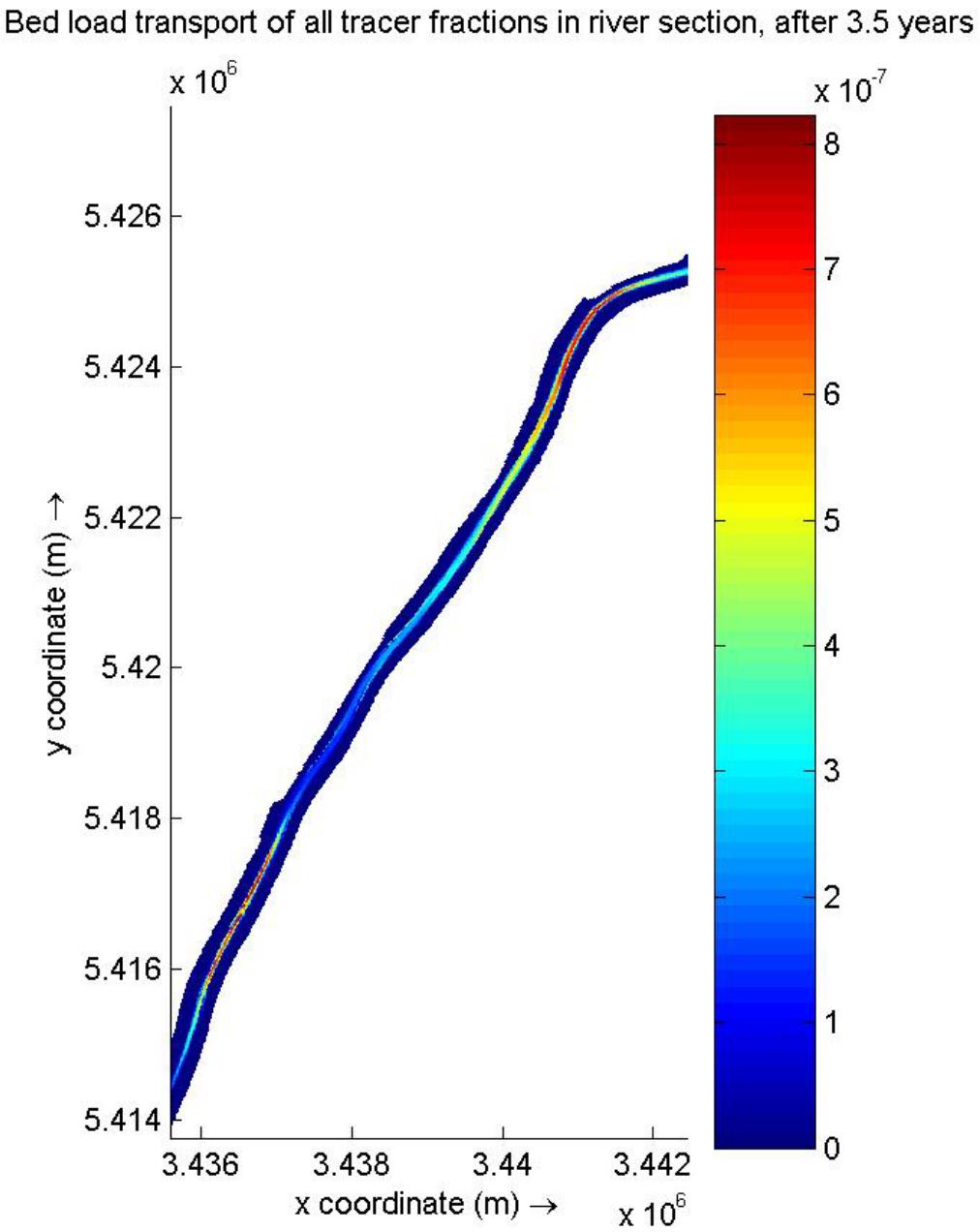

Figure 7.11 bed load transport, plain view

7.2 Changing the number of fractions

In this section, the effects of a different schematization of the sieve curve data into a discrete number of sediment fractions, is discussed.

Instead of the 10 fractions used in section 7.1, 8 fractions will be used for schematization of the original bed material in this section. The schematization of the tracer nourishment is the same as in 7.1.

7.2.1 Set-up

The following parameters have been used in the simulation described in this section:

Parameter	*value*
Thickness active layer	0.5 m
Number of fractions	8
Discharge	2000 m^3/s
Dredging and nourishment	not implemented
Other parameters	same as in 7.1

Table 7.4: important parameters reference case

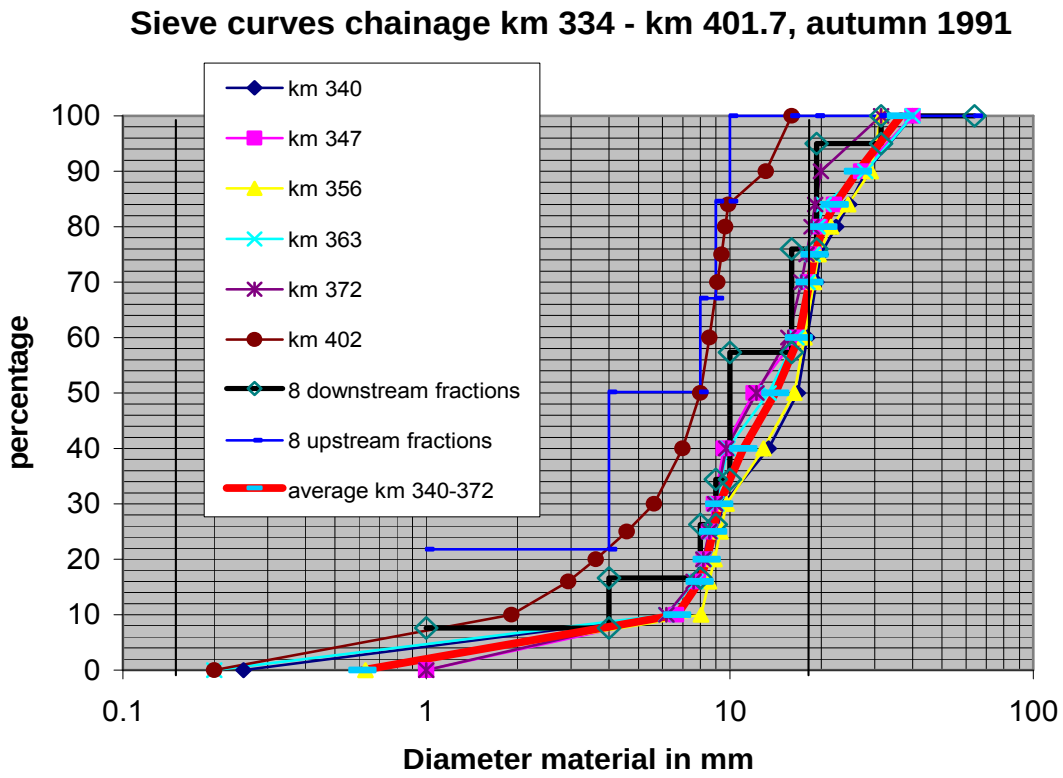

Figure 7.12: division of sieve curve data in 8 discrete fractions

Fraction schematization	sed1	sed2	sed3	sed4	sed5	sed6	sed7	sed8
lower border (mm)	2E-04	4	8	9	10	16	19.3	31.5
upper border (mm)	4	8	9	10	16	19.3	31.5	64
occurrence at upstream boundary	0.08	0.09	0.10	0.08	0.23	0.19	0.19	0.05
occurrence at downstream boundary	0.22	0.28	0.17	0.18	0.05	0.10	0.00	0.00

Table 7.5: division of sieve curve data in 8 discrete fractions

Compared to the model with 10 discrete fractions, exactly the same sieve curve data are used. The difference is the number of fractions used. In the model with 10 fractions, the 10-31.5mm diameter range is divided into 5 classes. In this model with 8 fractions, this range is divided into 3 classes.

For each fraction (or class), the representative grain size is calculated by:
$D_i = \sqrt{D_{\min} \bullet D_{\max}}$,
as is stated in section 3.2.6.

By changing the fractions, D_i is changed.

The sediment transport is related to D_i in a non linear way, as is described in section 3.1.2.1. Different transport rates for each fraction could cause a different transport of the fractions and a different total transport. This, of course, can have implications for the morphology.

7.2.2 Bed level implications

To see any implications on the bed level, a comparison is made between a calculation with 8 fractions and one with 10 fractions. The bed level shown is averaged over the cross direction of the summerbed.

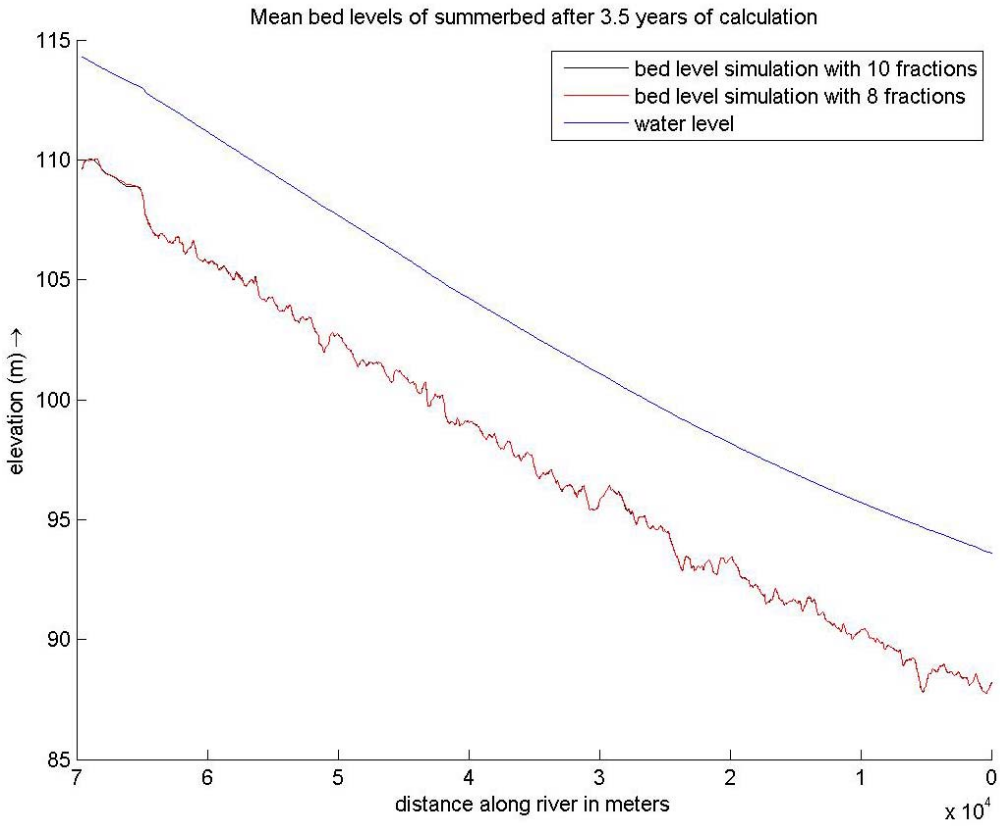

Figure 7.13: bed level comparison for model with 8 and model with 10 discrete fractions

Almost no significant differences can be found between the bed levels, only at the upstream end there is some difference, due to the upstream morphological boundary condition.

7.2.3 Sediment data

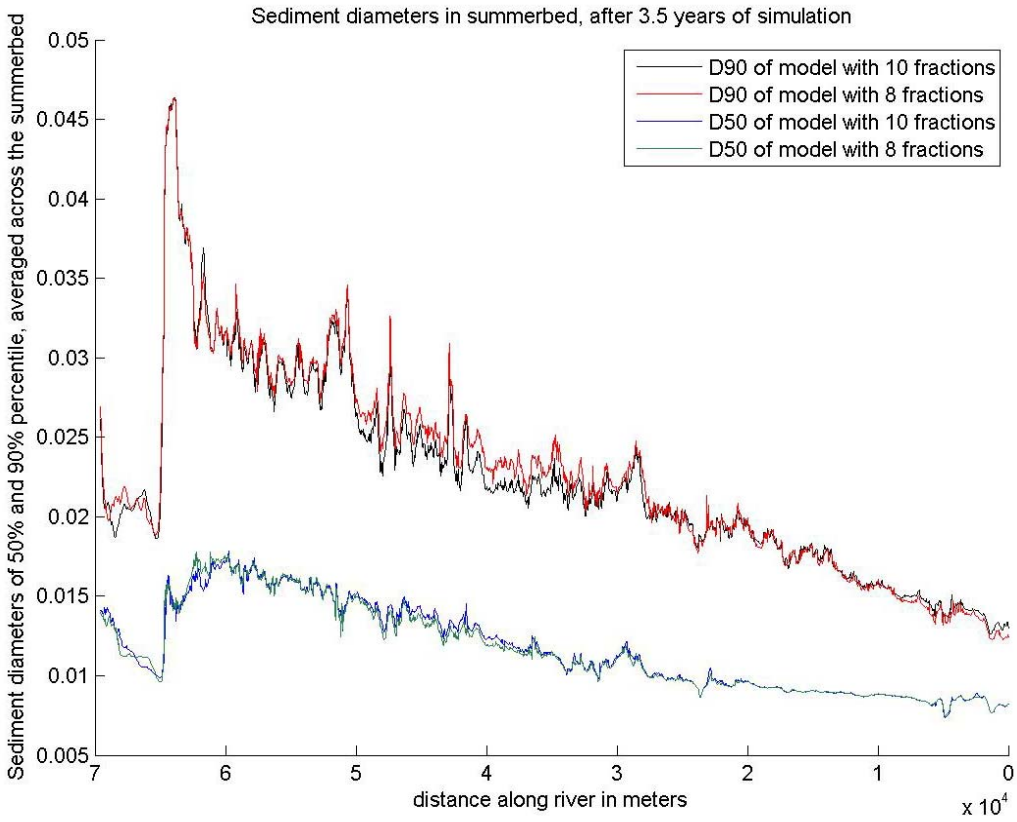

Figure 7.14: sediment data comparison for model with 8 and model with 10 discrete fractions

The 50% and 90% percentiles of the sediment diameter hardly change. This is, for example, an indication for the change of hiding and exposure effects, this change will not be significant in this case.

The difference between the total amounts of sediment transport across the summerbed is also negligible:

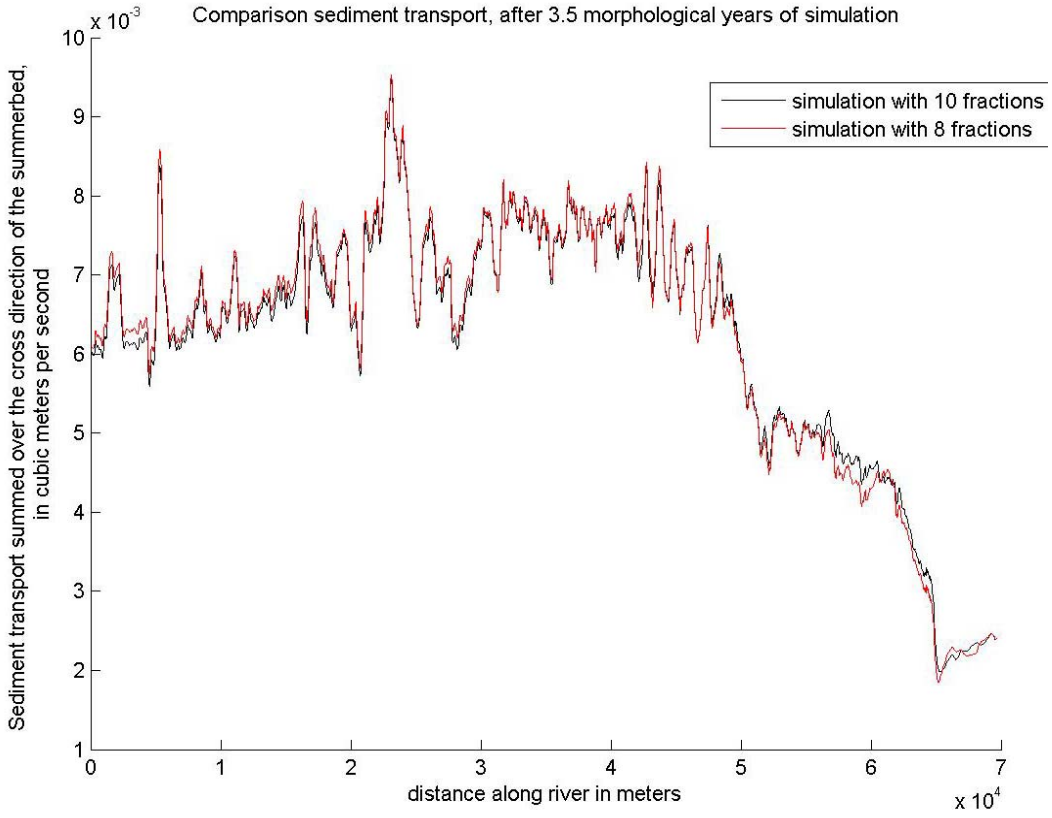

Figure 7.15: bed load transport comparison for model with 8 and model with 10 discrete fractions

This is the total transport of all fractions.

7.2.4 Tracer

Below a comparison is made between the propagation of the tracer fractions of a simulation with 8 fractions and one with 10 fractions. The number of tracer fractions is kept the same in both simulations.

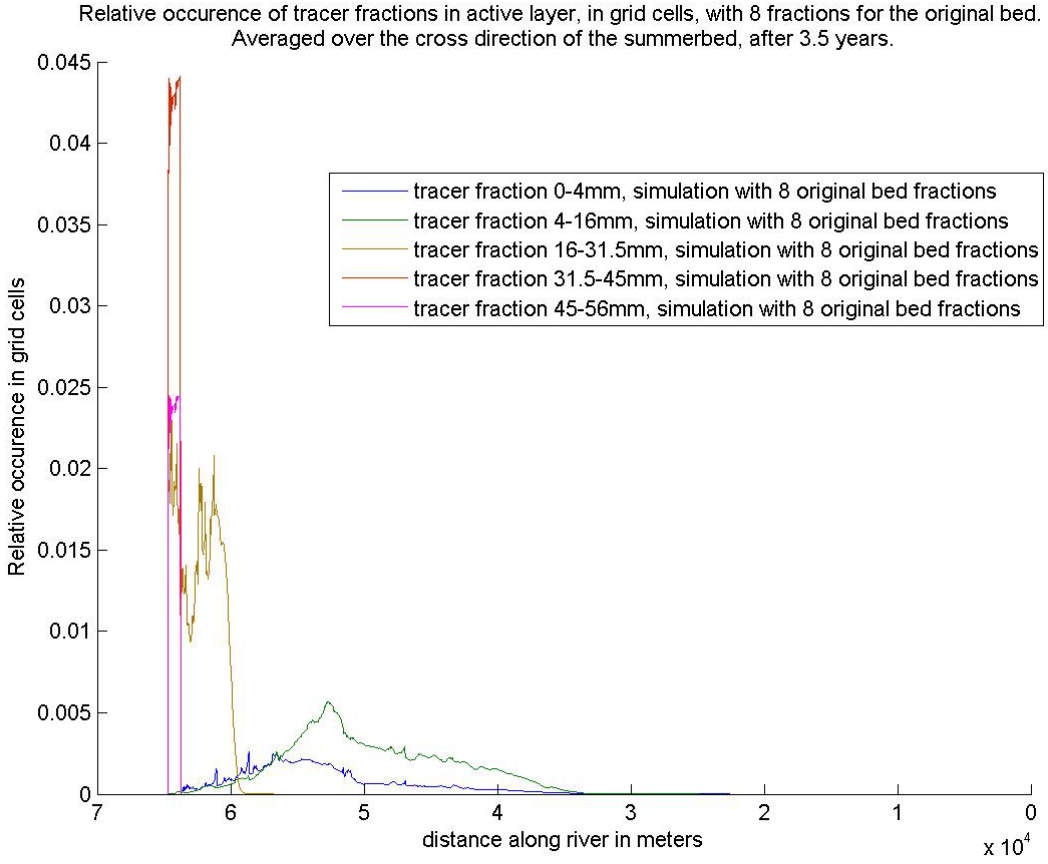

Figure 7.16: tracer nourishment propagation for model with 8 discrete fractions

Compared with the results from section 7.1.4, figure 7.9, there are almost no differences.

7.2.5 Discussion

The different number of fractions did not have much effect on the model results. Of course the change in the input was quite small: the same sieve curve was used, only this curve was slightly different divided into more fractions at the coarser part.

It could have been more interesting to investigate the effect of changing the upper border of the coarsest fraction, or the lower border of the finest fraction. The range in which the number of fractions was changed, is mobile in both simulations with 8 and 10 fractions. By lowering for instance the upper level of the coarsest fraction, this fraction might change from immobile (as is the case in the reference simulation in section 7.1) to mobile. This could have a large effect on, for example, the hiding and exposure relation.

Effects on hiding end exposure can already be studied by calculating the hiding and exposure coefficient by 'hand', when lowering the upper border of the coarsest fraction from 64 mm to 45 mm. This is studied for the initial bed composition at the upstream boundary of the model. In figure 7.17 the results are shown for fraction 4-8 mm and the coarsest fraction of the original bed:

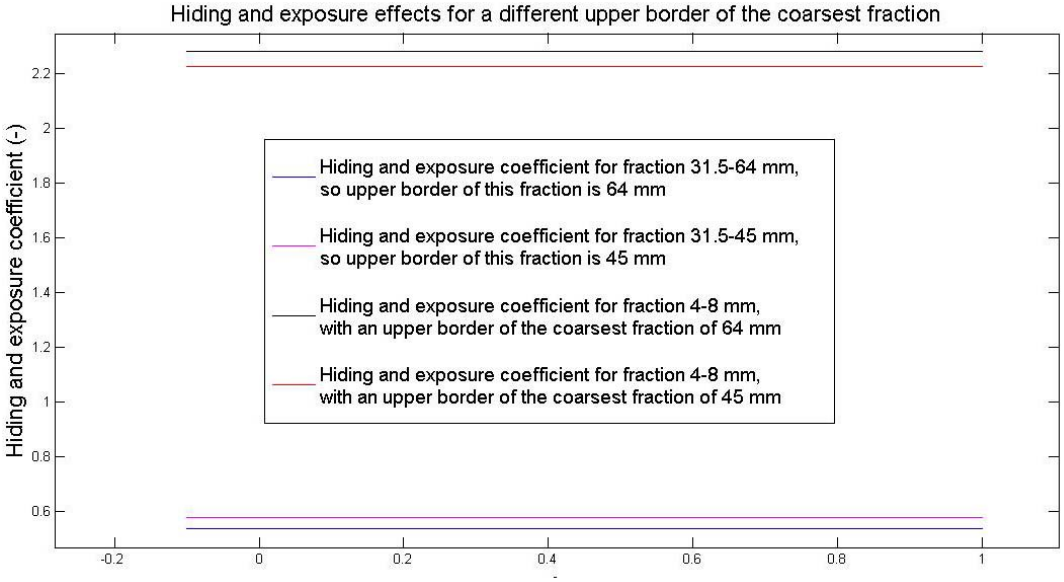

Figure 7.17: hiding and exposure effects for different upper border of coarsest fraction

As can be seen from figure 7.17, there is almost no effect on the hiding and exposure coefficient. However, this is the hiding and exposure effect of the initial bed only.

As stated before, difference in mobility of the coarsest fraction, can be important for differences in hiding and exposure effects in a later stadium of the computation. The hiding and exposure coefficient does not change much when choosing a different upper border. The mobility parameter θ_i in the transport formula does change significantly, because it is dependent on the characteristic fraction diameter D_i, as was explained in section 3.1.2.1. A comparison is made in table 7.6 between the sediment transports of the coarsest fraction, for different diameter values of the upper border, for the initial composition at the upstream boundary.

Upper border coarsest fraction (31.5-64 mm)	*Sediment transport in m^2/s*
64mm	0.00000987
45mm	0.00000816

Table 7.6: sediment transport for different upper borders of coarsest fraction

There is a difference in the sediment transport of the coarsest fraction, when changing the upper border. This must be born in mind when choosing a value for the upper border. A similar reasoning holds for the finest fraction.

In the model the coarsest fraction of the original bed shows no mobility at Q=2000 m^3/s, while from the 'hand' calculation it appears there is sediment transport at this discharge. After some parameters in the 'hand' calculation are changed to a value which corresponds slightly better with reality, however (summerbed slightly wider, depth slightly larger), the sediment transport of the coarsest fraction also drops to zero. This demonstrates that this sediment transport is quite sensitive to small changes.

The determination of the upper border of the coarsest fraction and the lower border of the finest fraction is done quite arbitrarily. The largest or smallest diameter found in measurements can differ in a wide range over time, see also 6.1.2. How these measurements are done and how the numbers are determined is not known exactly. More information about this could be advantageous for the choice of the upper border of the coarsest fraction and the lower border of the finest fraction.

That the results are not affected here by using 8 fractions instead of 10, is of course not a guarantee for similar situations in other models. A careful inspection of the situation is recommended before making a final choice about the fraction schematization. Using less fractions in the model significantly reduces simulation time, and hence the economic advantage could be large. One could for instance use the following schematization of 5 fractions, to reduce computation time even further:

Fraction	*Occurrence*
0.4-4 mm	8%
4-8 mm	9%
8-16 mm	41%
16-32 mm	38%
32-64 mm	5%

Table 7.7: fraction schematization of model with 5 classes

When calculating the summed sediment transport over all fractions by 'hand', with the help of $q_{s,i} = \alpha D_i \sqrt{\Delta g D_i} \left(\mu\theta_i - \xi\theta_{cr} \right)^c p_{i,a}$, it appears that the summed transport over all fractions has become smaller with a factor 2. This comparison has been made for the initial composition at the upstream boundary. This does not implicate that calculating with 5 fractions in this model cannot represent reality. A different calibration of the transport formula could give better results.

Caution should be taken with calibration of the sediment transport formula, $q_{s,i} = \alpha D_i \sqrt{\Delta g D_i} \left(\mu\theta_i - \xi\theta_{cr} \right)^c p_{i,a}$. Different combinations of dimensionless coefficients in the transport formula, could lead to the same sediment transport. For example when using a different combination of c and α coefficients. All combinations of c and α coefficients shown below in figure 7.18, give the same transport for the sum of all fractions.

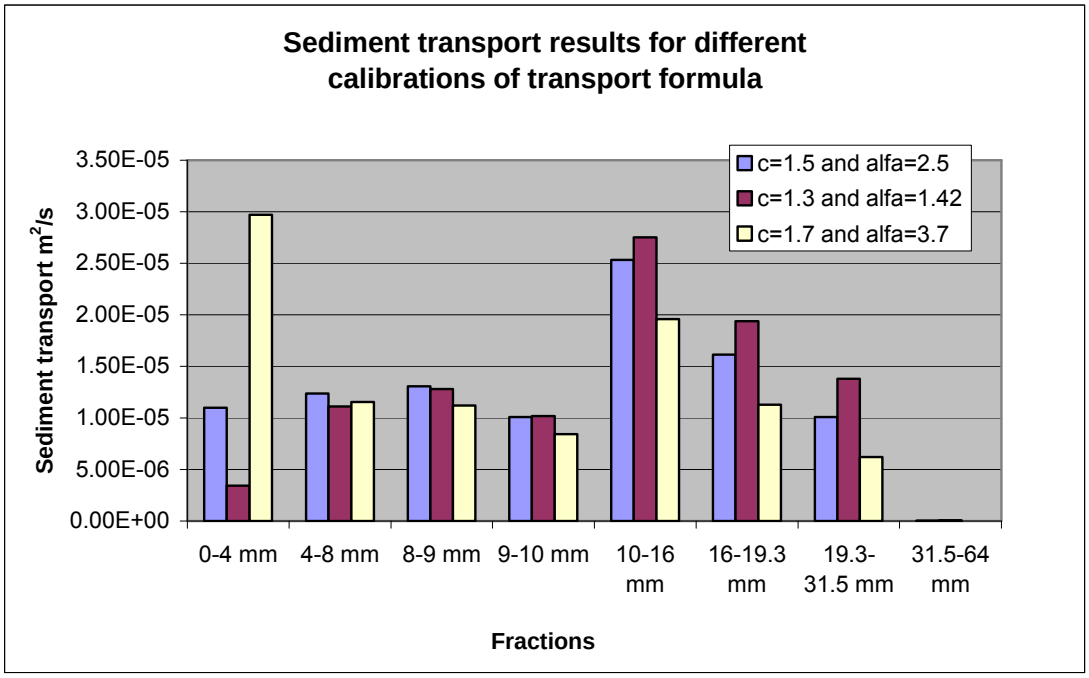

Figure 7.18: Sediment transport for each fraction, for initial composition at upstream boundary

As is clear from figure 7.18, the sediment transport for each individual fraction, can be very different, while the summed transport over all fractions is the same for the given sets of c and α.

This effect should be considered during calibration. For a good representation of the tracer fractions in the model, use of data available about this tracer for calibration of the transport formula, is recommended.

7.3 Changing the active layer thickness

This section deals with the effects of a different active layer thickness. This is a model parameter for which a certain value is chosen, see also section 3.1.2.

7.3.1 Set-up

The following parameters have been used in the reference case:

Parameter	*value*
Thickness active layer	0.1 m
Number of fractions	10
Discharge	2000 m^3/s
Dredging and nourishment	not implemented
Other parameters	As in 7.1

Table 7.8: important parameters of model-set-up

Compared to the reference case of 7.1, the active layer thickness is significantly smaller. This can have significant implications for morphology. The active layer thickness is an important parameter for the adjustment rate of the bed composition in this layer, but also for the propagation of fractions, as can be seen in Appendix II.

7.3.2 Bed level implications

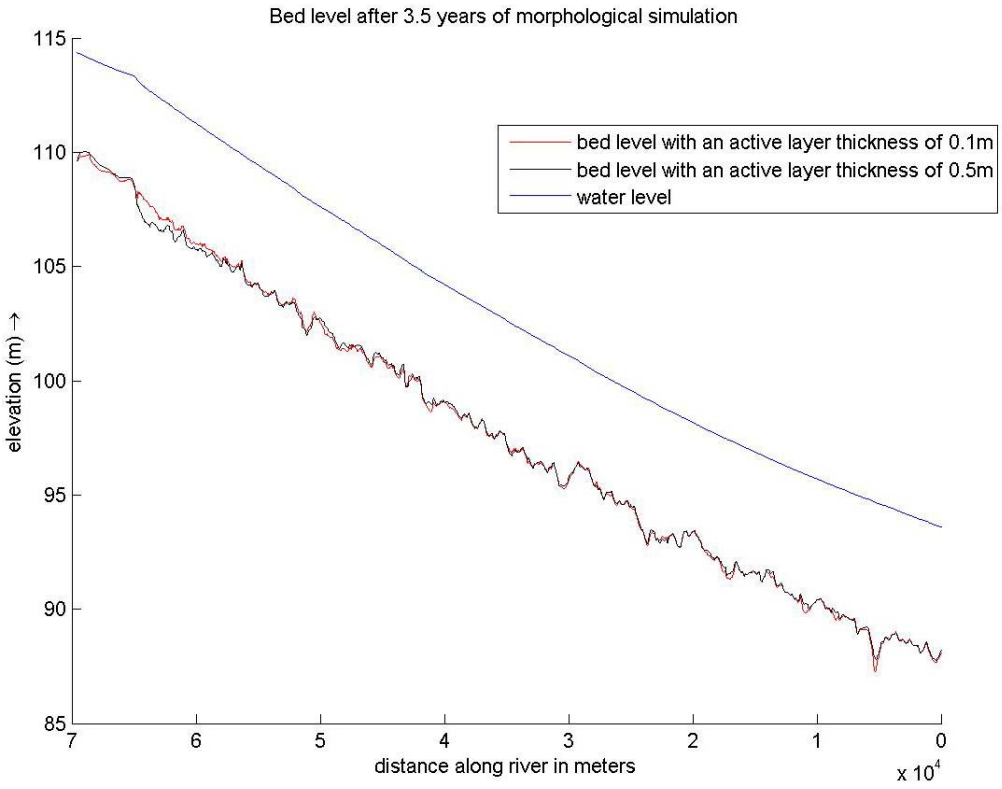

Figure 7.19: bed level comparison

Along most of the river, changing the active layer thickness does not have a large implication for the mean summerbed level. This is different for the area around 65000-60000 meters (around chainage km 336-342). The simulation with an active layer thickness of 0.1 m shows a significant smaller amount of erosion in this area. For an active layer thickness of 0.1 m, the bed composition in this active layer is adjusted at a much higher rate. The consequence is a quicker coarsening of the active layer, which results in less erosion of the bed.

7.3.3 Sediment data

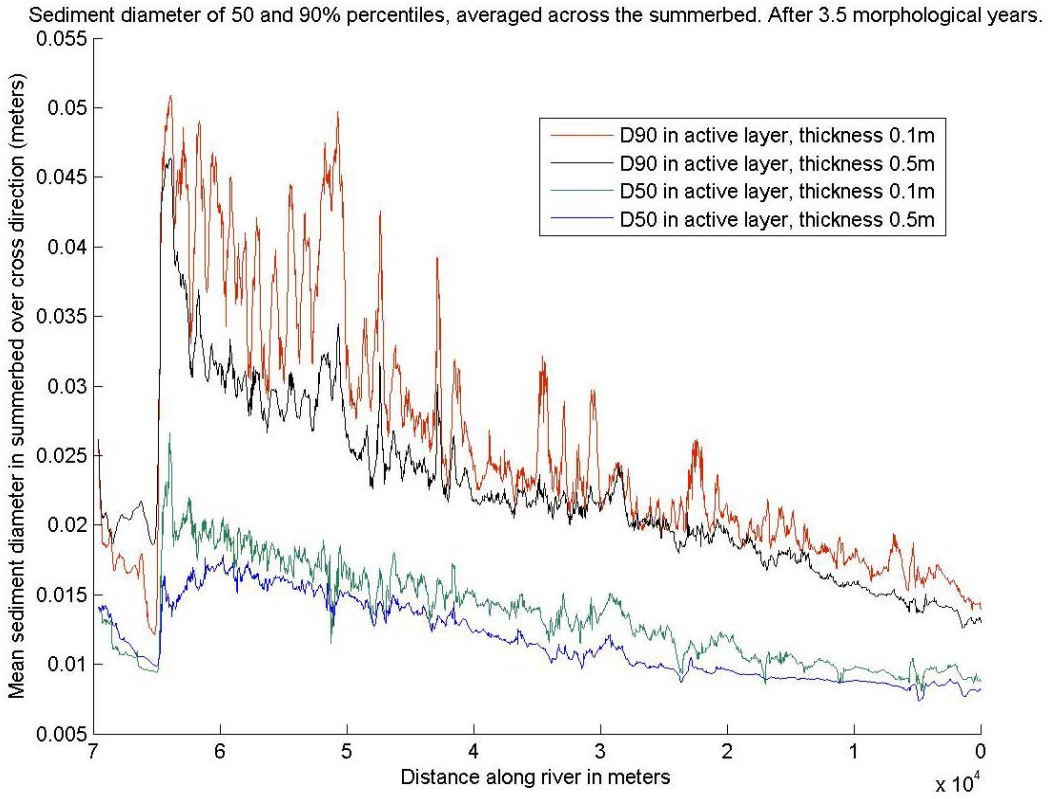

Figure 7.20: sediment data comparison

A coarsening of the active layer can be seen in most of the model, except for the area around 70000-65000 meters (around chainage km 331.3-336), where the active layer gets finer. This fining is due to the characteristics of the virtual extension onto the grid, in combination with the morphological upstream boundary condition. The results of the bed load transport in figure 7.21, correspond with the coarsening of most of the summerbed.

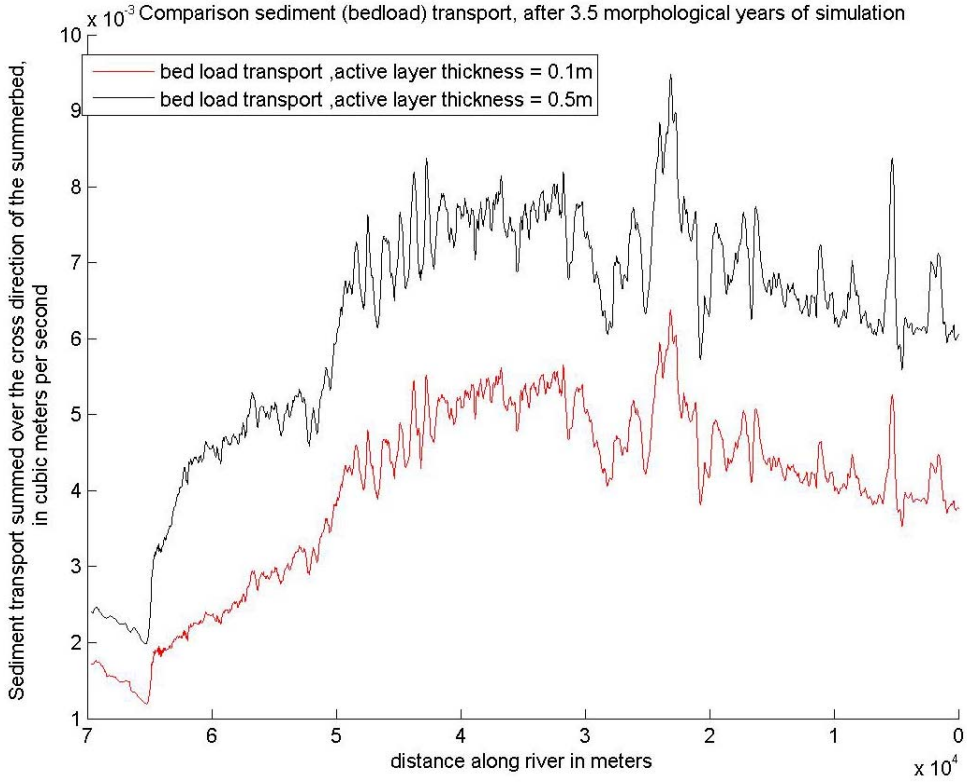

Figure 7.21: bed load transport comparison

7.3.4 Tracer

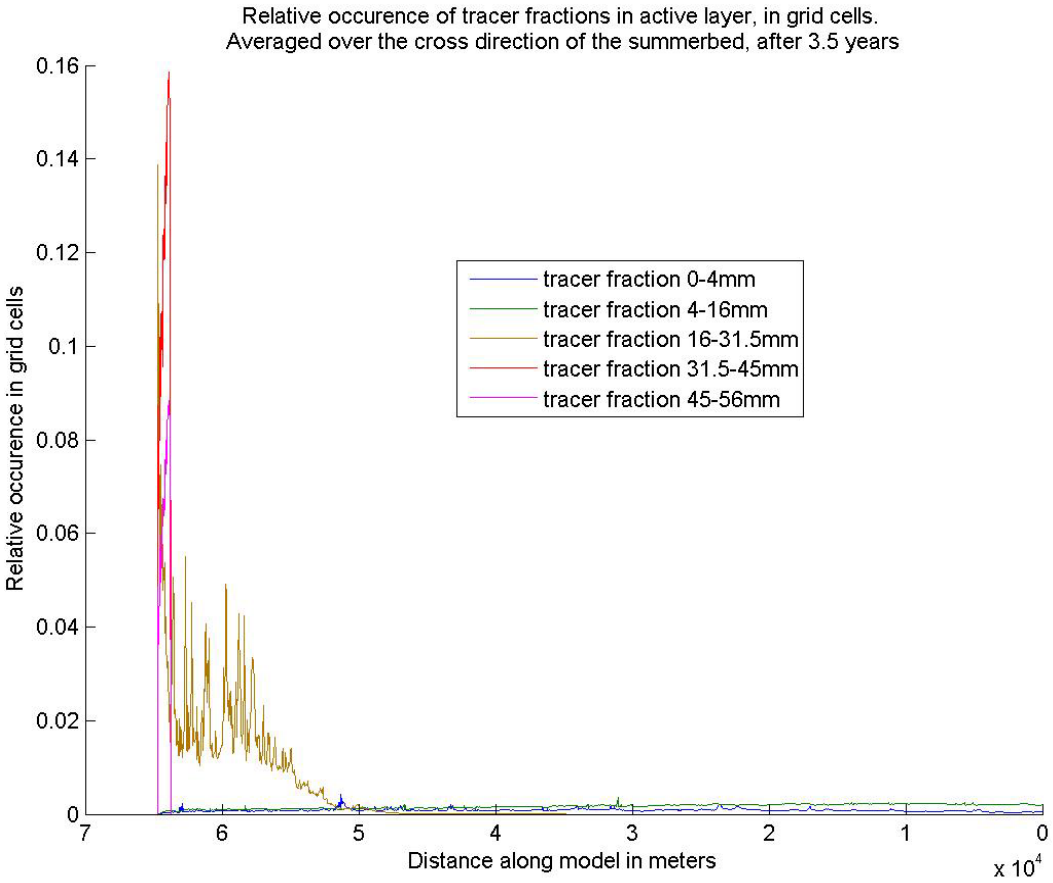

Figure 7.22: tracer propagation for active layer thickness of 0.1m

The above figure shows the spreading of tracer fractions in the active layer of 0.1 m thick. The two coarsest fractions still hardly spread. Compared to the case with an active layer thickness of 0.5 m, there are some important differences. The three finest fractions have spread over a larger area, and their peak has become lower compared to the simulation with a smaller active layer thickness. This also becomes clear in figure 7.23, where a comparison is made between the two finest fractions for different active layer thicknesses, after approximately 1.5 morphological years of simulation.

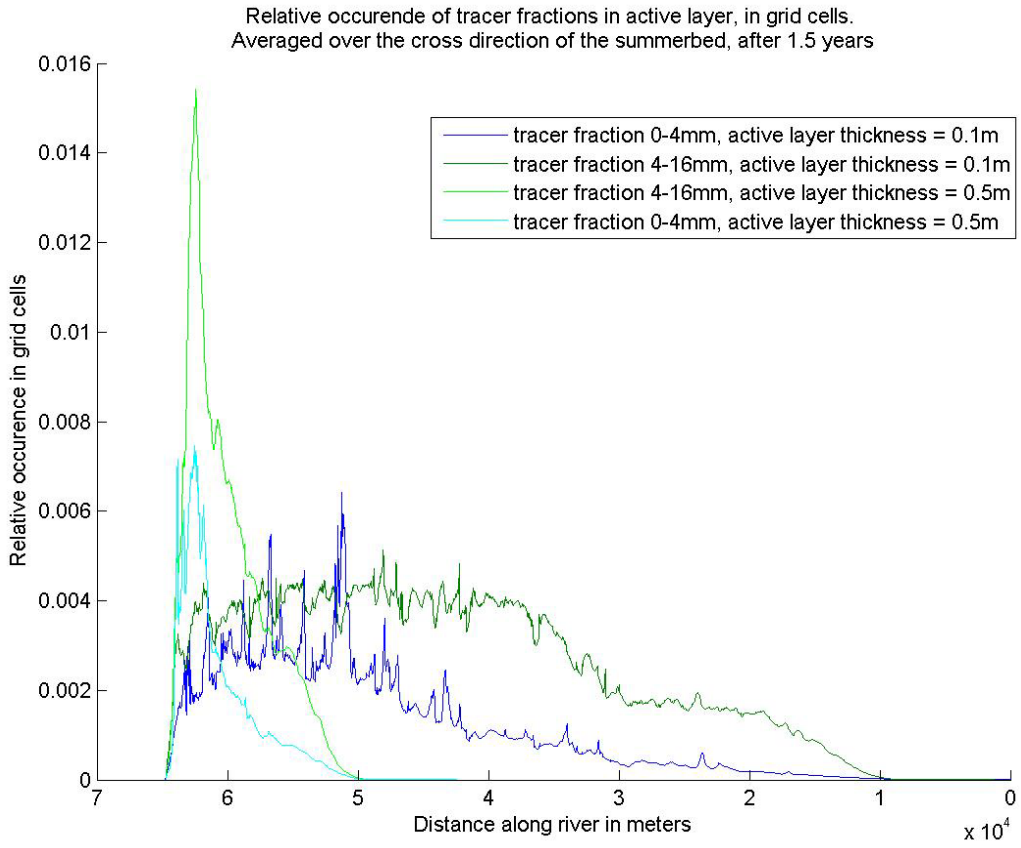

Figure 7.23: propagation of smallest tracer fractions

Figure 7.24 shows the availability of the sum of all tracer fractions in and below the active layer:

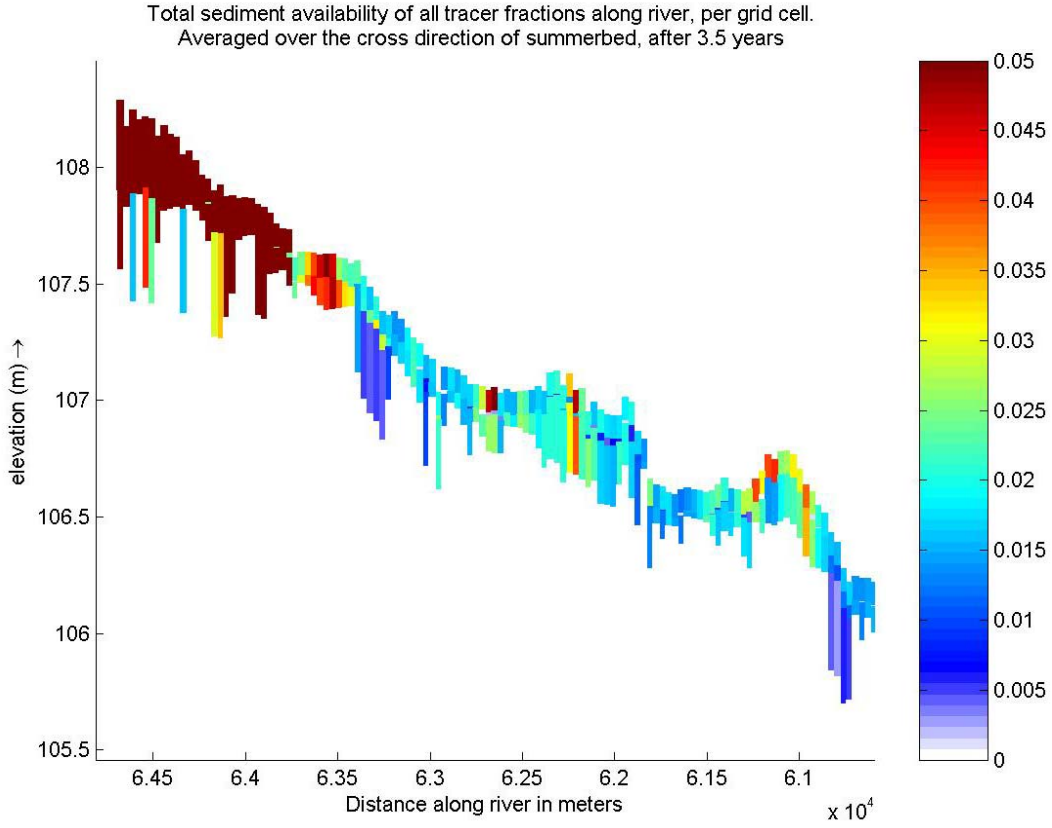

Figure 7.24: occurrence of tracer fractions in active layer and underlayer system

From the vertical axis it is clear that a lot of material is stored below the 0.1 m thick active layer, which is the top layer in figure 7.24. In figure 7.25 the availability of 4 tracer fractions is made visible.

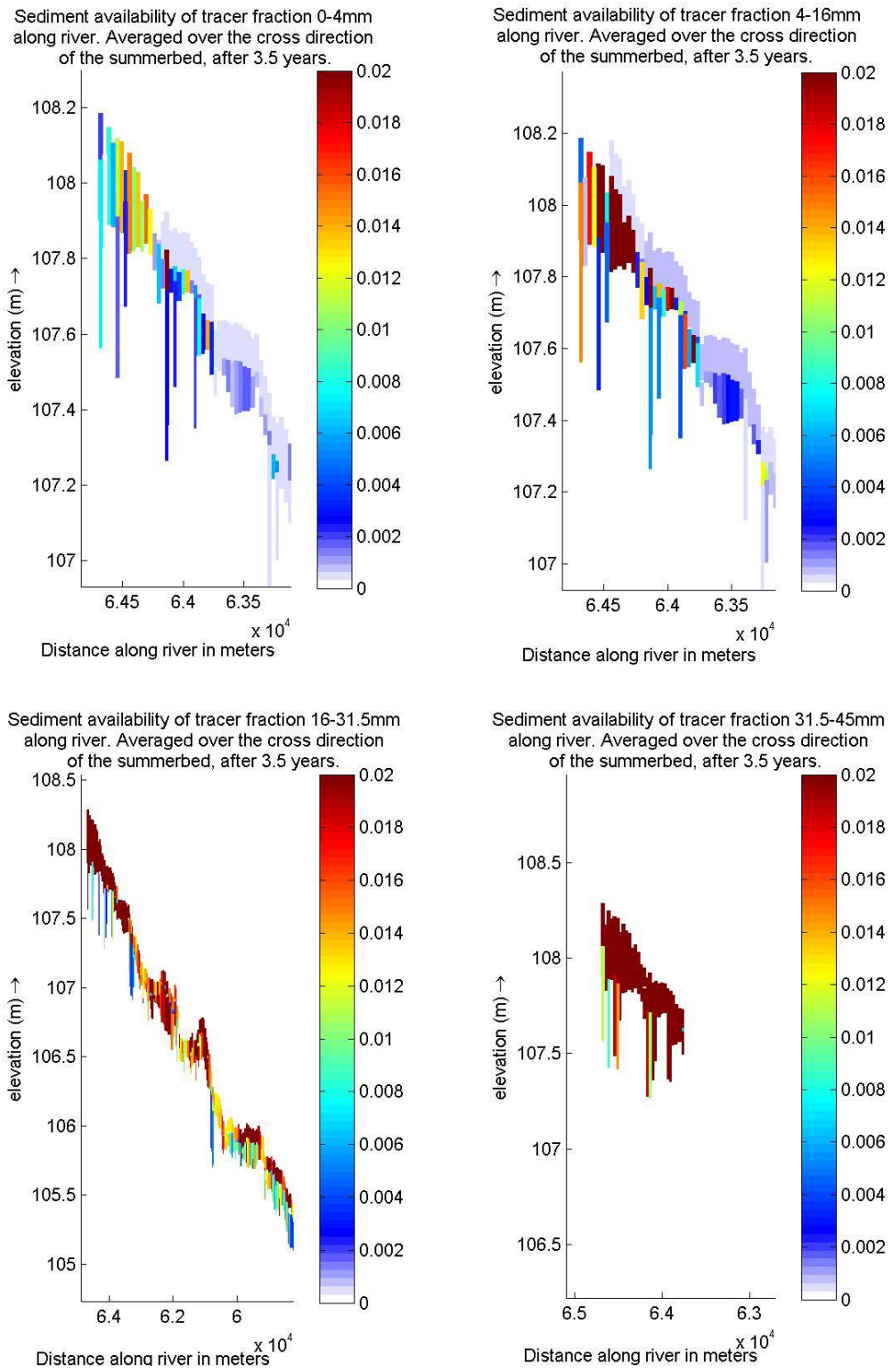

Figure 7.25: occurrence of tracer fractions in active layer and underlayer system

It appears that a large part of the two finest tracers is stored below the active layer. Also a significant amount of material of the two coarser fractions shown in figure 7.25, is clearly present below the active layer.

7.3.5 Discussion

The smaller active layer thickness has important implications for the model results.

It results in a quick coarsening compared to runs with a larger active layer thickness, especially in the parts with relatively much erosion. With a thinner active layer, there is less fine material available for erosion. This relatively small amount erodes quickly, and what is left in the active layer is relatively coarse material, which hides fine material in the underlayers.

Normally around 65000-60000 meters (around chainage km 336-342), a large erosion area grows, which would also be present in reality, if no nourishments would be done in this region. Due to the thin active layer and its coarsening, erosion in this area is stopped quickly.

Hence the choice of the active layer thickness has a large impact on the original bed properties.

The tracer is dumped at once from river chainage kilometre 336.2-337. With a tracer volume of 17500 cubic meters, a dump width of approximately 150 meters, and an equal distribution of the dumped volume over the whole area, this results in a thickness of the tracer nourishment of 0.15 metres. This is larger than the active layer thickness, which automatically means that significant amounts of tracer material 'disappear' in the underlayer system when the tracer is dumped at once. Especially at the dump site of the tracer, there is still a lot of tracer material present in the underlayers after 3.5 years of simulation.

This demonstrates the importance of the active layer thickness and dumping method: it has a large influence on amounts of storage and amounts of transportation. With a larger active layer more tracer material would be available for transport and less for storage in underlayers. A larger active layer thickness also results in a less coarser active layer. This means more sediment erosion in eroding river sections, which results in a larger contribution of underlayer material to the active layer, since the layer thickness is a constant. Hence the probability that tracer material which is 'trapped' in the underlayer, gets into the active layer again and is available for transport, is larger.

The celerity of the part of the tracer fractions that is transported, is larger with a smaller active layer thickness, when comparing simulation results. This can also be concluded from an analysis done in appendix II. According to this analysis, the kinematic celerity of fractions in the active layer can be stated as:

$$c_{mix} = \frac{\mu q_s}{\delta(1-\varepsilon)},$$

in which δ is the active layer thickness. A smaller active layer thickness could result in a higher celerity of the fractions in the active layer, according to this analysis.

In the above equation for the fraction celerity, this celerity is not dependent on the celerity of bed level perturbations. When assuming a coupling between the two celerities, there is a slight change in the absolute value, as was shown by *Mosselman et. al (WL Delft Hydraulics, may 2007)*.

7.4 Hiding and exposure relationship

This section discusses the effect of the hiding and exposure relationship used in the model. In the previous sections, hiding and exposure was implemented by using the formulation of Egiazaroff, modified by Ashida & Michiue (1973). A comparison is made with the case in which there are no hiding and exposure effects.

7.4.1 Set-up

The following parameters are used:

Parameter	*value*
Thickness active layer	0.25 m
Number of fractions	8
Discharge	2000 m^3/s
Dredging and nourishment	not implemented
Other parameters	As in 7.1, except for the number of fractions

Table 7.9: important parameters

In this section 8 fractions are used. As appeared from section 7.2, no large differences were found compared to calculating with 10 fractions. Simulating with less fractions saves computational time. Not implementing hiding and exposure, simply means that the hiding and exposure correction factor (ξ_i) is set to 1 in the sediment transport formula. This ξ_i factor is multiplied with the critical Shields parameter in the transport formula, and hence influences the initiation of motion of the sediment.

7.4.2 Bed level implications

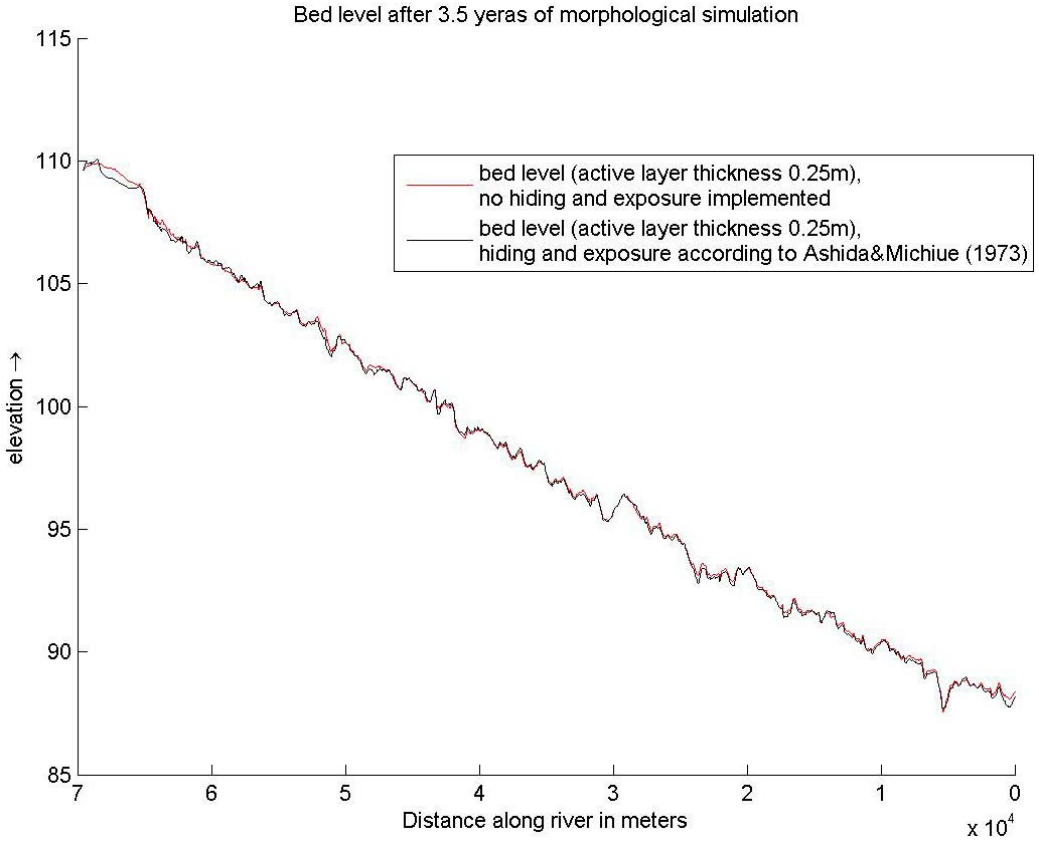

Figure 7.26: bed level comparison

For the bed level, the implications are not significant.

7.4.3 Sediment data

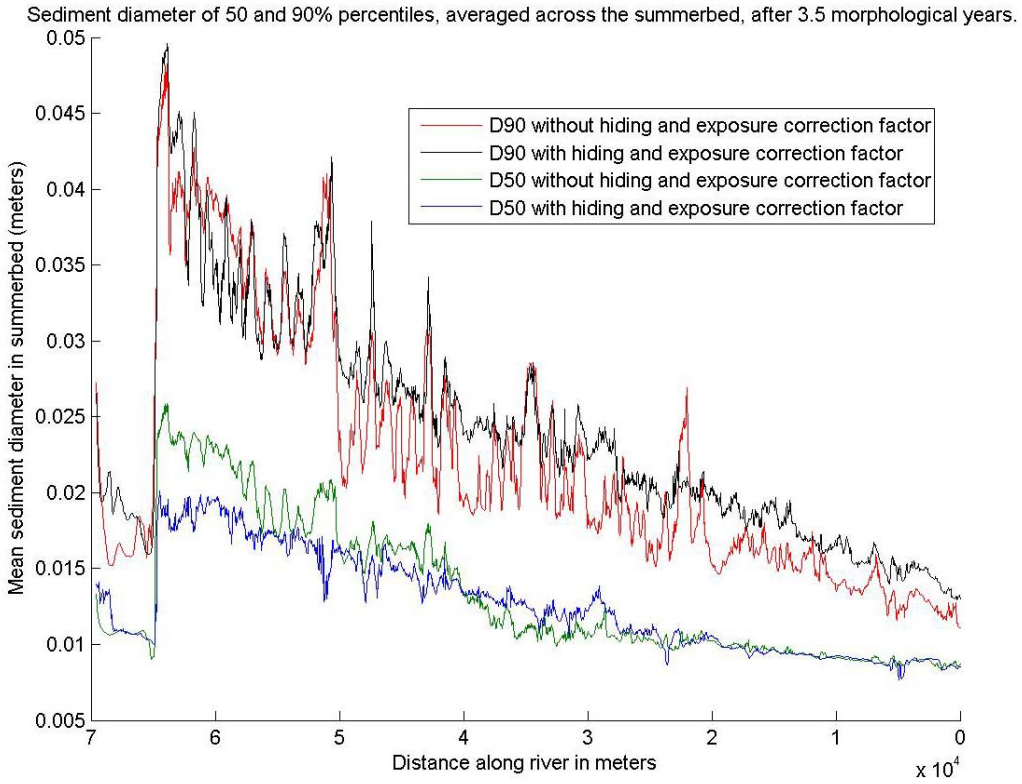

Figure 7.27: sediment data comparison

The global pattern is the same for simulations with and without hiding and exposure. Some differences can be found between the two cases, as is visible in the figure.

There is, for example, an increase of the D_{50} in the erosion area (chainage km 336-342, around 65000-60000m on the horizontal axis), when calculating without a hiding and exposure correction. In the case of not using a correction, less hiding of the finer fractions occurs, which contributes to a coarser composition in case of erosion. On the other hand, less exposure occurs of the coarser fraction, also leading to a coarser composition in case of erosion.

7.4.4 Tracer

The two coarsest fractions of the tracer hardly move with hiding and exposure implemented. Without hiding and exposure these fractions are, of course, also not mobile. In the figure below the difference in mobility of the two smallest tracer fractions is showed.

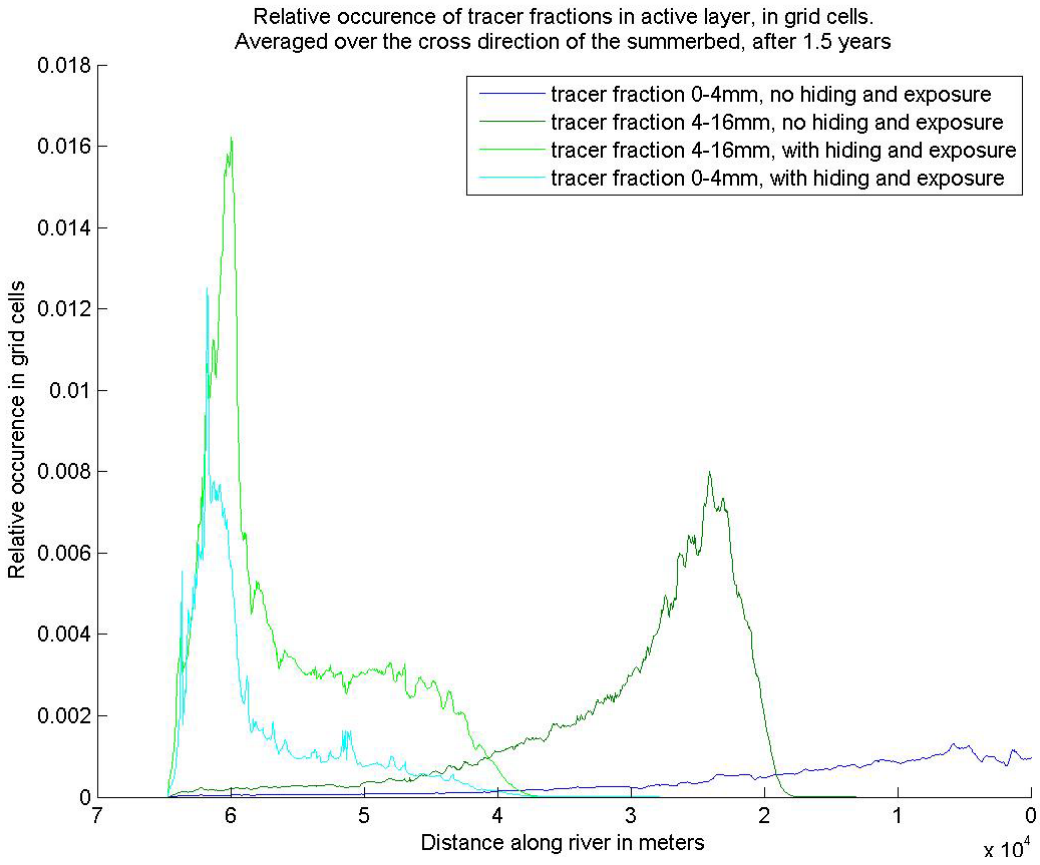

Figure 7.28: tracer propagation for smallest fractions

As can be seen in figure 7.28, the finest tracer fractions move much faster without implementation of hiding and exposure in the model. With the implementation of hiding and exposure, the smallest fraction (0-4 mm) moves even a bit slower than tracer fraction 4-16 mm. This is clearly caused by hiding and exposure, since the smallest fraction moves much faster than fraction 4-16 mm in the run where hiding and exposure is not implemented. Since the lower border of the smallest fraction was accidently set at a unrealistic low value, the characteristic diameter of this fraction is unrealistic low, resulting in large hiding effects for the smallest fraction.

7.4.5 Discussion

From 7.4.4 it is clear that hiding and exposure effects are important for the propagation speed of fractions.

In this research only one hiding and exposure relation was used, the Egiazaroff formulation, modified by Ashida & Michiue. Several other relationships have been derived in the past. A number of them is quite different from the Egiazaroff formulation, modified by Ashida & Michiue. Since the effects of implementing hiding and exposure in the model are large, it is useful to research the consequences of a different hiding and exposure relationship.

For this, a comparison between the Egiazaroff formulation, modified by Ashida & Michiue and the Parker, Klingeman & McLean or Soehngen, Kellermann & Loy formulation is made in the remainder of this section.

The Ashida & Michiue formulation, in the remainder of this section stated as 'relation1', holds:

$$\xi_i = \left\{ \begin{array}{l} 0.8429 \dfrac{D_m}{D_i}, if \ \dfrac{D_i}{D_m} \le \dfrac{7}{18} \\ \left[\dfrac{\log_{10} 19}{\log_{10} 19 + \log_{10}\left(D_i / D_m\right)} \right]^2, otherwise \end{array} \right\}$$

The Parker, Klingeman & McLean or Soehngen, Kellermann & Loy formulation, in the remainder of this section stated as 'relation 2', holds:

$$\xi_i = \left(\frac{D_m}{D_i} \right)^{\alpha},$$

in which coefficient alfa (α) is dimensionless, and ξ_i is the hiding and exposure coefficient for each fraction i.

For the initial bed composition of this model at the upstream boundary, a comparison is made between relation 1 and 2. This comparison is made for fraction 4-8mm and for fraction 31.5-64mm.

The used initial bed composition at the upstream boundary is given below:

Fraction schematization	sed1	sed2	sed3	sed4	sed5	sed6	sed7	sed8
lower border(mm)	2E-04	4	8	9	10	16	19.3	31.5
upper border (mm)	4	8	9	10	16	19.3	31.5	64
occurrence at upstream boundary	0.08	0.09	0.10	0.08	0.23	0.19	0.19	0.05

Table 7.10: bed composition

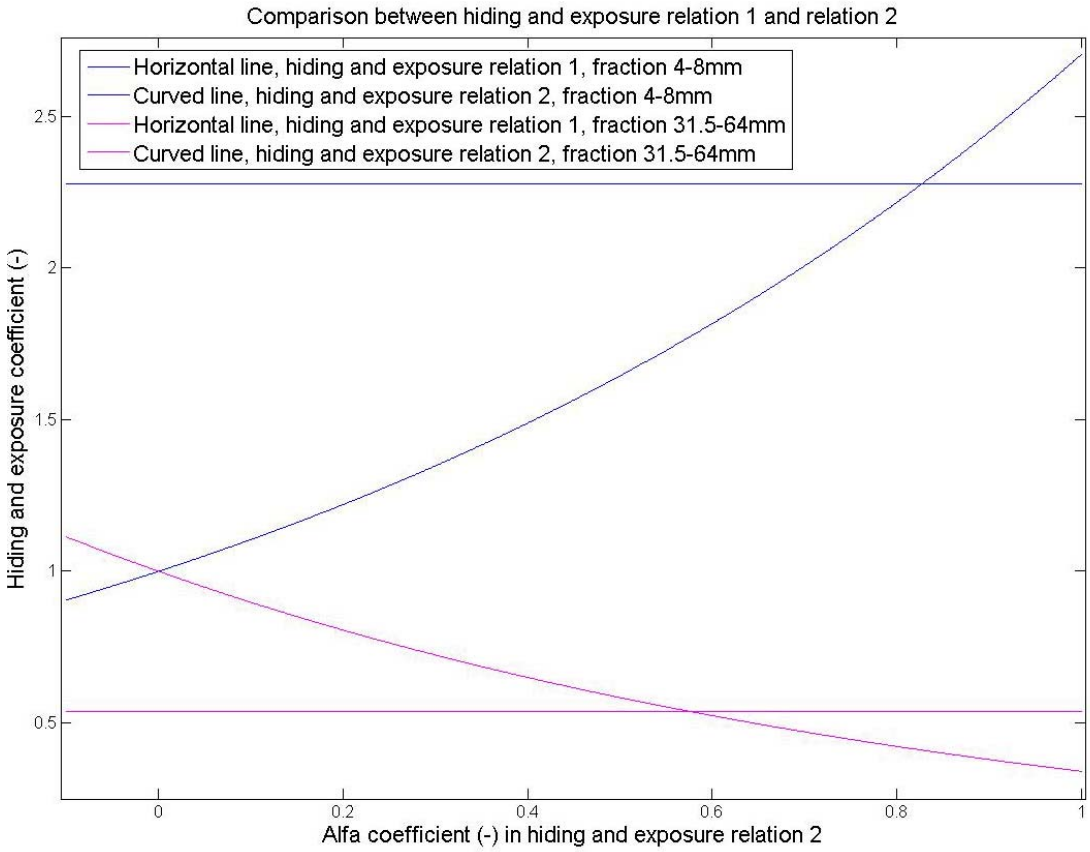

Figure 7.29: comparison between hiding and exposure coefficients of relation 1 and 2

The horizontal lines represent the values of the hiding and exposure coefficient, ξ_i, calculated with hiding and exposure relation 1, for the 4-8mm fraction and the 31.5-64mm fraction. These values are of course independent of the alfa-coefficient (α) on the horizontal axis, since this coefficient is only present in relation 2.

The curved lines show the dependence of the hiding and exposure coefficient of relation 2 on coefficient α.

No matter which coefficient α is chosen for relation 2, the hiding and exposure coefficients of relation 1 and 2 can never be exactly the same for both the fractions 4-8mm and 31.5-64mm simultaneously. The consequence is that there will always be a difference in ξ_i when using relation 1 instead of relation 2 and vice versa. From figure 7.29 it is clear that this difference can be large. If for instance α =0.575 is chosen, ξ_i is the same in relation 1 and relation 2 for fraction 31.5-64mm. For fraction 4-8mm however, ξ_i =2.25 in relation 1 and ξ_i =1.75 in relation 2.

Since it is clear from 7.4.4 that the hiding and exposure coefficient ξ_i can have a large implication on the tracer propagation, the choice for a certain hiding and exposure relation can be very important. This choice affects the calibration of coefficients in the sediment transport formula, since every calibration should result in the same yearly transport. Hence, this choice affects the propagation of individual fractions. A study about the background of all possible relations, could be advantageous for this choice. Simulations with all possible hiding and exposure relations could show more information about the differences between the relations, and show which relation suits the simulated river type best.

7.5 Higher discharge

The coarsest fraction of the original bed material, as well as the two coarsest fractions of the tracer, hardly moved at the representative discharge. In this section the consequences of a higher discharge are discussed.

7.5.1 Set-up

The following parameters are used:

Parameter	*value*
Thickness active layer	0.5 m
Number of fractions	10
Discharge	3000 m^3/s
Dredging and nourishment	not implemented
Other parameters	As in 7.1

Table 7.11: important parameters

The mobility of the coarsest fractions is compared to the reference case of 7.1.

7.5.2 Mobility of original bed fractions

For a discharge of 2000 m^3/s, the coarsest fraction 31.5 mm-64 mm does not move. For the higher discharge of 3000 m^3/s, this fraction becomes mobile. The other fractions of the original bed material of course also have a higher transport rate at this discharge.

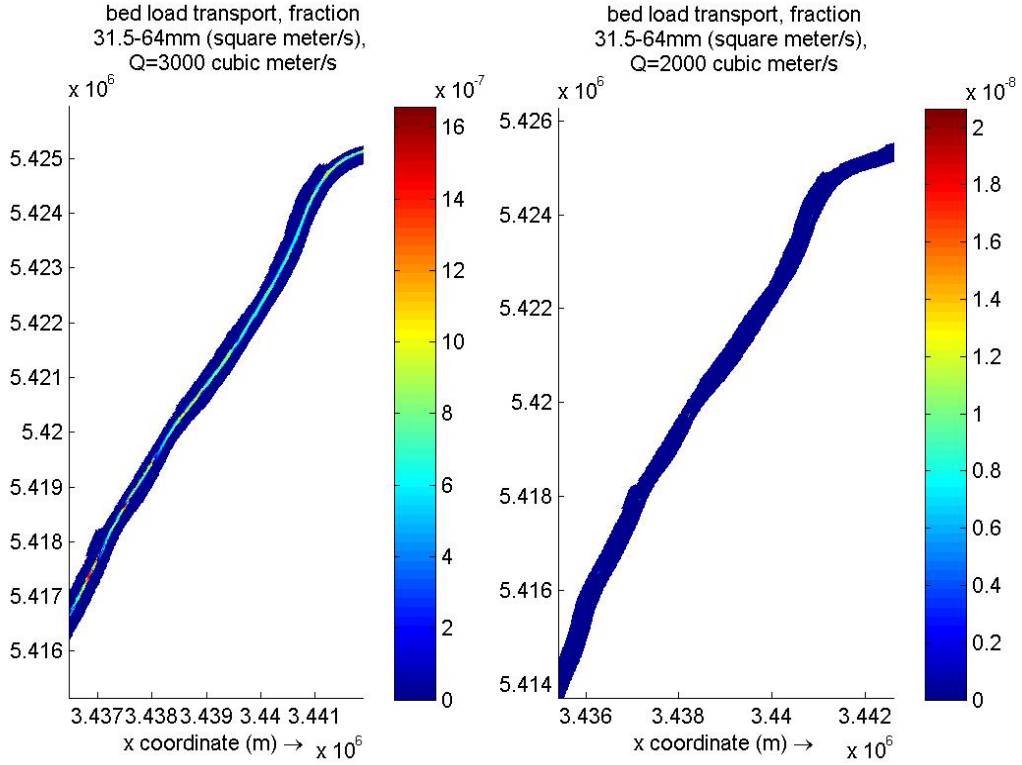

Figure 7.30: mobility at different discharges

As is visible from the plain view of figure 7.30, hardly any transport occurs at 2000 m^3/s, but significant transport occurs at 3000 m^3/s.

7.5.3 Mobility of tracer fractions

Figure 7.31 below gives the difference in mobility between the representative discharge (2000 m^3/s) and the higher discharge Q=3000 m^3/s .

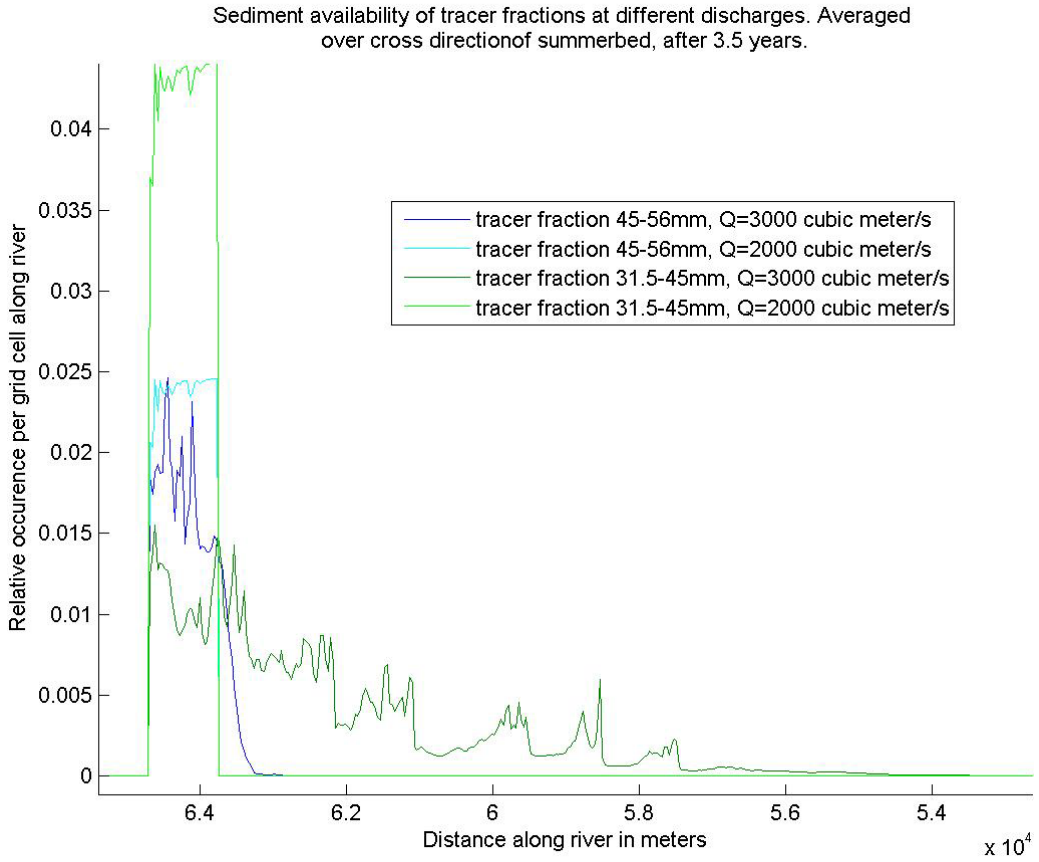

Figure 7.31: mobility of coarsest tracer fractions at different discharges

Tracer fraction 45-65 mm still hardly moves, but tracer fraction 31.5-45 mm shows a bit more mobility at the higher discharge.

7.5.4 Discussion

The results of a simulation with a higher discharge shows the importance of floods. Simulating with a constant representative discharge does not move the coarsest fractions. Simulating with a discharge which is higher than the representative discharge, gives a difference, as is clear from figure 7.31.

From the figure below it appears that the erosion area in the summerbed around 65000-60000m (around chainage km 336-342) is deeper at the higher discharge.

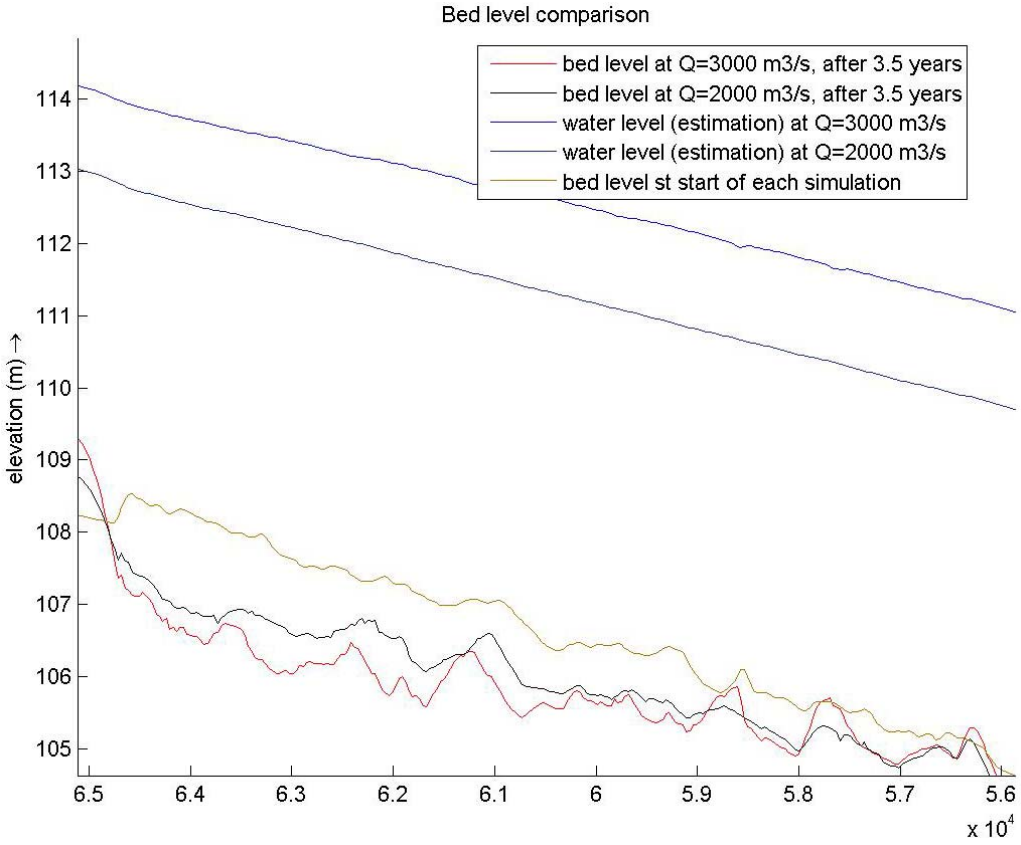

Figure 7.32: bed level comparison for different discharges

The propagation of the coarsest tracer fractions at Q=3000 m^3/s is still far smaller compared to field data from Germany. According to these field data, the propagation of tracer fraction 31.5-45 mm should be around 5-10km after 3.5 year. Of course the deeper erosion area results in a smaller velocity and hence less transport, but this cannot be the only reason for the large difference between the field data and the results of the propagation.

Apparently there are other parameters, or at least one other parameter, that need adjustment for a better representation of the fraction propagation.

When considering the kinematic celerity, $c_{mix} = \frac{\mu q_s}{\delta(1-\varepsilon)}$, the influences of several parameters can be considered. The active layer thickness δ already appeared to be an important factor in propagations of fractions. A combination of calculating with a hydrograph, which includes high discharges, and a lower active layer thickness might speed up the propagation. It is not likely, however, that this will compensate the large difference between the data and the model results. As was clear in section 7.3, a thin active layer of 0.1m did not move the coarsest tracer fractions at Q=2000 m^3/s. Since flood peaks (Q=3500 m^3/s) in the hydrograph only occur for a couple of days per year, these peaks will not be able to move the coarsest tracer fractions far enough.

Other parameters that one could change are the porosity and μ, but realistic values for these parameters do not have a wide range, and consequently the effect on the fraction celerity is relatively small.

What could have a serious effect on the fraction propagation, is the calibration of the sediment transport formula. The sediment transport formula in this research is calibrated on data containing the yearly transport and the discharge-transport relations along the river. The calibrated coefficients of the sediment transport formula are the same for all fractions in the model. A calibration that results in the same yearly transport of all fractions together, does not result in representative behaviour of individual fractions. This was already shown for the original bed fractions in section 7.2.5. In this section it appeared that individual fractions showed different behaviour, when sets of calibration coefficients were slightly different, while these sets resulted in the same transport of all fractions summed.

In conclusion, the calibrated values for transport formula coefficients do give the right yearly transport for the chosen representative discharge in this research, but apparently do not allow enough transport of the coarse tracer fractions. Also when the high discharge is used, as in this section, the coarse fractions move slowly.

Another set of coefficients, resulting in the same yearly transport, but allowing more transport of the coarsest tracer fractions, could give better results. One could choose for instance a lower θ_{cr} (critical Shields value) in the sediment transport formula $q_{s,i} = \alpha D_i \sqrt{\Delta g D_i} \left(\mu\theta_i - \xi_i\theta_{cr}\right)^c p_{i,a}$, which allows an easier initiation of motion. Also a lower hiding and exposure coefficient ξ_i for the coarser fractions, might be a solution. To represent the yearly transport correctly, other calibration coefficients in the transport formula now have to be adjusted.

One possible problem with the above adjustments could be the celerity of the finer fractions, which could change significantly. An important question for research is, if the used transport formula in this model can correctly reproduce the yearly transport and the celerities of all tracer fractions simultaneously.

7.6 Case study with hydrograph

In this paragraph the importance of computing with a hydrograph, instead of a constant discharge, is discussed.

7.6.1 Set-up

The following parameters are used:

Parameter	*value*
Thickness active layer	0.5 m
Number of fractions	8
Discharge	computation with hydrograph, as described in chapter 5
Dredging and nourishment	0 m^3
Other parameters	As in 7.1

Table 7.12: important parameters

A computation with a hydrograph practically means calculating with a certain discharge sequence each year. In the figure below this sequence is shown.

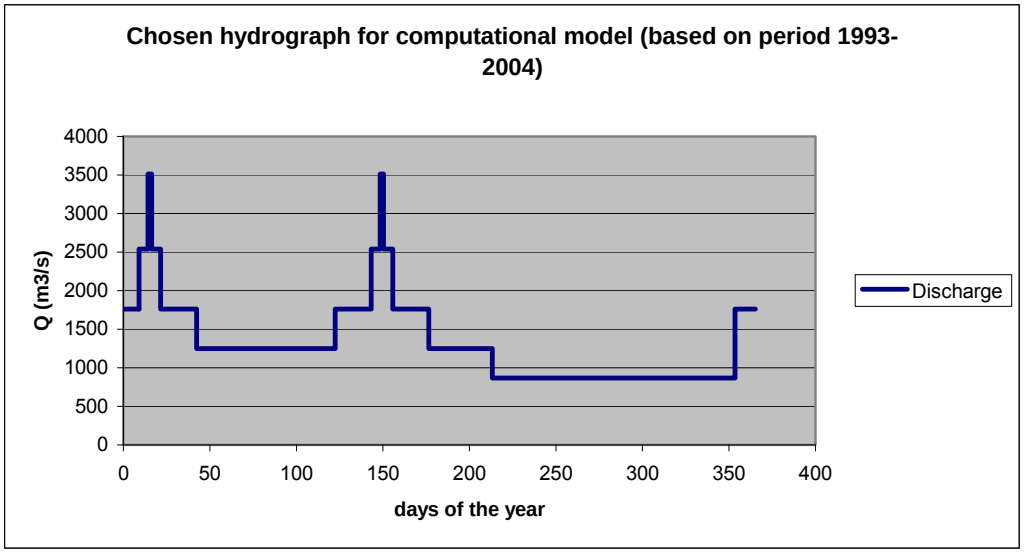

Figure 7.33: chosen hydrograph for simulation

The derivation of the above hydrograph can be read in chapter 5.

7.6.2 Bed level and sediment diameters

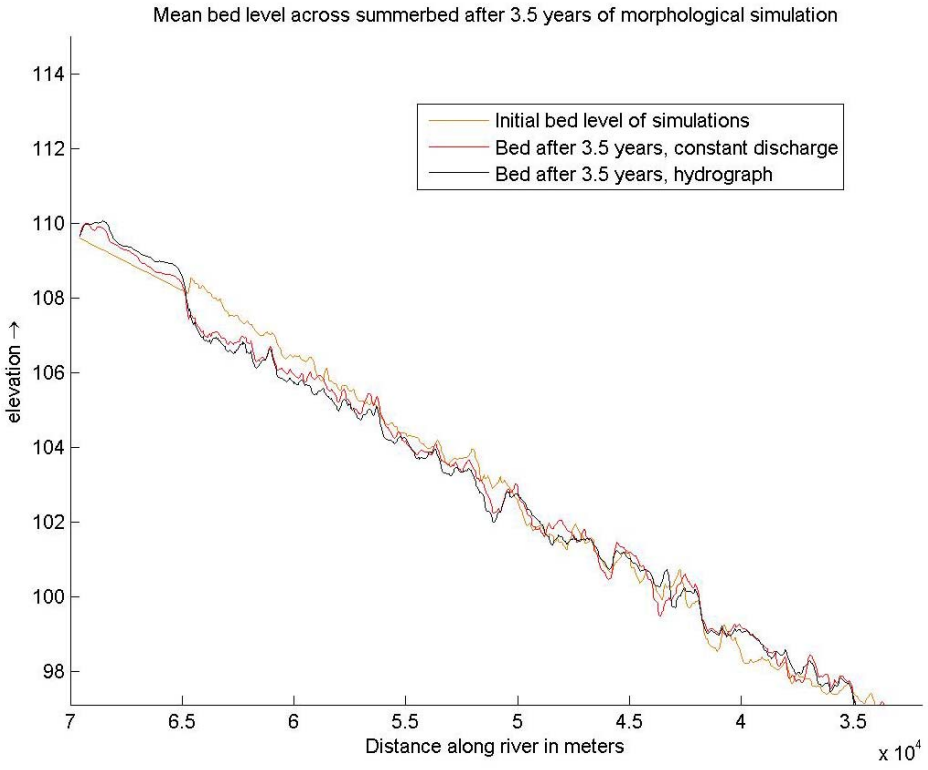

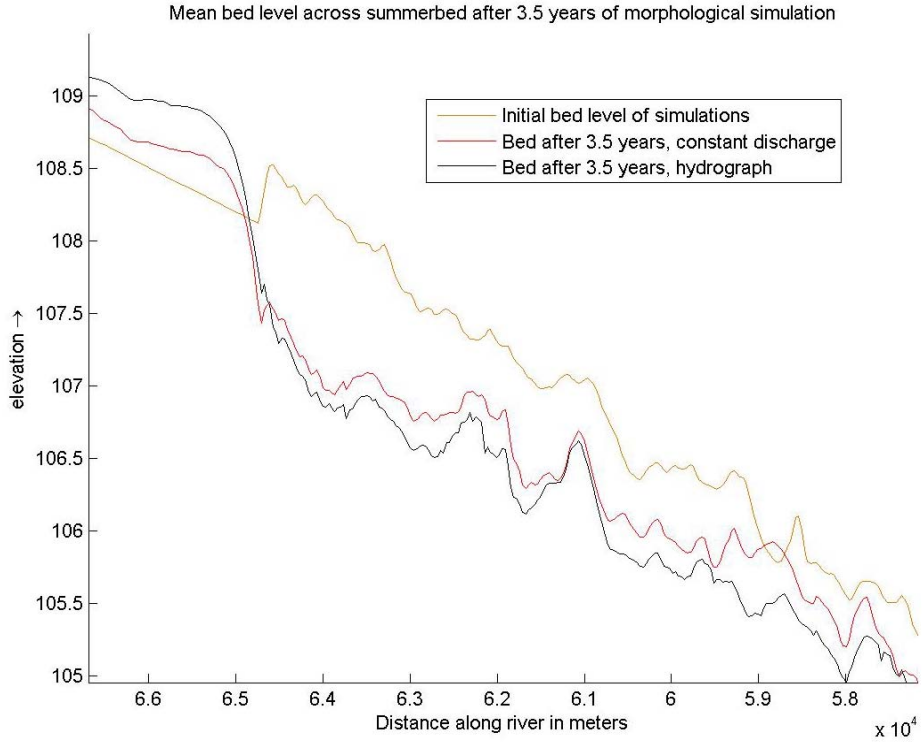

Figure 7.34 and 7.35: mean bed level averaged across summerbed

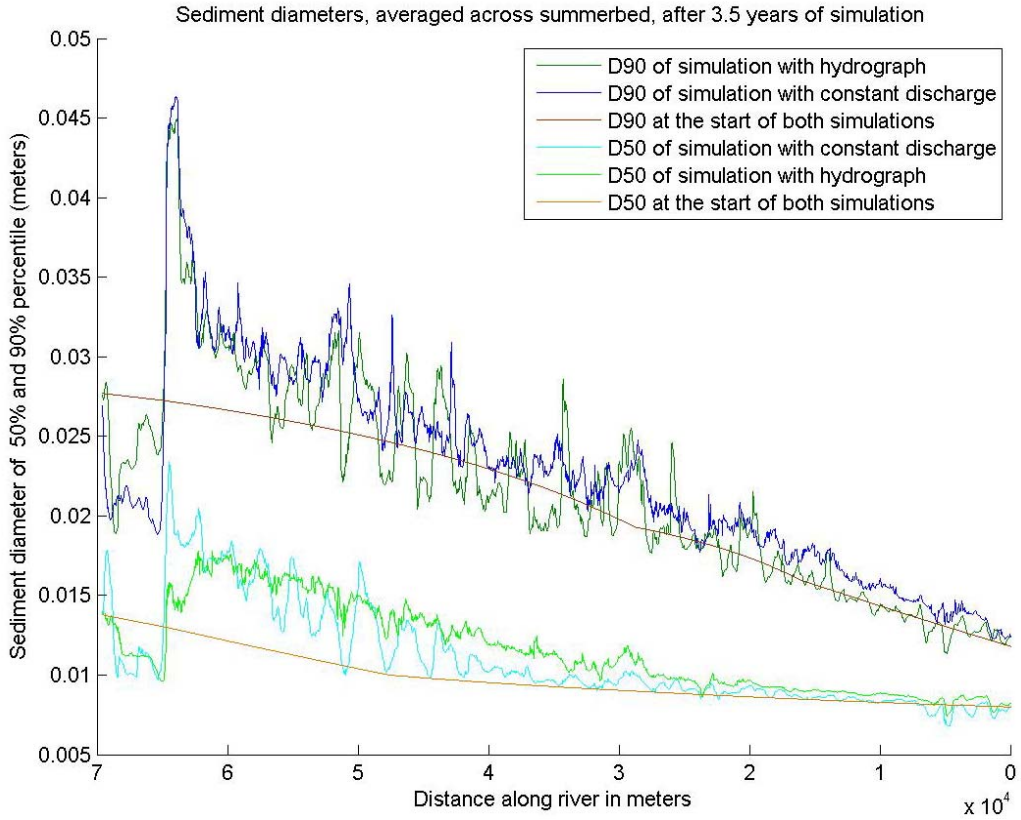

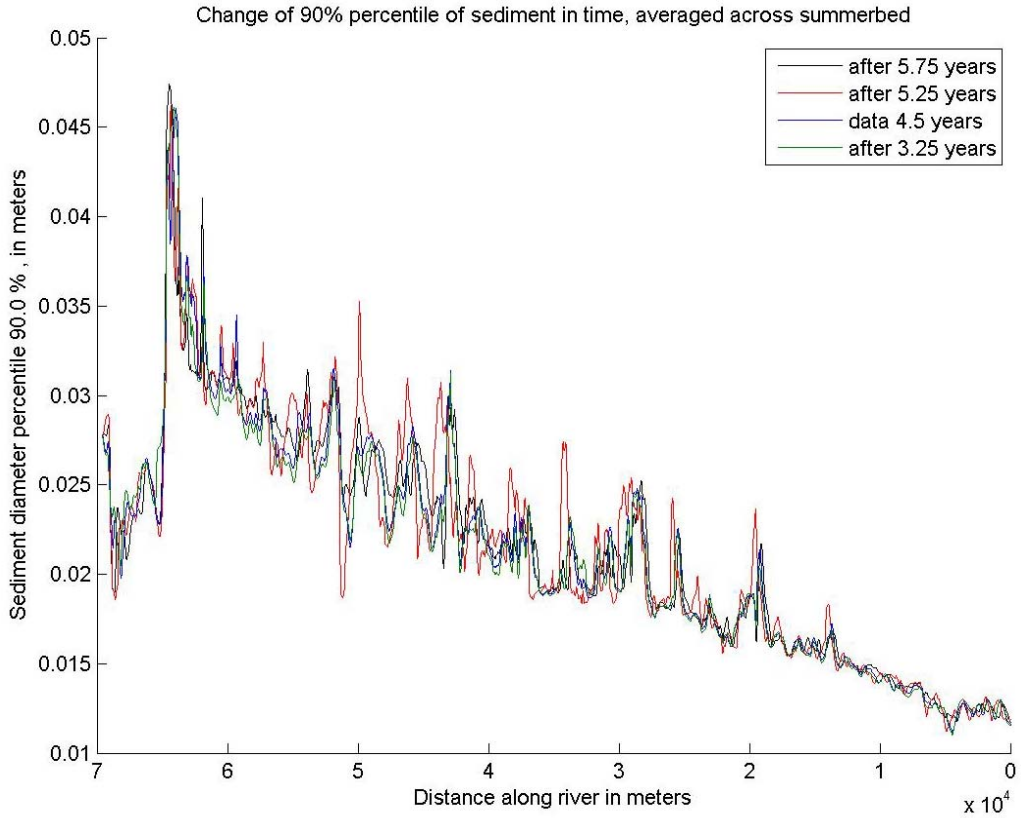

Figure 7.36 and 7.37 sediment data comparison

As can be seen in figure 7.36 and 7.37, both the bed level and the sediment size roughly show the same pattern for calculating with the representative discharge and calculating with a hydrograph. As will be showed in section 7.6.3, the tracer material shows a significant different behavior when calculating with a hydrograph.

7.6.3 Tracer

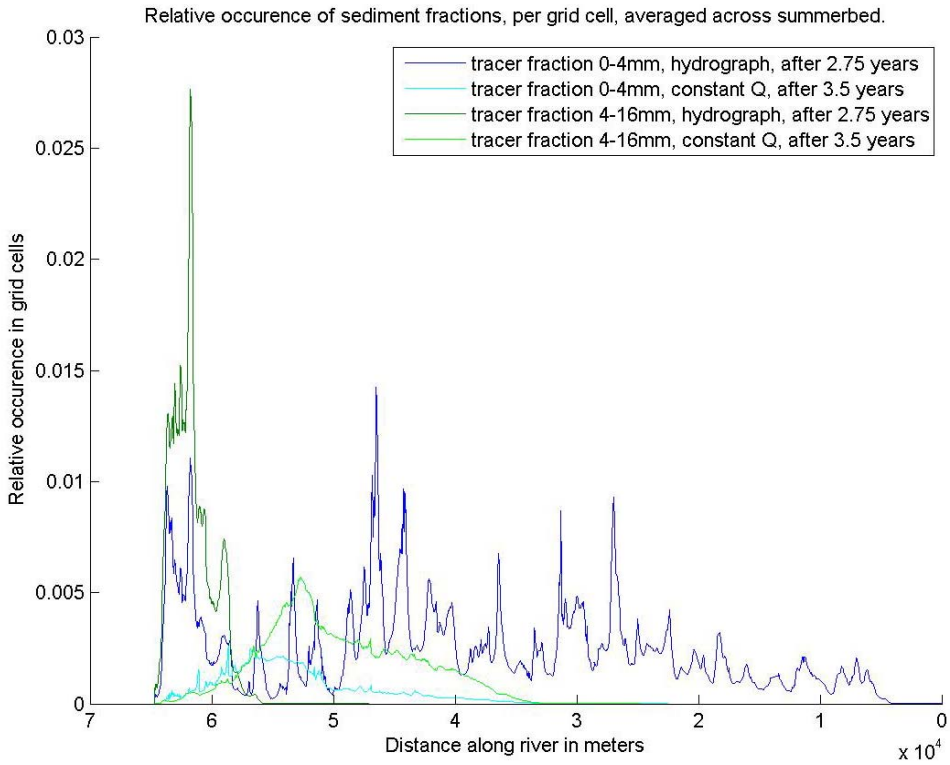

Figure 7.38: propagation of smallest tracer fractions, both for hydrograph and constant discharge

From figure 8.6 it is clear that a large difference occurs between simulation with a representative discharge and a hydrograph. Also in the simulation with a hydrograph, the two coarsest tracer fractions (31.5-45 mm and 45-56 mm) hardly move, which was already forecasted in section 7.5.4. As was already discussed in chapter 7, there is a large difference between the propagation of the coarsest fractions in the model, and the data from the BfG.

When looking at the two finest fractions of the tracer, the propagation is significantly different from the simulation with the representative discharge. The occurrence of the 5 different discharge levels apparently speeds up the 0-4 mm tracer fraction, but slows down the 4-16 mm fraction.

7.6.4 Discussion

A logical explanation for the different behaviour of the finest tracer fractions when computing with a hydrograph, can be the following. The hydrograph simulation is run with the same transport formula coefficients as the simulation with a constant discharge. The sediment transport of a tracer fraction, averaged over the period of 1 hydrograph, could be different compared to the transport rate of this fraction at the representative discharge. Also the percentage of time the critical value for initiation of motion is exceeded, for a certain fraction, could be quite different. In the hydrograph simulation, tracer fraction 4-16mm could be in transport percentually less time than in the simulation with the representative discharge. A plausible reason is that most of the time the discharge in the hydrograph simulation is significantly lower than the representative discharge. For the finer fraction of 0-4mm, the initiation of motion is exceeded at a lower discharge, allowing this fraction to be in transport much more.

Tracer fraction 4-16mm moves very slow compared with the data from the BfG, results of the representative constant discharge corresponded better with this data. According to the above explanation for the different behaviour of the finest tracer fractions when computing with a hydrograph, the solution for a good reproduction by the model is a different calibration of the transport formula coefficients. A properly chosen different set of coefficients, probably gives better results for the propagation of tracer fraction 4-16mm. As was already discussed in 7.5.4, this solution is also the best way to change the coarsest tracer fractions from not mobile to mobile. As was already discussed in 7.5.4 either, an important research question is if the used transport formula in this model can correctly reproduce the yearly transport and the celerities of all tracer fractions simultaneously.

Another option for changing the propagation speed of tracer fractions, is changing the hydrograph. The hydrograph can only be changed slightly, to still be characteristic for the analyzed period of flow. Hence the effect could be quite small.

7.7 Summary of the effects of all case studies

In table 7.13 all effects stated in previous sections of this chapter are summarized.

Effect	δ	ξ	c	α	Q	no. of fractions
Reference situation	0.5 m	yes	1.5	2.5	2000 m^3/s	10
Insignificant	0.5 m	yes	1.5	2.5	2000 m^3/s	8
Finest fraction more transported, coarser fractions less transported, the two coarsest fractions are not transported at all.		yes	1.7	3.7	2000 m^3/s	only study with simple excel sheet
Finest fraction less transported, coarser fractions more transported, the two coarsest fractions are not transported at all.		yes	1.3	1.4	2000 m^3/s	only study with simple excel sheet
Finest tracer fraction propagate much faster along river, two coarsest tracer fractions are still not mobile. A lot of dumped material 'disappears' in the underlayer system, because the dumping thickness is larger than the active layer thickness. Fast coarsening of active layer.	0.1 m	yes	1.5	2.5	2000 m^3/s	10
Much faster propagation of the smaller tracer fractions, the two coarsest fractions are still hardly mobile.	0.5 m	no	1.5	2.5	2000 m^3/s	8
Two coarsest tracer fraction still hardly mobile.	0.5 m	yes	1.5	2.5	3000 m^3/s	10
Faster propagation of 0-4 mm fraction, but slower propagation of 4-16 mm fraction. The two coarsest tracer fractions are still hardly mobile	0.5 m	yes	1.5	2.5	hydro-graph	10

Table 7.13: summary of the effect of all case studies

δ = active layer thickness [m]
ξ = hiding and exposure factor [-]
c, α = transport formula coefficients [-]
Q = discharge [m^3/s]

8 Conclusions and recommendations

8.1 Conclusions

- The quasi-3D graded sediment model used in this study has been able to reproduce significant propagation of sediment fractions within the tracer nourishment, along the river. Unfortunately, the finer fractions move too slowly and the coarsest fractions are hardly mobile, at all, when a comparison is made with the field data. A smaller active layer thickness and higher discharge did not help to obtain a more accurate prediction. Realistic options for a better result, within the model concepts used, are:
    1. A lower critical Shield value θ_{cr} in the sediment transport formula. A lower critical Shields value will result in more mobility.
    2. A different hiding and exposure formulation. Since hiding and exposure has a significant influence on mobility, a different formulation might give better results. Since existing formulations to describe the hiding and exposure phenomenon give very different results, the choice for a certain formulation in a model is important for the propagation of the sediment fractions present in the nourishment.
    3. A larger active layer thickness. From a physical point of view the active layer thickness could be increased above 0.5 m, which is the largest thickness discussed in this report. Dunes in the river reach just downstream Iffezheim typically have a height of 0.8 m at the representative discharge *(Gehres, 2009)*. The dune height is believed to be an important parameter for the thickness of the active layer in the river. *Mosselman and Sloff (2007)* show that the thickness of the active layer might even be significantly larger than the dune height, due to variations in transverse slopes and due to sandwaves caused by discharge variations.
       When interpreting the kinematic celerity of sediment fractions $c_{mix} = \frac{\mu q_s}{\delta(1-\varepsilon)}$, at first sight this celerity is smaller with a larger active layer thickness δ. However, a larger active layer thickness can certainly result in a different sediment composition in the active layer. A different sediment composition will result in a different sediment transport rate q_s and a different factor μ. This might result in a larger celerity of sediment fractions when the active layer thickness is larger.

  It is uncertain however, if the model concepts used can give a good representation of the behavior of all sediment fractions simultaneously. For instance, in the case one calibrates the critical Shields value θ_{cr} and the calibration coefficients c and α on the sediment transport of the coarsest fractions, it is uncertain that the same θ_{cr}, c and α give a satisfactory approximation for the sediment transport of the smaller fractions and vice versa.

- It is questionable if the concepts used in this model are able to reproduce the behaviour of the tracer nourishment with a satisfactory approximation. Not all physical processes occurring in the river reach downstream Iffezheim are implemented in the model concept used. Below is a list of considerations that are important for the predictive capability of the model.
    1. Vertical sorting processes are also not fully implemented in the current model. The active layer in the model, which represents the mixing layer, is assumed to be fully mixed. The same holds for the substratum or underlayer system.

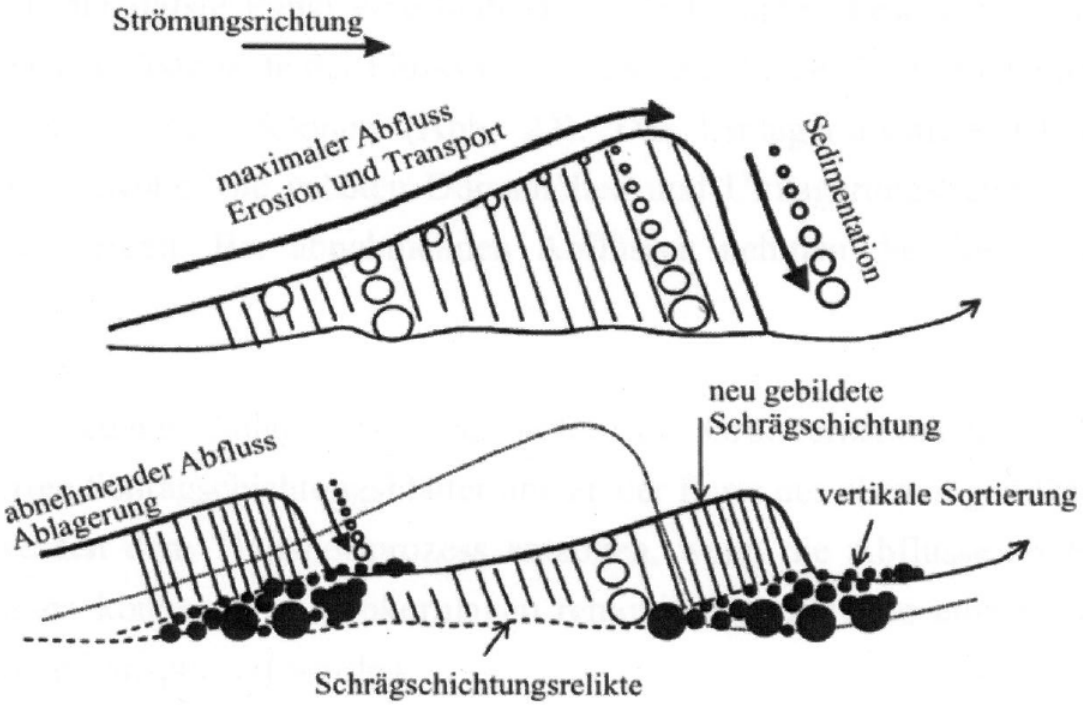

Figure 8.1: Dune processes in the river reach just downstream Iffezheim *(BfG, 2009)*

From figure 8.1 it is clear that both horizontal and vertical sorting occurs in the river reach just downstream of Iffezheim. Nourishing material also introduces vertical sorting processes that are not included in the current model. The material in the tracer nourishment of this study, is on average coarser than the original bed. After dumping of the tracer nourishment in the model, this nourishment is assumed to be instantly fully mixed with the rest of the active layer. In reality a different process will occur: the coarse material of the nourishment will be present on top of the original bed for a longer time.
All these sorting processes have consequences for the availability of sediment particles for transport and hiding and exposure of both the original bed material and the nourishment material.

2. The active layer thickness in this model is constant in time and space, which is not physically realistic. The dune height is an important parameter for the thickness of the active layer. In the river reach downstream of Iffezheim the dune height is dependent on the water depth according to the following relation: $\Phi = 0{,}167h$ *(Gehres, 2009)*.

In this relation h is the waterdepth in metres and Φ is the dune height in metres. Since the water depth is variable with time, the active layer thickness is also variable with time.

3. There are significant dunes in the river reach downstream Iffezheim, this is a different situation than the plane bed supposed in the model. The near-bed flow conditions will be different for the situation with dunes. In the model concept used, the mobility parameter θ_i is the same when the depth-averaged velocity is equal and the sediment size is equal. A sediment particle on the stoss side of a dune can be exposed to the same depth-averaged velocity as an equally sized particle on the lee side of the dune, but it is very unlikely that they will have the same critical Shields value for initiation of motion, due to different hydrodynamic forcing and conditions on both sides of the dune. Also the variation in dune size may have an influence, larger and more powerful eddies may for instance develop at dunes with a deeper trough.
4. Appendix V shows that the critical Shields parameter θ_{cr} varies with the sediment diameter, even when no hiding and exposure effects are taken into account. The contrary is stated in the modified Meyer-Peter-Müller formula for graded sediment, where the critical Shields parameter θ_{cr} is the same for all sediment diameters. Hydrodynamic conditions are different for finer sediment particles compared to coarser sediment particles, since the smaller grains are more submerged in the viscous sublayer.
5. On the river reach downstream of Iffezheim, intensive shipping occurs, while this is not taken into account in the model. In 2003 almost 40000 commercial vessels passed the locks near the Iffezheim weir, transporting 30 million tons of goods. These vessels might have a significant influence on the near-bed velocities and hence on the mobility of the tracer material.
6. It is difficult to choose the maximum and minimum sediment size present in the model. In reality cobbles up to 100 mm are present in the river reach downstream Iffezheim. The occurrence of these cobbles is rare, hence the effect on the morphology is almost nil. It is hard to say at what level of occurrence the stones start to have a significant contribution to morphology and so it is hard to determine the sediment size that should be included in the model.
7. A number of other factors might be important as well. In graded sediment mixtures the coarser grains are assumed to be more exposed to the flow compared with a more uniform mixture with only coarser grains. In a well graded mixture the finer grains can fill up pores between the larger sediment particles, possibly contributing to the skin friction experienced by the coarser grains. Sediment properties are assumed to be constant in time and space, but in reality this will not hold for roundness of grains, porosity, etcetera.

- Even if for the river reach discussed in this report the model concepts used are able to reproduce the behaviour of the tracer nourishment satisfactory, it is questionable if these model concepts are able to make rough predictions of nourishments in other river reaches.

- Calculating with a hydrograph instead of calculating with a constant discharge, is better for a number of reasons:
  * Flood periods move also the coarser fractions.
  * The average transport rate is different.
  * There are long low water periods which lead to a faster spreading of the fine material, because the coarser fractions are not transported during this period.

- When the thickness of the nourishment is initially larger than the thickness of the active layer, a part of the nourishment is stored below the active layer. This can slow down the propagation of the nourishment significantly, since it will be stored under the active layer until sufficient erosion transfers the nourishment back into this layer. This holds for both the active layer in the model as for the in reality occurring active layer in the river. At what time of the year the nourishment is done, can have an influence on storage below the active layer. During floods the active layer thickness will be much larger, at least in reality, which has consequences for the probability of storage of nourishment material below the active layer.

- For calibration of graded sediment models, field data about the different sediment fractions might help to reproduce behaviour of these fractions better in a model. When calibrating the transport formula on yearly transport only, no specific information about the behaviour of each fraction is implemented in the model. It is questionable if this fact does not present errors in the propagation of the different fractions that are larger than the desired level. For the graded sediment model used in this research, calibration on specific field data might also improve results, but the shortcomings of the modeling concepts earlier discussed in this section might be too large.

8.2 Recommendations

- It is suggested to release a tracer nourishment as quickly as possible in for instance the Bovenrijn, if one is interested in nourishments as a measure against bed degradation in a number of the Dutch river branches. When nourishing large volumes to counter the effect of bed degradation, a small tracer nourishment can already provide field data for a better prediction of the behaviour of large nourishments. Computational models might not give an accurate prediction of nourishment propagation yet according to section 8.1, but rough estimations will already be better once propagation data about specific sediment fractions are available from the field.
  The tracer nourishment should preferably contain all possible sediment sizes of future nourishments, to be sure of gaining sufficient field data from this tracer nourishment. The period of time the displacement of the tracer nourishment should be studied, should be at least several years, to include enough flood periods for displacement of the coarser material.
  Not only field data about longitudinal propagation, but also field data about transverse propagation might be interesting, to know how fast nourishments can spread over the width of the river after dumping.

- This paragraph gives practical recommendations for nourishing material in the Dutch river branches to counter bed degradation, based on the currently available knowledge.

  To dump material fast, with as less obstruction to navigation as possible, split barges or bottom door barges can be used. Bottom door barges need a significant larger depth to operate than split barges: bottom door barges need at least a waterdepth of 3 metre.

Figure 8.3: large split barge at sea

Split barges and bottom door barges used for river management purposes can approximately dump 600 tons of material per time, this is around 350 m^3 of nourishment. This results in a lot of times a split barge or bottom door barge has to dump, to complete the large scale nourishments that are needed to counter bed degradation, resulting in a longer dumping period. Dumping the whole nourishment in a short period of time is not recommended anyway,

since it is difficult to forecast the behaviour precisely, starting with smaller amounts is safer.

During the long period of nourishing, it is advised to measure the bottom regularly, to see where the nourishment has had effect so far. Predictions about nourishment propagation are still hard to make and a dumping plan based on rough predictions only could lead to an overload of nourishment on some locations and a shortage of nourishments on other locations.
When performing the nourishments, it is advisable to nourish at enough different locations over the width of the summerbed and not only on the same location of the summerbed cross-section along the whole degradation zone. This can prevent piling up of too much material on a certain location in the summerbed cross-section.

A suitable moment for dumping could be just before the start of the winter, for several reasons:
*Dumping at low waters can give operational problems (bottom door barges need a waterdepth of 3 m to operate).
*Dumping at low waters can create problems for the navigation depth, when the dumping thickness is too large.
*During the winter and (early) spring there is a larger probability of floods and higher discharges, which can transport the nourished material faster from the dumping site to locations where less or zero nourishment material is present. When the next low water occurs, the initial dumping thickness has already been reduced significantly.

An important question is of course what kind of mixture the nourishments should preferably contain.
The nourishment material should not be too fine. Problems with nourishments that have a fine mixture, is that downstream migration might be too fast, resulting in quickly returning degradation problems at the upstream end of the degradation zone. Nourishment material should also not be too coarse: very coarse material hides the fractions in the original bed too much, resulting in downstream erosion problems.
A nourishment that is relatively coarse compared to the original bed material, will armour the bed more and results in less nourishments needed to keep the river bed on a certain level. Another advantage of a coarsening of the bed could be the river slope, which could be steeper for coarser material. An on average steeper river slope in the Merwede, Waal and Bovenrijn could result in less bed degradation problems, especially in the Bovenrijn since it is further away from the sea.

One could for instance start with supplying a relatively coarse, but well graded nourishment in the Bovenrijn and/or the upstream part of the Waal. The coarse material of the mixture will armour the bed near the dumpsite and will possibly contribute to a steepening of the river, while the finer material travels more downstream and reduces bed degradation there in several possible ways:
* The material traveling downstream results in a higher river bed level.
* Material that is easily transported downstream in the Bovenrijn, might be less mobile in the Merwede, where it contributes to protecting the bed against erosion.

A positive side effect of a coarser river bed is a less steep transverse slope in river bends, leading to better nautical conditions *(Mosselman et. al, 2004)*

- Development of a model which takes into account more important physical processes, could be beneficial for the prediction of sediment nourishments. Another submodel of the river bed is for instance needed, to be able to represent the processes of vertical sorting of the river reach downstream Iffezheim better. Research on this has already be done by for instance *Blom (2008)*. Other important physical processes which are not implemented in the model, like the variability of the critical Shields value with the sediment diameter and the velocity increase due to navigation, also need consideration.

- The schematization of the characteristic sediment diameter of the coarsest and finest sediment fraction is done quite arbitrarily, research towards the effects of a different schematization is very useful. It is hard to define how the upper border of the largest sediment fraction and the lower border of the smallest sediment fraction should be chosen, for instance. The choice of these borders affect the characteristic diameter of the largest and smallest fraction significantly, and hence influence the amount of sediment transport and morphology.

- Investigation towards the effects of a different initial bottom, by changing the initial sediment composition. Instead of choosing the composition of autumn 1991 as initial bottom for this model, the initial bottom of spring 1996 can be chosen. As can be seen in section 6.1.2, there is quite a lot of change in the sediment composition in time, and it is not totally clear which choice for an initial composition is the best.

References

Ashida, K., Michiue, M.(1973).
"Studies on bed-load transport in open-channel flows". Proc. Int. Symp. on River Mechanics, IAHR, Bangkok, Thailand, paper A36, pp.407-418

Blom, A. (2008).
''Different approaches to handling vertical and streamwise sorting in modeling river morphodynamics''. Water resources research, volume 44.

Frings, R.M., Vollmer, S. (2008).
"Morphological development of the Rhine between 1996 and 2006". Bundesanstalt für gewässerkunde, Koblenz.

Gehres, N. (2009).
''Flussbettentwicklung und sohldynamik des frei fließenden Oberrheins von Iffezheim bis Mainz''. Bundesanstalt für Gewässerkunde.

Gölz, E., Theis, H., Trompeter, U. (2006).
"Tracerversuch Iffezheim". Bundesanstalt für Gewässerkunde and Wasser -und schifffahrtsamt, Koblenz/Freiburg.

Havinga, F.J., Havinga, H., Visser, P.J., de Vriend, H.J., Wang, Z.B. (2004).
"Lecture notes river engineering". Delft University of Technology.

Hirano, M. (1971).
"River bed degradation with armouring '. Trans. of JSCE, Vol. 3, Part 2.

Jansen, P.Ph.(ed.) (1979).
"Principles of river engineering: the non-tidal alluvial river". Areaman, London (1979).

Koch, F.G., Flokstra, C. (1980).
"Bed level computations for curved alluvial channels". Proc. XIX Congress of the IAHR, Vol. 2, New Delhi, India, p. 357.

Meyer-Peter, E., Müller, R. (1948).
"Formulas for bed-load transport". Proc. 2nd Congress IAHR, Stockholm, Paper No.2, pp.39-64.

Mosselman, E., Sloff, C.J. (2007).
"The importance of floods for bed topography and bed sediment composition, numerical modelling of Rhine bifurcation at Pannerden". Delft University of Technology & WL | Delft Hydraulics.

Mosselman, E., Sloff, C.J., Yossef, M., Ottevanger, W., van Vuren, S. (2007).
"Case studies Duurzame Vaardiepte Rijndelta". WL Delft Hydraulics.

Mosselman, E., Wijbenga, A. (2007).
''Morfologische effecten van zandwinning in de Merwedes''. WL Delft Hydraulics.

Mosselman, E., Sloff, C.J., Kerssens, P., van der Knaap, F., Schwanenberg, D. (2004). ''Sustainable river fairway maintenance and improvement''. WL Delft Hydraulics.

Ribberink, J.S. (1987).
"Mathematical modelling of one-dimensional morphological changes in rivers with non-uniform sediment". Delft University of Technology.

Sieben, J., Sloff, C.J. (2007).
"Model assesment of sediment nourishments in rivers with graded sediment" Delft University of Technology, WL | Delft Hydraulics & Ministry of Transport, Public Works and Water Management, Institute of Inland Water Management and Water Treatment.

Talmon, A.C., Struiksma, N., Van Mierlo, M.C.L.M. (1995).
"Laboratory measurements of the direction of sediment transport on transverse alluvial-bed slopes". J. Hydraulic Research 33, pp. 495-518
WL Delft Hydraulics (1986).
"Aantasting van dwarsprofielen in vaarwegen: retourstroom, waterbeweging stabiliteit''.
WL Delft Hydraulics (2007).
"Delft 3D flow user manual".

Appendix I

Yearly transports along chainage km 325 – 625 of the Rhine river, over the period 1996-2006 (*Frings et. al, bundesanstalt fur gewasserkunde, oktober 2008)*.

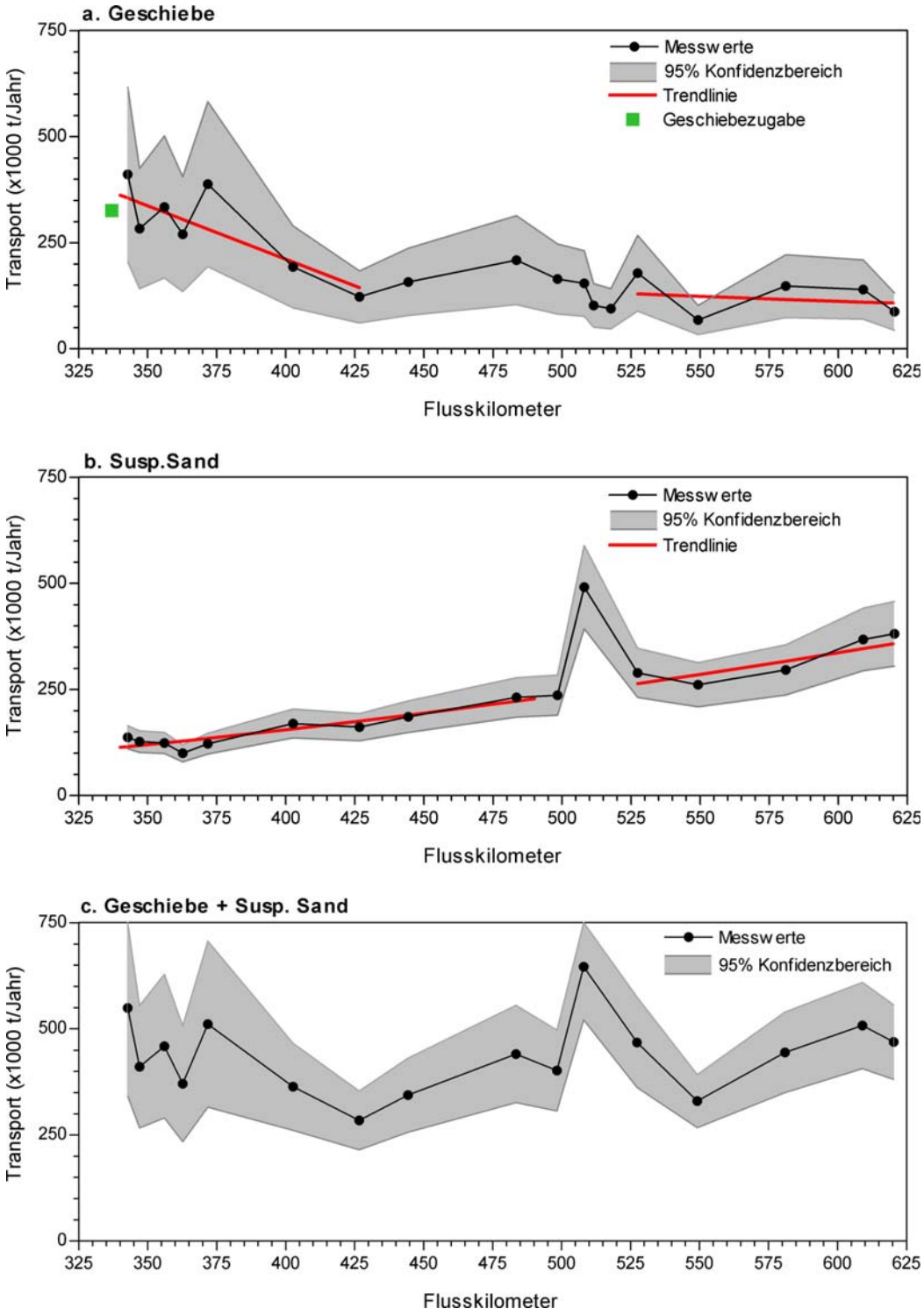

Figure A.1: transport along the river Rhine

Appendix II

This appendix holds an analysis on the bed composition of a graded sediment system, which leads to the celerity of the kinematic bed composition wave. This analysis has been done by *Ribberink (1987)*, and is 1-dimensional.

The mass balance for the total sediment package holds:

$$(1-\varepsilon)\frac{\partial z_b}{\partial t}+\frac{\partial q_s}{\partial x}=0 \qquad \text{(A-1)}$$

in which

q_s = total sediment transport per unit of width, without pores (m^2/s)
t = time (s)
ε = porosity (-)

For every sediment fraction the following balance equation holds

$$(1-\varepsilon)\left[\frac{\partial p_{i,a}\delta}{\partial t}+p_i(z_0)\frac{\partial z_0}{\partial t}\right]+\frac{\partial q_{s,i}}{\partial x}=0 \qquad \text{(A-2)}$$

waarin

$p_{i,a}$ = relative occurrence of sediment fraction *i* in active layer (-)
$p_i(z_0)$ = relative occurrence of sediment fraction *i* on level z_0 (-)
$q_{s,i}$ = sediment transport of sediment fraction *i* per meter width, without pores (m^2/s)
z_0 = level of upper limit of (first) underlayer (m + NAP)
δ = thickness of active layer (m)

The active layer thickness is chosen constant, which gives $\partial z_0/\partial t=\partial z_b/\partial t$. The transport per fraction is:

$$q_{s,i}=p_{iT}q_s \qquad \text{(A-3)}$$

in which

p_{iT} = Relative occurrence of sediment fraction *i* in bedload transport (-)

Equation (A-I) is being used to eliminate $\partial q_s/\partial x$. The result is:

$$(1-\varepsilon)\left[\delta\frac{\partial p_{i,a}}{\partial t}+\left(p_i(z_0)-p_{iT}\right)\frac{\partial z_b}{\partial t}\right]+q_s\frac{\partial p_{iT}}{\partial x}=0 \qquad \text{(A-4)}$$

Assumed is that the relative occurrence of each sediment fraction at level z_0 is always equal to the relative occurrence of that fraction in the active layer ($p_i(z_0) = p_{i,a}$). The values of D_i are constant for the selected sediment fractions. Multiplication of all terms with D_i and summation over all fractions, gives:

$$(1-\varepsilon)\left[\delta\frac{\partial D_m}{\partial t}+(D_m-D_{mT})\frac{\partial z_b}{\partial t}\right]+q_s\frac{\partial D_{mT}}{\partial x}=0 \qquad \text{(A-5)}$$

with

$$D_m=\sum_i p_{i,a}D_i \qquad \text{(A-6)}$$

$$D_{mT}=\sum_i p_{iT}D_i \qquad \text{(A-7)}$$

With the assumption that the division between the mean grain size of the bedload transport and the mean grain size of the active layer results in a constant value, equation (A-13) can be written as:

$$\frac{\partial D_m}{\partial t}+\frac{\mu q_s}{\delta(1-\varepsilon)}\frac{\partial D_m}{\partial x}=\frac{D_{mT}-D_m}{\delta}\frac{\partial z_b}{\partial t} \qquad \text{(A-8)}$$

with

μ = division between mean grain size of bed load transport and mean grain size in active layer: $\mu = D_{mT}/D_m$ (-)

This equation can be interpreted as the description of a kinematic bed composition wave, which develops due to bed level changes and differences between the grain size distributions of the bedload transport and the active layer. The comprehending celerity is:

$$c_{mix}=\frac{\mu q_s}{\delta(1-\varepsilon)} \qquad \text{(A-9)}$$

Appendix III – List of symbols

Symbol	Description	Unit	Value
α	Dimensionless coefficient in sediment transport formula	-	
β	Dimensionless coefficient in sediment transport formula	-	
δ	Active layer thickness	m	
ε	Porosity	-	0.4
μ	Ripple factor	-	1
θ	Angle between gridlines	°	
θ_i	Shields parameter for fraction *i*	-	
θ_{cr}	Critical shields parameter (initiation of motion)	-	
ρ	Mass density	kg/m^3	2650
ξ_i	Hiding and exposure parameter for fraction *i*	-	
Δ	Relative mass density	-	1.65
c	Dimensionless coefficient in sediment transport formula	-	1.5
C	Chezy coefficient	-	
c_b	bed celerity	m/s	
c_{mix}	celerity of mixture	m/s	
c_w	celerity of free surface waves	m/s	
$C_{g,90}$	Chezy coefficient related to grains	-	
A_{sh}	Coefficient related to adjustment of bed load transport direction	-	
B_{sh}	Coefficient related to adjustment of bed load transport direction	-	
D_i	Grain diameter of fraction *i*	m	
$D_{\min}$	Lower border of sediment fraction	m	
$D_{\max}$	Upper border of sediment fraction	m	
D_m	Mean diameter	m	
D_{mT}	Mean diameter of sediment in bedload transport	m	
$f(\theta)$	Coefficient related to adjustment of bed load transport direction	-	
g	Gravitational accelaration	m/s^2	9.81
h	Water depth	m	
k	Nikuradse roughness value	m	
$p_{i,a}$	Relative occurence of sediment fraction *i* in active layer	-	
$p_i(z_0)$	Relative occurence of sediment fraction *i* on level z_0	-	
p_{iT}	Relative occurence of sediment fraction *i* in bedload transport	-	
q	Discharge per unit of width	m^2/s	
$q_{s,i}$	Sediment transport of fraction *i*, per unit of width	m^2/s	
$q_{s,total}$	Total sediment transport of all fractions, per unit of width	m^2/s	

t	Time variable	s	
u	Flow velocity component along x coordinate	m/s	
u_*	Shear stress velocity	m/s	
w_s	Fall velocity of sediment	m/s	
x	Coordinate along river axis	m	
z_0	Level of upper limit of (first) underlayer	m	
z_b	Bed level	m	
Q	Total discharge through cross section of river	m^3/s	
φ_s	Original direction of bed load transport, equal to direction of depth averaged velocity	°	
φ_x	Adjusted direction of bed load transport	°	
I	Helical flow intensity	m/s	
I_e	Equilibrium helical flow intensity	m/s	
R	Radius of streamline curvature	m	
s	Coordinate along streamline	m	
u_s	Flow velocity component along streamline	m/s	
u_r	Flow velocity component perpendicular to streamline	m/s	
α_τ	Angle between depth-averaged flow and near-bed flow, caused by helical flow	°	
κ	Von Karman constant	-	0.4
C_{sh}	Coefficient related to adjustment of bed load transport direction	-	
D_{sh}	Coefficient related to adjustment of bed load transport direction	-	
v	Flow velocity component along y coordinate	m/s	
y	Coordinate perpendicular to river axis	m	
$q_{sx,i}$	Sediment transport component along x coordinate, of fraction *i*, per unit of width	m^2/s	
$q_{sy,i}$	Sediment transport component along y coordinate, of fraction *i*, per unit of width	m^2/s	
ε_H	Horizontal eddy viscosity	m^2/s	
Φ	Dune height	m	
D	Diameter of sediment	mm	

Appendix IV

In this appendix a rough estimation is given of the number of simulations and the runtime of these.

Type of simulation	*number of simulations needed*	*rough average runtime*
hydraulic calibration	26	15 hrs.
morphological set-up	26	30 hrs.
case studies with constant discharge	17	7 days
case studies with hydrograph	13	15 days

Table A.1: runtime needed

In total, around 1 year of runtime was needed for these simulations. To be able to run these simulations within 4 months, many simulations have been run simultaneously. Many simulations in the hydraulic calibration and the morphological set-up were also needed to 'debug' to model. Bugs in the model were, for example, present in the boundary formulations and the initial condition formulations.

In this report, one morphological simulation with a hydrograph is analyzed. In total 13 simulations with a hydrograph have been run, unfortunately analyses with the other 12 simulations could not be done anymore. The data of these simulation are useful for further research. In table A.2 these simulations are described.

Type of simulation with hydrograph	*Number of simulations*
Simulations with different amount of dredging/nourishment	3
Simulation with different initial bottom	1
Simulations with different active layer thickness	4
Simulations with different hiding and exposure formulation	2
Simulations with different critical Shields value in sediment transport formula	2
Simulation with 45 mm as upper border of the coarsest fraction (instead of 64 mm)	1

Table A.2: unanalysed simulations, useful for further research

Appendix V

In the figure on the next page, figure A.2, curves of equal transport are constructed from laboratory tests. These tests were done with various grain sizes and various flow conditions, but always with a uniform grain bed, excluding hiding and exposure effects.

The curves are constructed in a graph with mobility parameter ψ on the vertical axis and parameter Re_* on the horizontal axis.

$$\psi = \frac{u_*^2}{\Delta g D} \qquad \text{(A-10)}$$

$$\mathrm{Re}_* = \frac{u_* D}{\nu} \qquad \text{(A-11)}$$

$$u_* = \sqrt{ghi} \qquad \text{(A-12)}$$

If the river part discussed in this report is considered,
$u_* = \sqrt{ghi}$ = 0.1 m/s

With the assumption that the curve of equal transport which represents the curve for initiation of motion, has a minimum around ψ =0.03 and Re_* =10, the following critical Shield values $\psi_{critical}$ ($= \theta_{cr}$) can be calculated.

For $D = 1mm$: $\psi_{critical}$ ($= \theta_{cr}$) = 0.045
For $D > 6mm$: $\psi_{critical}$ ($= \theta_{cr}$) = 0.063

This shows that the critical value for initiation of motion, without hiding and exposure effects, is different for small material and coarser material. When the diameter of the sediment is larger than 6 mm, this critical value is constant in respect to the sediment diameter.

For the Bovenrijn the conditions are a bit different (water slope is less steep), which results in the fact that the critical moment for initiation is constant for $D > 9mm$.

Figure A.2 is obtained from laboratory tests of *WL Delft Hydraulics (1986).*

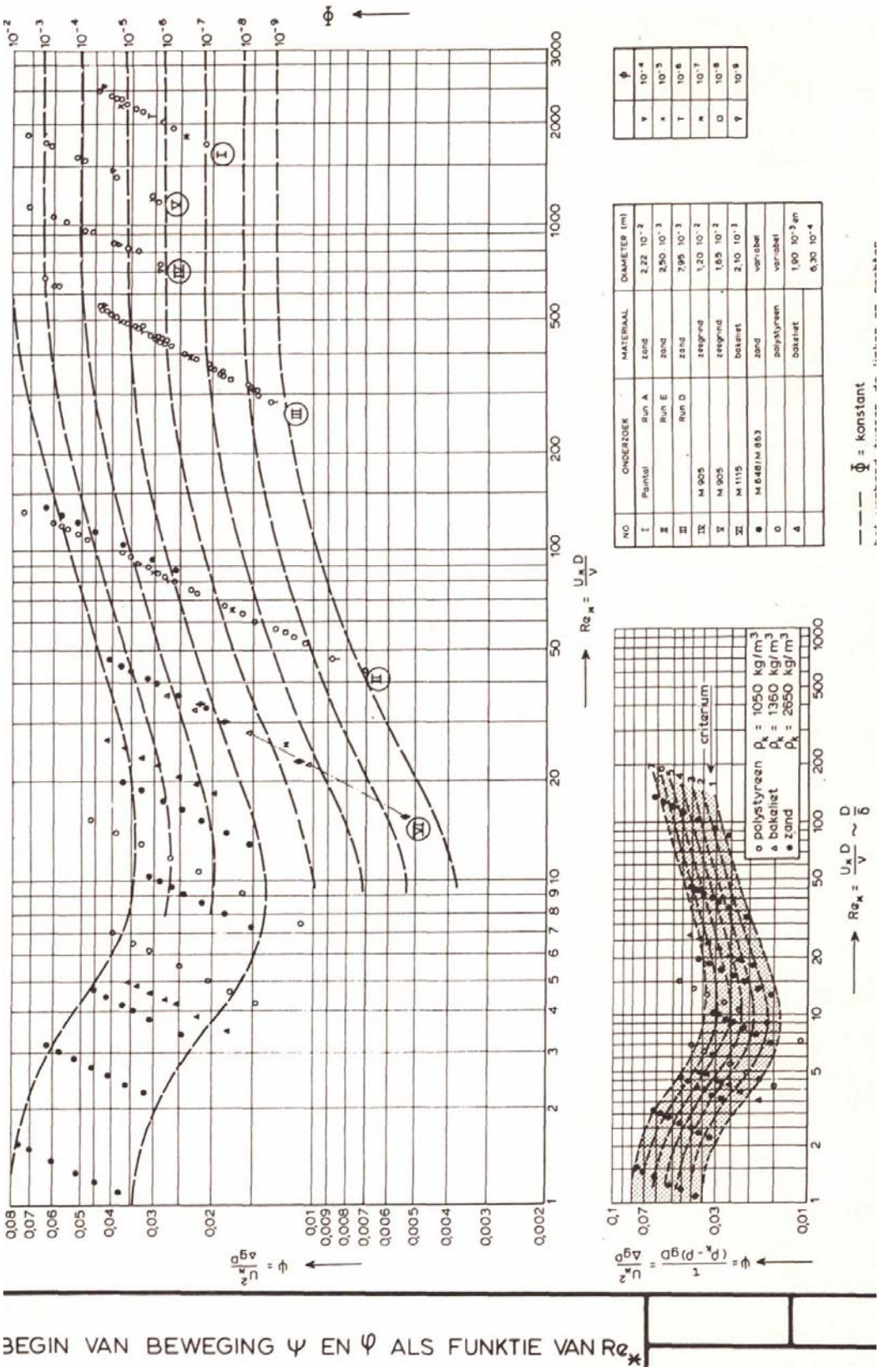

Figure A.2: curves of equal transport, for mobility parameter ψ and Re_*